

This electronic thesis or dissertation has been downloaded from the King's Research Portal at <https://kclpure.kcl.ac.uk/portal/>



### **3 Dimensional echocardiographic assessment of left ventricular dyssynchrony in the optimisation of pacing therapy.**

Adhya, Shaumik

*Awarding institution:*  
King's College London

The copyright of this thesis rests with the author and no quotation from it or information derived from it may be published without proper acknowledgement.

#### **END USER LICENCE AGREEMENT**



**Unless another licence is stated on the immediately following page** this work is licensed

under a Creative Commons Attribution-NonCommercial-NoDerivatives 4.0 International

licence. <https://creativecommons.org/licenses/by-nc-nd/4.0/>

You are free to copy, distribute and transmit the work

Under the following conditions:

- Attribution: You must attribute the work in the manner specified by the author (but not in any way that suggests that they endorse you or your use of the work).
- Non Commercial: You may not use this work for commercial purposes.
- No Derivative Works - You may not alter, transform, or build upon this work.

Any of these conditions can be waived if you receive permission from the author. Your fair dealings and other rights are in no way affected by the above.

#### **Take down policy**

If you believe that this document breaches copyright please contact [librarypure@kcl.ac.uk](mailto:librarypure@kcl.ac.uk) providing details, and we will remove access to the work immediately and investigate your claim.

3 Dimensional echocardiographic  
assessment of left ventricular  
dyssynchrony in the optimisation of  
pacing therapy.

---

Shaumik Adhya

Submitted for the degree MD (Res)

# Acknowledgements

Thanks to my wife for all her support – this would never have happened without her.

Thank you to Mark and Francis, my supervisors for their unfailing generosity. Thanks also to the Kings Research Fellows – Amit, Cliona, Lindsay and Alexandros, and the Kings sonographers in particular Pete, Jo, Norman and Nikki. They have helped in numerous practical ways and taught me so much.

This work was funded by a departmental grant from Medtronic.

# Table of Contents

<b>Acknowledgements .....</b>	<b>2</b>
<b>Table of Contents .....</b>	<b>3</b>
<b>Table of Figures .....</b>	<b>6</b>
<b>Abstract .....</b>	<b>13</b>
<b>Chapter 1 Introduction.....</b>	<b>15</b>
<b>1.1 Abstract.....</b>	<b>15</b>
<b>1.2 History of pacing .....</b>	<b>16</b>
<b>1.3 Definition of dyssynchrony .....</b>	<b>21</b>
<b>1.4 Techniques to assess dyssynchrony .....</b>	<b>21</b>
1.4.1 Indirect techniques.....	22
1.4.2 Direct Techniques - electrical.....	23
1.4.2.1 Electrocardiogram (ECG).....	23
1.4.3 Direct techniques - non-echocardiographic methods .....	24
1.4.3.1 Nuclear imaging .....	24
1.4.3.2 Cardiac Magnetic Resonance Imaging.....	25
1.4.3.3 Cardiac Computed Tomography .....	25
1.4.4 Direct techniques - echocardiographic methods .....	26
1.4.4.1 Motion-mode .....	26
1.4.4.2 Doppler imaging .....	27
1.4.4.3 Two and Three dimensional imaging .....	30
1.4.4.4 Measurement Variability .....	33
1.4.4.4.1 Doppler and two-dimensional methods.....	33
1.4.4.4.2 Three-dimensional methods .....	34
<b>1.5 Assessment of Dyssynchrony.....</b>	<b>35</b>
1.5.1 Dyssynchrony in healthy subjects.....	35
1.5.2 Dyssynchrony due to right ventricular pacing. ....	38
1.5.2.1 Atrioventricular dyssynchrony .....	38
1.5.2.2 Intra-ventricular dyssynchrony, and the effect of pacing at different right ventricular sites. ....	39
1.5.3 Dyssynchrony in left bundle branch block.....	44
1.5.3.1 Electrical mapping of left bundle branch block.....	45
1.5.3.2 Echocardiographic assessment of left bundle branch block and its utility in CRT .....	46



1.5.3.2.1 M-mode and 2D echocardiographic assessment.....	46
1.5.3.2.2 Doppler assessment.....	46
1.5.3.2.3 Speckle tracking.....	47
1.5.3.2.4 3D echocardiography .....	48
<b>1.6 Optimisation of pacing.....</b>	<b>56</b>
1.6.1 Why the interest in AV optimisation?.....	56
1.6.2 Methods to optimise AV and VV delays. ....	58
1.6.3 The role of AV optimisation in biventricular pacemakers.....	60
1.6.4 The clinical basis for AV optimisation. ....	64
1.6.5 The role of VV optimisation .....	65
1.6.6 AV & VV optimisation .....	67
<b>1.7 Summary.....</b>	<b>70</b>
<b>Chapter 2 AdviseCRT .....</b>	<b>71</b>
<b>2.1 Abstract.....</b>	<b>71</b>
<b>2.2 Introduction .....</b>	<b>71</b>
<b>2.3 Methods.....</b>	<b>72</b>
2.3.1 Study Objectives.....	72
2.3.2 Study design.....	72
2.3.3 Patient eligibility criteria .....	73
2.3.4 Implant set-up.....	74
2.3.5 Implant measurements.....	77
2.3.6 Post Procedure echocardiogram .....	78
<b>2.4 Results .....</b>	<b>80</b>
2.4.1 Patients .....	80
2.4.2 Optimum AV delay .....	83
2.4.3 3-Dimensional echocardiography to determine optimum AV delay .....	83
2.4.4 Doppler echocardiography and Cardiac Impedance to determine optimum AV delay .....	84
<b>2.5 Conclusions.....</b>	<b>85</b>
<b>Chapter 3 RV mid-septal or apical pacing.....</b>	<b>88</b>
<b>3.1 Abstract.....</b>	<b>88</b>
<b>3.2 Introduction .....</b>	<b>88</b>
<b>3.3 Methods.....</b>	<b>90</b>
<b>3.4 Results .....</b>	<b>92</b>
<b>3.5 Conclusions.....</b>	<b>102</b>
<b>Chapter 4 Do we need to optimise?.....</b>	<b>105</b>

<b>4.1 Abstract.....</b>	<b>105</b>
<b>4.2 Introduction .....</b>	<b>105</b>
<b>4.3 Methods.....</b>	<b>106</b>
4.3.1 Patients .....	106
4.3.2 Study Procedures.....	107
4.3.3 Outcome measures .....	112
4.3.4 Statistical analysis.....	113
<b>4.4 Results .....</b>	<b>114</b>
4.4.1 Baseline Characteristics.....	115
4.4.2 Inter-observer variability. ....	116
4.4.3 Response to CRT .....	116
4.4.4 Determinants of response .....	120
4.4.5 Effect of optimisation.....	126
4.4.6 Clinical outcome of CRT .....	129
<b>4.5 Conclusions.....</b>	<b>131</b>
 <b>Chapter 5 Three-dimensional echocardiographic Speckle tracking</b>	
<b>.....</b>	<b>133</b>
<b>5.1 Abstract.....</b>	<b>133</b>
<b>5.2 Introduction .....</b>	<b>133</b>
<b>5.3 Methods.....</b>	<b>134</b>
5.3.1 Statistics.....	139
<b>5.4 Results .....</b>	<b>140</b>
<b>5.5 Conclusions.....</b>	<b>156</b>
 <b>Chapter 6 Conclusions .....</b>	<b>158</b>
<b>6.1 Aims of this thesis.....</b>	<b>158</b>
<b>6.2 Summary of main findings.....</b>	<b>158</b>
<b>6.3 Conclusion.....</b>	<b>161</b>
 <b>7 References.....</b>	<b>162</b>

## Table of Figures

Figure 1.1 Image demonstrating septal to posterior wall motion delay. It is the interval between maximal posterior and septal displacement of left posterior and septal wall using a mono-dimensional short-axis view at the papillary muscle level. Intraventricular dyssynchrony is defined by a septal-to-posterior wall motion delay of .130 ms. Reproduced from Schmidt et al. <sup>47</sup> .....	27
Figure 1.2 Illustration of Myocardial Performance Index, or Tei-index. <sup>50</sup> ..	28
Figure 1.3. Regional myocardial velocity curves obtained by tissue Doppler imaging at the basal septal (yellow) and basal lateral (green) segments. In the color 2D pictures, movement of the myocardium toward the probe (during contraction) is shown in red, whereas movement away from the probe (during relaxation) is shown in blue. Panel A, In a patient with LBBB, there was delay in the onset and peak sustained systolic contraction (SM) in the lateral compared with the septal wall. Regional contraction occurred in a haphazard manner in various segments as illustrated by the patchy areas of blue colors (arrowheads). Panel B, After biventricular pacing, there was dramatic improvement in the synchronicity, as reflected by the overlapping of velocity curves in the basal septal and basal lateral segments and the homogenous red color in the two-dimensional picture. <sup>51</sup> .....	29
Figure 1.4 Example of 3D speckle tracking derived strain. The segments are demonstrated in the upper left endocardial cast, bulls-eye plot upper right, and individual segments plotted against time on the lower right panel. Numerical results are in the lower left panel.....	33
Figure 1.5 Example of the Ritter method for AV optimisation. <sup>117</sup> . This method programs two extreme AV intervals: a long AV interval with A wave attenuation (AVlong) and a short AV interval with A wave truncation (AVshort). For each AV interval, the time between the QRS	

complex onset to the completion of the A-wave is measured. The optimal AV interval is then calculated as below. ....	57
Figure 1.6. Iterative method. Initially a long AV delay is programmed and the mitral inflow interrogated. The AV delay is shortened in 20ms increments until truncation of the A wave occurs. It is then lengthened in 10ms increments until the A wave is no longer truncated <sup>117</sup> . ....	59
Table 2.1 – Table of impedance vectors .....	78
Figure 2.1 Pressure volume loops. An example patient during intrinsic rhythm (upper panel), LV pacing with an AV delay of 160ms (middle panel) and 120ms (lower panel). The segmental loops are on the left, the global LV loop is bottom right and summary data in the upper right. In intrinsic rhythm the cardiac function is poor with a stroke volume of 31ml and the shape of the loop indicates inefficient cardiac work. During LV pacing there is a “square” shaped loop indicating efficient cardiac function and much better haemodynamics with a stroke volume of 63 ml. There is little difference between the AV delays shown. ....	82
Figure 2.2 – Frequency histogram of optimum AV delays. ....	83
Figure 2.3 – Box plot showing median, interuartile ranges and 95% confidence interval of the % difference between 3D methods and dp/dt. ....	84
Figure 2.4 – Box plot of difference in AV delay for each method against dp/dt. The box indicates the median difference and the interquartile range. The whiskers indicate the 95% confidence interval. ....	85
Table 3.1 - Baseline characteristics. Asterix indicates p value <0.05 .....	93
Table 3.2 - Effects of pacing at different locations. Asterix indicates P value <0.05 .....	94
Figure 3.1 3D analysis of a patient in baseline rhythm. The upper left panel shows a short axis cut of the endocardial cast. The upper right panel shows the 4ch cut, and the lowere left panel shows a bullseye plot. The volume graphs for each of 16 segments is shown in the lower	

right panel. There is very little dispersion in the time to minimum volume across the segments, indicating synchronous contraction.	
Ejection fraction was 47%, SDI 1.9% .....	95
Figure 3.2. The same patient with apical RV pacing. There is now more dispersion seen in the time to minimum volume in the lower right panel. The EF was 39%, SDI 5.8%. .....	96
Figure 3.3 Another patient at baseline. EF is 63%, SDI 2.7% .....	96
Figure 3.4. The same patient as 3.3 during mid-septal RV pacing. The dispersion of time to minimum volume remains small Ef 61%, SDI 2%.. .....	97
Table 3.3 - Effects of pacing in patients with normal ejection fraction.	
Asterisk indicates $p < 0.01$ .....	98
Table 3.4 - effects of pacing in patients with low ejection fraction .....	99
Figure 3.5 - Figure 1. Box and whisker plot showing LV ejection fraction during intrinsic rhythm and pacing in apex and mid-septal regions. Paired t-test indicates a significant fall in ejection fraction in both groups, $p < 0.01$ .....	100
Figure 3.6 - Box and Whisker plot showing change in LV ejection fraction due to pacing in apex and mid-septal regions. Box indicates 25th and 75th percentiles with whiskers indicating 5th and 95th percentiles. P value for difference = 0.02. ....	100
Figure 3.7 - Box and Whisker plot showing change in SDI due to pacing in apex and mid-septal regions. Box indicates 25th and 75th percentiles with whiskers indicating 5th and 95th percentiles. P value for difference between apex and mid-septum = 0.03. ....	101
Figure 3.8 - Box and Whisker plot showing absolute change in LV ejection fraction due to pacing in apex and mid-septal regions, stratified by baseline LV ejection fraction. Box indicates 25th and 75th percentiles with whiskers indicating 5th and 95th percentiles. P value for	

difference between apex and mid septum in patients with low baseline  
 LV ejection fraction = 0.03..... 102

Figure 4.1 Four images demonstrating the calculation of the Myocardial  
 performance index. The A-E time is measured at least 3 times. The  
 Ejection time is also measured at least 3 times. The echo machine has  
 been programmed to automatically calculate the average MPI. The  
 panels show a measurement at 2 example sensed AV delays of 160ms  
 and 120ms. 120ms is determined to be the optimum setting with an  
 MPI of 0.67, as compared to 160ms which has a higher MPI of 1.05 109

Table 4.1 Baseline Characteristics ..... 115

Figure 4.2 3D assessment of a single patient at baseline. The upper left  
 panel shows a short axis view of the endocardial case, the upper right a  
 long axis view. The lower left panel is a bulls eye plot of all 16  
 segments. The activation wavefront is seen over the endocardial casts.  
 Individual segmental motion is plotted in the lower right panel. The  
 ejection fraction was 16% and SDI 14.0% ..... 117

Figure 4.3 3D assessment of the same patient after CRT. The panels are in  
 the same order as Figure 4.2. The graph indicates some improvement in  
 dyssynchrony. The EF was 26% and SDI 7.7%..... 118

Figure 4.4 The same patient before optimisation. In this figure the lower  
 right panel gives the numerical results..... 118

Figure 4.5. After optimisation (AV and VV). The ejection fraction has  
 increased from 30 to 32% with a small drop in SDI from 5.7 to 5.4. . 119

Graph 4.1 This graph shows a box plot of ejection fraction at baseline (EF  
 1), within 72 hours of CRT implant (EF 2), before optimisation (EF 3) and  
 immediately after optimisation. The horizontal line indicates the  
 median ejection fraction at each time point, the boxes enclose the 25th  
 to 75th percentiles of the range and the whiskers enclose approximately  
 95% of the range. When assessed with a repeated measures ANOVA

test, the serial change in ejection fraction over the 4 time points was statistically significant $p < 0.001$ .....	120
Graph 4.2 A plot of relative change in ejection fraction against change in SDI post CRT. A Linear regression line is plotted and the $R^2$ value of 0.195. ....	122
Graph 4.3 Relative change in Ejection fraction plotted against Systolic Dyssynchrony Index at baseline. A linear regression line is plotted. The $R^2$ value of 0.113. ....	123
Graph 4.4 Relative change in Ejection Fraction plotted against QRS. A linear regression line is shown. The $R^2$ value of 0.052.....	124
Graph 4.5 Box-plot demonstrating the relative change in ejection fraction between baseline and before optimisation categorised by QRS morphology. Normal refers to a QRS of $\leq 120$ ms. NSIVCD refers to a QRS of $> 120$ ms that did not meet WHO criteria for left or right bundle branch block.....	125
Graph 4.6 Graph showing mean and 95% confidence intervals for the relative change in ejection fraction between baseline and before optimisation as categorised by QRS morphology. P value for comparison $< 0.05$ .....	126
Graph 4.7 Absolute change in ejection fraction peri-optimisation plotted against absolute change in SDI before and after CRT implantation. Regression confirms no statistical correlation between change in ejection fraction and change in SDI (R square 0.01) .....	127
Graph 4.8 plots absolute change in ejection fraction due to optimisation against SDI2. Regression confirms no statistical correlation between change in ejection fraction and SDI2 (R square 0.14).....	128
Graph 4.9 Change in Mean Ejection fraction due to optimisation stratified by SDI2. Graph shows mean $\pm$ 95% confidence intervals. P value $< 0.05$ .....	129

Graph 4.10 Plot of patients stratified according to NYHA functional class pre CRT implantation, at optimisation and at follow up. The width of the boxes indicates the proportion of patients in each class.....	130
Figure 5.1 Aligned volume. The volume has been opened in LV analysis 4.0. The volume has been rotated along the axes to that the axis goes through the apex and the mitral valve. The aortic valve has been marked in the short axis view (SAX, upper left panel) to aid the software in recognizing the standard 2,3 and 4 chamber long axis cuts (3Ch upper right, 2Ch lower left and 4Ch lower right respectively).....	137
Figure 5.2. The software generates an endocardial border at a single timepoint in the cardiac cycle. This is visible next to the moving image and can be manipulated to ensure accurate placement of the border. After this step the software tracks the border and generates the moving endocardial cast. This can then be visualised throughout the cardiac cycle to ensure a good fit. ....	138
Figure 5.3 Output of LV analysis 4.0. This figure shows the 3D cast in the upper right panel, bullseye plot upper left panel, numerical results lower left panel and graph of 3D strain against time in lower right panel. ....	139
Table 5.1. P values for bias between Chicago and Kings are all non significant ( $>0.05$ ) .....	141
Figure 5.4 Bland Altman plot for End Diastolic Volume. Solid line indicates bias and dashed lines indicate 95% confidence intervals. ..	144
Figure 5.5 Bland Altman plot for End Systolic Volume. Solid line indicates bias and dashed lines indicate 95% confidence intervals. ....	144
Figure 5.6 Bland Altman plot for Stroke Volume. Solid line indicates bias (-1.4 ml), dashed lines indicate 95% confidence intervals ( $\pm 19$ ml) ..	145
Figure 5.7 Bland Altman plot for Ejection Fraction. Solid line indicates bias and dashed lines indicate 95% confidence intervals .....	145
Figure 5.8 Bland Altman plot for SDI-I. Solid line indicates bias and dashed lines indicate 95% confidence intervals .....	146



Figure 5.9 Bland Altman plot for SDI-II .....	146
Figure 5.10 Bland-Altman plot for End Diastolic Volume.....	148
Figure 5.11 Bland-Altman plot for End Systolic Volume.....	148
Figure 5.12 Bland-Altman plot for Stroke Volume .....	149
Figure 5.13 Bland-Altman plot for Ejection Fraction .....	149
Figure 5.14 Bland-Altman plot for SDI-I.....	150
Figure 5.15 Bland-Altman plot for SDI-II.....	150
Figure 5.16 Bland-Altman plot for GLS .....	151
Figure 5.17 Bland-Altman plot for Twist .....	151
Table 5.2 .....	153
Figure 5.18 Bland-Altman plot for SDI-I.....	155
Figure 5.19 Bland-Altman plot for SDI-II.....	155
Figure 5.20 Bland-Altman plot for SDI time to 3D minimum strain.....	156

## Abstract

Over the past 50 years, cardiac pacemakers have been used to treat bradycardia such as complete heart block, with single chamber pacing, then dual chamber pacing with the advantage of atrioventricular synchrony and more recently the development of biventricular pacing for heart failure, severely impaired left ventricular function and left bundle branch block. Throughout this pacemaker therapy has been designed to approach normal physiology. Indeed biventricular pacing is conceived as resynchronisation therapy, and is commonly referred to as such.

Alongside such developments in pacemaker therapy, real-time three-dimensional echocardiography has emerged as a technique to accurately measure left ventricular function and assess dyssynchrony.

This thesis uses this technique in four discrete projects. The first investigated the optimal timing of pacing stimuli compared to impedance and invasive haemodynamics. The second investigated mid-septal as compared to conventional right ventricular pacing. The third investigated the utility of dyssynchrony assessment after biventricular pacing to predict medium term response and the need for optimisation. The final chapter investigated the reliability and reproducibility of novel three-dimensional speckle tracking techniques.

The concordance of impedance, haemodynamic and echocardiographic measurements in selecting the optimum atrioventricular pacing interval was poor. Right ventricular pacing resulted in an acute decrement in left ventricular function, particularly in patients with pre-existing left ventricular dysfunction. In these patients mid-septal pacing caused less of a decline in left ventricular function than apical pacing. The assessment of dyssynchrony after biventricular pacemaker therapy was a powerful predictor of medium term response, as well as identifying a group of patients with a higher probability of acute response to optimisation of timing of pacing stimuli. Novel three-dimensional speckle tracking

methods have good reproducibility for calculation of left ventricular volumes, but not for dyssynchrony measurements. After training and with better quality datasets, reproducibility is improved.

Three-dimensional echocardiography is an attractive technique in the evaluation of patients with pacemakers. Some of the changes induced by altering pacemaker settings are near the limit of resolution of the technique. Speckle tracking is attractive and the improvement in software may improve its reliability and utility.

# Chapter I Introduction

## I.1 Abstract

In recent years biventricular pacing has emerged as a treatment for patients with heart failure, systolic left ventricular dysfunction and left bundle branch block. The mechanism of this treatment is generally accepted to be the amelioration of dyssynchronous cardiac contraction. It has therefore focussed attention to the assessment of cardiac dyssynchrony as well as the effect of right ventricular pacing on dyssynchrony and cardiac function.

Over the same period advances in echocardiography have led to the development of 3-dimensional techniques in the assessment of cardiac function and dyssynchrony. This thesis uses these methods to investigate their use in determining optimal timing of biventricular pacing, to determine the effects of pacing the right ventricle in different sites, the prediction of benefit from optimisation of timing of biventricular pacing as well as evaluating the reproducibility and the determinants of this in novel methods of 3D echocardiographic analysis.

The rest of this introduction will briefly review the history of pacing, define dyssynchrony and describe techniques used in its assessment before covering the effects of left bundle branch block, right ventricular pacing and biventricular pacing on dyssynchrony. Finally I will review the development and evidence base for biventricular pacing and the evidence behind optimisation of timing of pacing. Novel speckle tracking methods will be mentioned and the chapter will close with the open questions that this thesis answers.

## 1.2 History of pacing

In 1889 Andrew McWilliam made the discovery that regular electrical impulses caused cardiac contractions in cats and dogs<sup>1</sup>. Later in the 1920's Dr Mark Lidwell, an Australian anaesthetist attempted to use electrical impulses delivered via a needle electrode to revive stillborn infants. One such infant apparently did not respond to adrenaline therapy but underwent pacing for 10 minutes before regaining spontaneous circulation and surviving<sup>2</sup>. In the 1920's Hyman in New York, created a device to deliver electrical stimuli to the heart, but this did not generate sufficient current to be practicable. In the 1940's Bigelow in Canada was working on the use of hypothermia to reduce metabolism and allow cardiac surgery. Hypothermia of 21 degrees Celsius resulted in asystole but the heart could not be re-started by warming. This led to the development of the first catheter electrode to allow atrial pacing and control of the heart rate in animals<sup>3</sup>. In 1952, Zoll reported his experience with external transcutaneous pacing in 2 patients, one of whom recovered an idioventricular rhythm and survived until discharge<sup>4</sup>. Lillehei in Minnesota started to develop a system to be used during cardiac surgery. Both Zoll and Lillehei's apparatus was dependent on external stimulators and mains electricity. Lillehei collaborated with a medical engineer Earl Bakken to develop the worlds first battery powered pacemaker. This was successfully used in a child for a few days until it was removed after the recovery of spontaneous rhythm. The first person to have a completely internal pacemaker system implanted was Arne Larsson in Sweden. He had complete heart block and his wife persuaded Ake Senning and Rune Elmqvist to create and implant a pacemaker<sup>5</sup>. This device used an epicardial electrode. Although this only lasted 8 hours before it needed replacement, Mr Larsson went on to have a total of 26 pacemakers before dying at the age of 85 due to non-cardiac causes<sup>6</sup>.

Subsequently, Furman reported temporary transvenous pacing of the right ventricle in 2 patients, with the electrode site being either the right ventricular apex or the right ventricular outflow tract<sup>7</sup>.

The first pacemakers simply delivered regular electrical stimuli, to a single cardiac chamber. Improvements have led to the ability to sense intrinsic cardiac electrical activity, and thus inhibit or indeed trigger pacemaker stimulation, activity sensors so that the pacing rate can be altered to meet changing physiological demands, dual chamber pacemakers and biventricular pacemakers{Mohee:uz}.

Developments in battery and lead technology allowed for a system to be placed transvenously, with leads placed in the right ventricle and, with the advent of dual chamber devices a further lead in the right atrium. The right ventricular apex became the default location for transvenous ventricular pacing because lead angulation, trabeculations and gravity meant that this location was the least likely to be complicated by lead displacement<sup>8</sup>.

Ever since the development of the pacemaker, there has been tremendous interest in maximising the benefit and minimising the complications of pacing. One of the major themes is making pacing as physiological as possible. The most obvious example is that of rhythm - the initial single chamber pacemakers meant that the ventricular rate was independent of the sinus rate. Pacemaker syndrome - a constellation of symptoms and signs due to discordant atrioventricular contraction was first described in 1969<sup>9</sup>. Intuitively, dual chamber pacemakers would better approximate sinus rhythm and therefore ameliorate pacemaker syndrome and improve clinical outcomes. However, overt symptoms of pacemaker syndrome are not seen in the majority of patients with single chamber pacemakers. Therefore it was initially unclear if dual chamber pacing would bring benefits to the majority of patients requiring pacemakers. Dual chamber pacing poses an additional cost, the procedure is more complex,

takes longer, has a higher infection rate, prolongs follow up visits and adds the risk of pacemaker mediated tachycardia.

Physiological studies have demonstrated higher left ventricular end-diastolic pressures, higher systolic and mean blood pressure, and lower right atrial and pulmonary capillary wedge pressures, as well as an increase in cardiac output with AV sequential pacing compared to with single chamber ventricular pacing. A number of small crossover trials compared AV sequential pacing modes to fixed-rate ventricular pacing and later against rate-adaptive ventricular pacing. Dual chamber pacing improves effort tolerance compared with fixed-rate ventricular pacing, but not compared to rate-adaptive ventricular pacing indicating that the increase in heart rate with exercise has a greater physiological impact than AV synchrony. Similarly, several crossover studies compared quality of life between dual chamber and ventricular pacing. Although very few of these studies used standardised or validated quality of life assessments, they did demonstrate improvements in quality of life with dual-chamber over ventricular pacing<sup>10</sup>.

Observational studies have also implied that dual-chamber pacing reduces the risk of atrial fibrillation, stroke and death compared with ventricular pacing. Indeed the largest of these studies reported in 1995 on outcomes of over 36,000 patients and suggested a mortality benefit from dual chamber pacing<sup>11</sup>. It was in the context of physiological data, crossover and observational studies that guidelines issued by the British Pacing and Electrophysiology Group, as well as the American Heart Association and American College of Cardiology favoured the implantation of dual chamber pacemakers in patients without chronic atrial fibrillation<sup>12,13</sup>.

However, it was only in 1994 that the first randomised controlled trial demonstrated a demonstrated a reduction in stroke with atrial pacing as

compared to ventricular pacing in sick-sinus syndrome<sup>14</sup> with longer term follow up of the same cohort demonstrating lower mortality in the atrial pacing group<sup>15</sup>. Despite the guidelines in favour of dual chamber pacing, a series of randomised controlled trial comparing single chamber ventricular pacing against dual-chamber pacing were performed - PASE<sup>16</sup>, CTOPP<sup>17,18</sup> MOST<sup>19</sup> and UKPACE<sup>20</sup> - which failed to show a mortality benefit from dual chamber pacing, though in CTOPP and MOST there was a reduction in atrial fibrillation, but not stroke. Nevertheless when patients were able to choose programming a pacemaker to single chamber or dual chamber pacing, they preferred dual chamber pacing<sup>16</sup>.

Simultaneously, work was being performed to investigate if patients with heart failure and without a conventional bradycardia indication for pacing, would benefit from pacemaker therapy. The concept behind this was that in heart failure there is frequently prolongation of the pr interval suggesting imperfect co-ordination of atrial and ventricular contraction that could potentially be ameliorated by pacing. Initial reports suggested remarkable early<sup>21,22</sup> and late<sup>23</sup> benefit. However, data from patients who were being considered for cardiac transplantation and had a permanent pacemaker suggested that their outcomes were significantly worse than matched patients without a pacemaker<sup>24</sup>. The authors suggested that this might be due to inappropriate pacing on under-sensed ventricular ectopics leading to an increased risk of ventricular fibrillation, or due to the effects of pacing induced dyssynchrony.

The DAVID trial was the first large study to demonstrate clinical adverse events associated with RV apical pacing<sup>25</sup>. This trial randomised patients without an indication for pacemaker therapy but undergoing implant of a defibrillator to a strategy of dual chamber rate-responsive pacing at a lower rate of 70 beats per minute or ventricular back up pacing at a rate of 40 beats per minute. They found that the back up pacing mode was associated with a lower rate of mortality and hospitalisation for heart failure.



The MOST trial confirmed the adverse clinical effects of right ventricular apical pacing. This trial randomised 2010 patients with sinus node disease to dual or single chamber rate responsive pacing. Overall, there was no difference in outcomes between the groups<sup>19</sup>, however when the population was studied on the basis of the percentage of ventricular pacing, it became clear that there was a relationship between the frequency of ventricular pacing and the risk of heart failure optimisation<sup>26</sup>. This was different for the two modes. In DDDR mode, there was a linear relationship between a ventricular pacing frequency from 0% to 40% after which the risk reached a plateau; in VVIR mode the linear relationship held from 0% to 80%. Ventricular pacing was also associated with an increased risk of atrial fibrillation.

These data have led to studies to understand the mechanism for these deleterious effects, strategies to minimise right ventricular pacing<sup>27</sup> where possible and to investigate the utility of pacing alternative right ventricular sites. These themes will be explored in greater detail below.

The concept that biventricular stimulation could resynchronise the heart was demonstrated in man by Cazeau and others in 1994<sup>28</sup>. They reported on a single case of a 54 year old man with dilated cardiomyopathy in whom pacing of all 4 cardiac chambers resulted in acute haemodynamic improvement and significant clinical benefit after only 6 weeks of therapy. They hypothesised that the benefit was derived from both ventricular resynchronisation as well as optimising the atrioventricular sequence of contraction on both sides of the heart. Later clinical studies including MUSTIC<sup>29,30</sup>, MIRACLE<sup>31</sup>, PATH-CHF<sup>32</sup>, COMPANION<sup>33</sup>, CARE-HF<sup>34</sup> and MADI-CRT<sup>35</sup> demonstrated significant improvements in morbidity and mortality in patients with heart failure, significantly impaired left ventricular function and left bundle branch block. This therapy has come to be known as cardiac resynchronisation therapy or CRT, and the strong evidence from these randomised controlled trials has led to its adoption in international

guidelines.<sup>36</sup> However, even in these trials it has been noted that up to 30% of patients do not derive symptomatic benefit from CRT.

### **1.3 Definition of dyssynchrony**

Dyssynchrony refers to imperfect timing of the activity of different parts of the heart. It can be thought of as occurring at three levels, atrio-ventricular, inter-ventricular and intra-ventricular<sup>37</sup>. Atrio-ventricular dyssynchrony refers to the lack of co-ordination in timing between atrial contraction and ventricular contraction. At its worst, this can lead to the atrium contracting against a closed mitral valve, which leads to gross elevation of the atrial pressure visible as “cannon waves” in the jugular veins. At a more subtle level, imperfect timing of atrial and ventricular contraction means that work done in atrial contraction is not completely translated into maximal left ventricular filling. Inter-ventricular dyssynchrony describes differences in the timing between right and left ventricular contraction or relaxation. Finally intra-ventricular dyssynchrony refers to differences in segmental timing within the ventricle. Most of the focus for investigation has been on the left ventricle rather than the right ventricle, and a great deal of data has been accumulated in the context of left bundle branch block, heart failure, right ventricular and biventricular pacing. A further distinction can be made between electrical and mechanical dyssynchrony, as these are not necessarily concordant.

### **1.4 Techniques to assess dyssynchrony**

There are a number of techniques that have been used in the assessment of dyssynchrony. They can be divided into indirect methods that measure the functional consequences of dyssynchrony, and those that attempt to characterise myocardial mechanics directly. The latter techniques have generally been applied to intra-ventricular dyssynchrony.

### 1.4.1 Indirect techniques

Clinical examination by an astute observer can reveal cannon waves in the jugular venous pressure as well as variations in the character of the pulse that may occur with the variations in filling seen in atrio-ventricular dyssynchrony, or reverse splitting of the second heart sounds indicating inter-ventricular dyssynchrony. Clinical examination is not sensitive enough to detect intra-ventricular dyssynchrony.

Phono-cardiography is a development of clinical examination which uses microphones to accurately record the heart sounds. This can give information on the timing of heart valve closure and thus inter-ventricular dyssynchrony. Invasive jugular venous and intra-cardiac pressure measurements can be made and parameters obtained including peak pressures, their time as well as the rate of change of pressure. The rate of change of pressure at the beginning of systole has been used as an index of ventricular performance, but this is dependent on the cardiac pre-load. If combined with simultaneous volume measurements, the cardiac workload can be accurately calculated from pressure-volume loops. Pressure gradients can also be estimated non-invasively using Doppler echocardiography, though these measurements are angle dependent. There are also numerous methods to measure cardiac output which is a global measure that is impaired by dyssynchrony. These include invasive dilution cardiac output measurements, arterial pulse pressure contour measurements, the rate of change of left ventricular pressure, as well as non-invasive measurements using thoracic impedance, finger plethysmography as well as Doppler echocardiography.

## 1.4.2 Direct Techniques - electrical

### 1.4.2.1 Electrocardiogram (ECG)

Myocardial contraction is dependent on intracellular calcium flux, which is triggered by rhythmic alterations in the voltage gradient across individual myocardial fibres. The changes in voltage across individual fibres sum to create a wave of electrical activity that is detectable on the surface of the body. Einthoven developed the string galvanometer in the early 20th century which was sensitive enough to detect and record the electrical changes that occur on the body surface with individual heart beats{Barold;2003vy}. Einthoven termed the deflection of the ECG due to atrial depolarisation the p wave and that of ventricular depolarisation the QRS complex. In healthy subjects the QRS complex lasts approximately 80 milliseconds. This rapid depolarisation of the ventricles is dependent upon specialised conduction fibres within the heart which have a distinct anatomical organisation, arising from the atrioventricular node and forming the His bundle, before dividing into a right and left bundles. The left bundle is further subdivided into anterior and posterior fascicles which terminate in sub-endocardial branches. The right bundle directly terminates in sub-endocardial branches.

The relationship of these intervals is one of the earliest measures of dyssynchrony. Prolongation of basic intervals such as that of the between p wave and QRS complex is indicative of atrio-ventricular dyssynchrony. Prolongation of the QRS duration is indicative of inter and intra-ventricular dyssynchrony. The pattern of the QRS complex gives further information than the duration alone - for example right bundle branch block indicating that the right ventricle is being activated later than the left ventricle,.

Infrequently, healthy subjects may have prolongation of the QRS in a pattern that reflects right bundle branch block<sup>38</sup> or rarely left bundle branch block<sup>39</sup>. In patients with heart failure, the presence of bundle branch block

is much higher<sup>40</sup>, as is prolongation of the interval between atrial and ventricular depolarisation<sup>41</sup>. The ECG can therefore give information on electrical dyssynchrony at all levels. However, the relationship between electrical and mechanical dyssynchrony may not be fixed, but rather variable between patients.

The surface ECG has been extended by the ability to make intracardiac recordings. The use of recordings from multiple intracardiac locations allows for accurate mapping of electrical activation patterns, though with anatomical locations determined by fluoroscopy which may be relatively crude. Electro-anatomical and non-contact mapping have been designed to improve this which allow the precise 3-dimensional location of the catheter in relation to a magnetic or electrical field to be determined. These systems can allow the import of previously acquired CT or MRI images of the heart to reduce the need for point-by-point reconstruction of cardiac anatomy.

### **1.4.3 Direct techniques - non-echocardiographic methods**

#### **1.4.3.1 Nuclear imaging**

Single positron emission computed tomography, or SPECT is a 3-dimensional nuclear medicine technique. It requires the injection of a radioactive isotope that emits gamma radiation that is detected by a camera that rotates around the patient. The acquisition of data is temporally gated against the ECG to allow the regional onset of myocardial contraction to be determined<sup>42</sup>. Although the temporal resolution is relatively low at 8 or 16Hz, Fourier transformation of the data allows interpolation with effective frame rates of up to 75 Hertz. This technique has been validated in single studies against 2-D and 3-D tissue Doppler echocardiography, and been used in patients undergoing CRT and found to correlate with response and have good predictive value<sup>43,44</sup>.

#### **1.4.3.2 Cardiac Magnetic Resonance Imaging**

Various cardiac magnetic resonance imaging techniques have also been used, incorporating cine, phase contrast and tagged imaging. MRI has been used to predict the response to cardiac resynchronisation therapy. A detailed review of these techniques is outside the scope of this thesis, but is covered by Pennell<sup>45</sup>. Potential advantages of CMR based techniques include high spatial resolution and the fact that this is a 3-dimensional technique that can tag tissue characteristics to measure local strain. However, the disadvantages include cost, long imaging time, complex and long analysis times and incompatibility with implanted devices. Although recently developed systems are available with MRI compatibility, CMR dyssynchrony has not yet been assessed in cohorts of patients with implanted devices.

#### **1.4.3.3 Cardiac Computed Tomography**

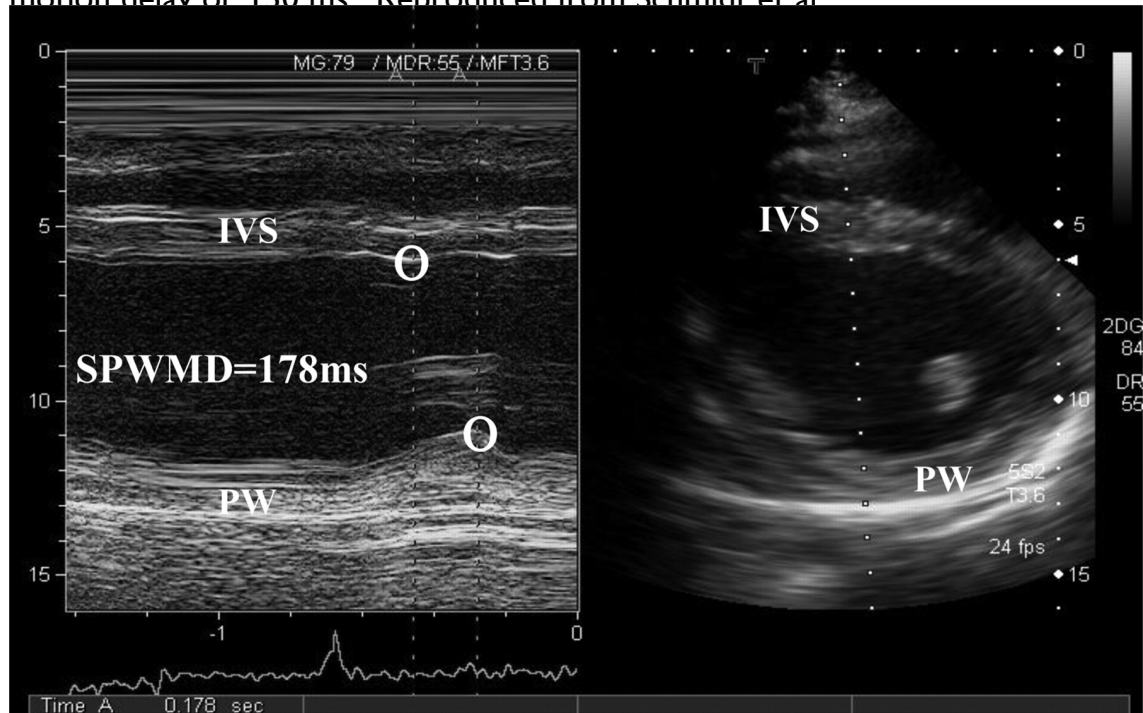
Cardiac CT has been studied in a single study of 38 patients. They examined 3 indices of dyssynchrony - the standard deviation of the time from the R wave to maximal wall thickness, the standard deviation of the time to maximal wall motion and the standard deviation of time to minimal systolic area. They also looked at segmental measures - the average of the maximal difference in time to max wall thickness or motion among 3 pairs of opposing walls. The global indices had a reasonable reproducibility, but their role in the assessment of patients requires further study<sup>46</sup>. However, this technique is limited as it delivers ionising radiation to patients and therefore carries a risk of inducing cancer. This effectively excludes this technique from routine clinical use.

## **1.4.4 Direct techniques - echocardiographic methods**

### **1.4.4.1 Motion-mode**

Echocardiography relies on the rendering of reflected ultrasound waves to produce an image. The simplest technique is that of M-mode or motion mode echocardiography, which uses a single point beam and displays the result against time. When applied to the heart from the para-sternum, this allows the motion of the mitral valve and the inter-ventricular septum and posterior walls to be interrogated. This allows the motion of opposing walls to be compared, and the difference in the time to peak systolic motion of those opposing walls has been used as one of the first methods of quantifying intra-ventricular dyssynchrony. Although it has the benefit of high frame rates and therefore good temporal resolution, it is limited by the fact that the line of ultrasound may not be perpendicular to the radial motion of the ventricle which therefore can give spurious results. This has been improved by technologies which allow simultaneous 2-D imaging to help alignment, as well as angle correction. It is also limited in that this measure only interrogates the inter-ventricular septum and posterior walls.

Figure 1.1 Image demonstrating septal to posterior wall motion delay. It is the interval between maximal posterior and septal displacement of left posterior and septal wall using a mono-dimensional short-axis view at the papillary muscle level. Intraventricular dyssynchrony is defined by a septal-to-posterior wall motion delay of  $\geq 130$  ms. Reproduced from Schmidt et al.<sup>47</sup>



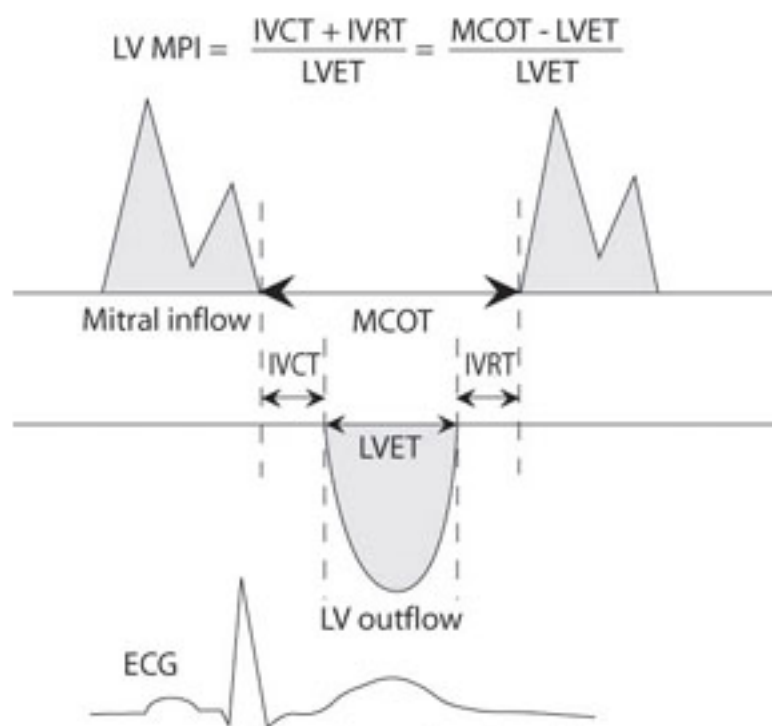
#### 1.4.4.2 Doppler imaging

Doppler imaging relies on the movement of myocardium or blood to alter the frequency of the reflected sound wave. The amount of the the Doppler shift is proportional to the velocity, and therefore this imaging mode allows the quantification of velocity of both blood flow or myocardium. The application of Doppler imaging to myocardial motion is termed tissue Doppler imaging<sup>48</sup>. In both instances, the display can be either colour coded for a relatively large sample area, or concentrated on a small sample area which is graphically displayed against time. Doppler measurements of flow can be used as an estimate of pressure and as a surrogate of cardiac output - both of which can be used as indirect



measures of dyssynchrony. Also, rather than simply quantifying flow, Doppler measurements can be used to compare timing, for example, to calculate the difference in time to onset of right and left ventricular flow as an index of inter-ventricular dyssynchrony. A measurement known as the myocardial performance index, or Tei-index has also been proposed as a global measure of cardiac function which is calculated as the ratio of isovolumic times to ejection time<sup>49</sup>. Furthermore, the onset of left ventricular ejection has also been proposed as a global marker for intra-ventricular dyssynchrony.

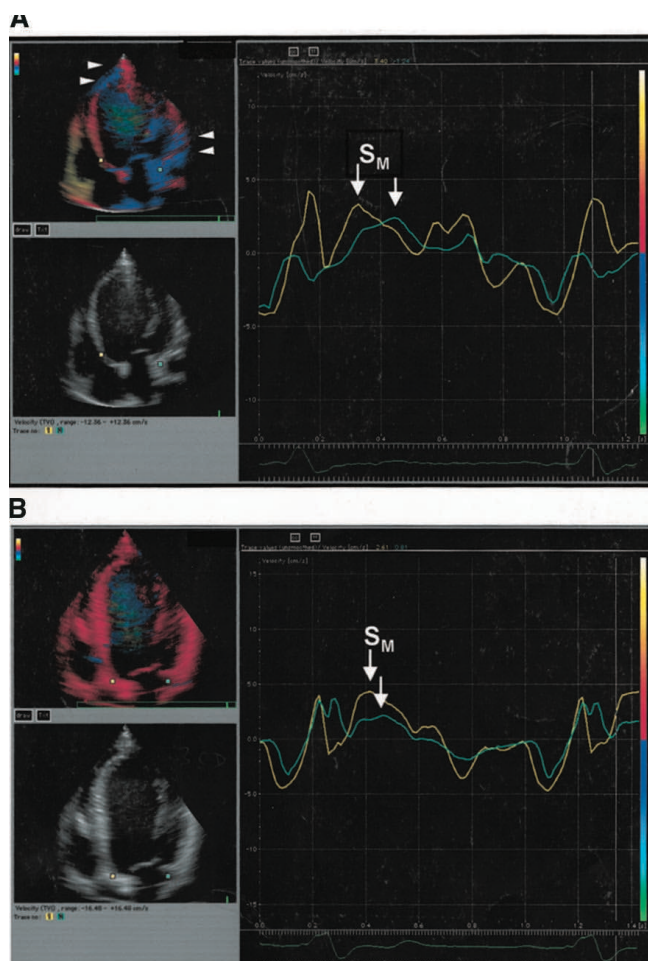
Figure 1.2 Illustration of Myocardial Performance Index, or Tei-index.<sup>50</sup>



Doppler measurements can also be made of the myocardial tissue. The timing of tissue Doppler measurements of myocardial motion can be employed to get a more comprehensive assessment of segmental motion. Differences between 2 segments, or the maximum difference between 3 pairs of opposing segments can be calculated. The standard deviation of the time to peak velocity of the 12 basal and mid segments as interrogated

from the left ventricular apex, also known as the Yu index, is the epitome of this technique.

Figure I.3. Regional myocardial velocity curves obtained by tissue Doppler imaging at the basal septal (yellow) and basal lateral (green) segments. In the color 2D pictures, movement of the myocardium toward the probe (during contraction) is shown in red, whereas movement away from the probe (during relaxation) is shown in blue. Panel A, In a patient with LBBB, there was delay in the onset and peak sustained systolic contraction ( $S_M$ ) in the lateral compared with the septal wall. Regional contraction occurred in a haphazard manner in various segments as illustrated by the patchy areas of blue colors (arrowheads). Panel B, After biventricular pacing, there was dramatic improvement in the synchronicity, as reflected by the overlapping of velocity curves in the basal septal and basal lateral segments and the homogenous red color in the two-dimensional picture.<sup>51</sup>



Doppler measurements of flow and of myocardial velocity also have the advantage of high temporal resolution, but are significantly angle dependent which may impact on their reproducibility.

#### **1.4.4.3 Two and Three dimensional imaging**

Two dimensional imaging requires the ultrasound beam to sweep along a line, whereas 3 dimensional imaging requires the ultrasound beam to move in two orthogonal directions. To allow time for emission and receiving of ultrasound signals as well as motion of the ultrasound beam, the temporal resolution of the resulting images is diminished. The advent of matrix transducers has enabled the use of multiple ultrasound emitters and receivers and thus increased the temporal resolution of these methods, but nevertheless 3-dimensional imaging has a lower temporal resolution than 2-dimensional imaging, which again has a lower temporal resolution than 1-dimensional imaging such as M-mode. Live 3D volumes often have volume rates of 20Hz or so, though parallel processing can allow over 60 volumes per second. In patients who have a heart rate above 60 beats per minute, the number of volumes per heart cycle falls further. Acquiring multiple heart cycles with ECG gating increases the temporal and spatial resolution, but at a cost of stitching artefacts that arise because of variability in heart rate as well as respiratory motion of the heart. Despite the lower temporal resolution, the addition of extra dimensions decreases the need for mental reconstruction of constituent images, and allows the exact relationship of lines or planes through the heart to be determined.

Two dimensional and 3 dimensional imaging can be used to qualitatively describe the motion of the left ventricle. Quantification of intra-ventricular dyssynchrony has focussed on the differences in time to peak displacement or strain. This can be calculated for an absolute difference between two segments, the maximum difference between 3 pairs

of opposing segments, or the standard deviation of a number of segments - 6 basal, 12 mid and basal segments or 16 or 17 segments for the entire left ventricle depending on the segmentation model used.

Whilst measuring the magnitude of displacement is a simple concept, that of strain is more complex. Strain is the quantity that reflects change in length - when applied to echocardiography two points are chosen and the difference in length between those points between diastole and systole is the strain. It has a directional component to it, and in 2-dimensional echocardiography the directions considered are longitudinal, circumferential or rotational and radial. It may be derived from tissue Doppler imaging as the integral of the velocities that Doppler imaging directly measures, or more recently by speckle tracking.

When looking at a rendered echocardiographic image, a pattern of speckles is obvious within the myocardial tissue. These arise due to tissue features smaller than the wavelength of the ultrasound resulting in constructive and destructive interference in the reflected sound waves. The pattern of speckles is therefore characteristic of the myocardial tissue and the pattern can be tracked from frame to frame throughout the cardiac cycle and therefore allow tissue motion to be characterised. This is angle independent and allows the calculation of velocities and strain<sup>52</sup>. The velocity of the myocardium is an obvious target to measure, but strain is a relatively novel concept in echocardiography.

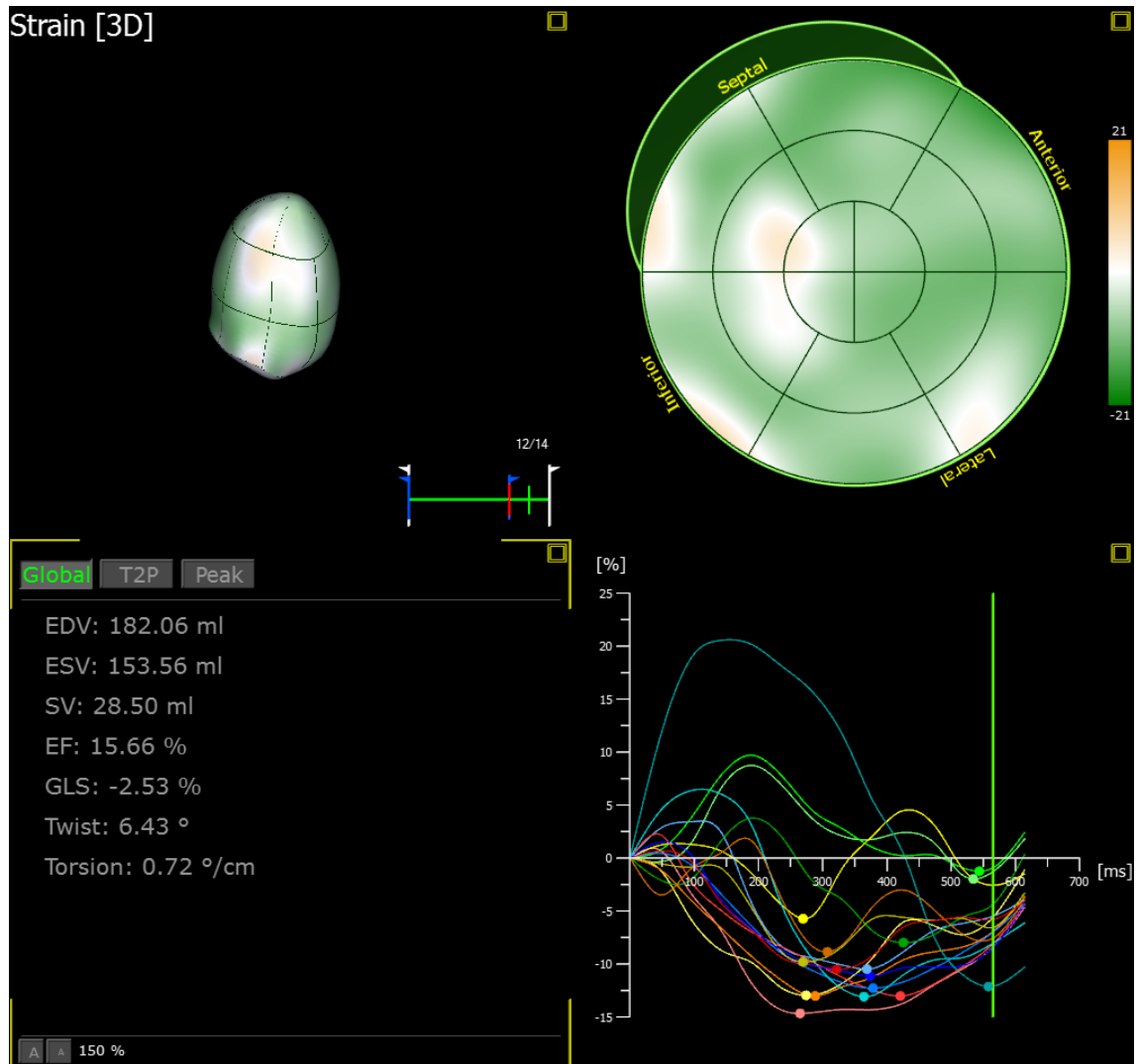
Speckle tracking derived strain is an attractive parameter because it is not angle dependent and measures tissue contraction rather than displacement which may occur passively for example when a scarred non-contractile segment is pulled on by neighbouring contractile segments.

Although modern techniques can assess motion or strain for hundreds or thousands of segments of myocardium, most techniques involve

amalgamating the data from these smaller segments into the 16 or 17 larger segments as used in clinical practice.

Disadvantages of speckle tracking are that it requires a high frame rate and extremely good image quality of the whole myocardium throughout the cardiac cycle. It is a summative approach - i.e. current techniques do not have the resolution to track the individual layers of the myocardium whose fibres are arranged in different directions and would therefore be expected to show different values. Current approaches average values for the whole trans-mural segment. Furthermore, it may be impacted on by the translational motion of speckles in the plane orthogonal to the echo plane.

Figure I.4 Example of 3D speckle tracking derived strain. The segments are demonstrated in the upper left endocardial cast, bulls-eye plot upper right, and individual segments plotted against time on the lower right panel. Numerical results are in the lower left panel.



#### I.4.4.4 Measurement Variability

##### I.4.4.4.1 Doppler and two-dimensional methods

Any method that purports to measure dyssynchrony must be reliable and reproducible. This is particularly important for those techniques that have a significant learning curve. 3D echocardiography requires expertise not only in the acquisition of datasets, but also in their analysis.

The PROSPECT study was a multi-centre study of 498 patients that investigated the utility of M-mode, pulsed Doppler and tissue Doppler derived indices of dyssynchrony as predictors of response to CRT<sup>53</sup>. Response was defined using a clinical composite score as well as a 15% or greater reduction in left ventricular end-systolic volume (LVESV) at 6 months compared to baseline. Each centre underwent training and was required to submit a high-quality study before patient enrolment. The core laboratories had access to a written measurement manual that had been approved by the steering committee. Intra-observer variability was similar in all core laboratories, and was low for left ventricular end systolic volume and left ventricular pre-ejection interval (Coefficient of Variation(CV), 3.8% and 3.7%, respectively). Variability was moderate for the standard deviation of the time to peak systolic velocity of 12 mid and basal myocardial segments (Ts-SD)(CV 11.4%) and the maximum time difference between the peak systolic velocity of the 6 basal segments (Ts-peak) (CV 15.8%). There was high variability for Septal to Posterior Wall Motion Delay (SPWMD) (CV, 24.3%). Inter-observer variability was higher for each parameter than intra-observer variability, with high variability for Ts-peak, Ts-SD, and SPWMD (CV, 31.9%, 33.7%, and 72.1%, respectively). Furthermore, a significant proportion of studies were deemed not to be interpretable, ranging between 61% and 95% for the routine non-TDI methods and between 37% and 82% for TDI-based tests

They concluded that the interpretability and variability of measurements accounted for the lack of sensitivity and specificity of any of these measures in predicting outcome from CRT.

#### **1.4.4.4.2 Three-dimensional methods**

Few studies have looked for intra-patient reproducibility, but one observer studied 15 patients within 24 hours and showed good intra-class correlation coefficients (ICC) and variability for end-diastolic volume (EDV),

left ventricular ejection fraction (LVEF), and SDI-16 were 0.99 and 1%, 0.98 and 3.7%, and 0.88 and 4.6%, respectively<sup>54</sup>. Soliman and others also performed test-retest reproducibility on 10 subjects and showed an ICC of 0.951, and a variability of 10%<sup>55</sup>.

Intra-observer and inter-observer reproducibility has been reported by most groups, with a range of intra-observer correlation coefficients for SDI-16 between 0.86592 to 0.99614, and inter-observer correlation of between 0.8182 and 0.99314. Reproducibility is also better in patients with good quality datasets when compared to moderate quality datasets<sup>55</sup>.

Inter-institutional variability for SDI-16 has also been reported<sup>56</sup>. This group recruited 120 healthy subjects in Switzerland, and their datasets were analysed in both Switzerland and in Minnesota, USA. Although the mean values and 95% confidence intervals of SDI-16 did not overlap, the concordance correlation coefficient and the limits of agreement suggested that there is no significant difference in the measurements between the two institutions.

These publications did not include Bland-Altman plots<sup>57</sup> as a method to assess reproducibility of these measurements. The statistical literature conflicts, with some authors suggesting intraclass correlation is the best measure of reliability<sup>58</sup>, whilst Bland et al suggest this is reasonable for validation studies only<sup>59</sup>.

## **1.5 Assessment of Dyssynchrony**

### **1.5.1 Dyssynchrony in healthy subjects.**

Healthy subjects have been assessed by all the techniques delineated above. The surface ECG demonstrates a p wave indicating atrial activity that lasts 80 to 110 ms. The interval between the p wave and the onset of the QRS complex is termed the pr interval and is normally 120 to 200ms. The QRS complex is generated by ventricular depolarisation and normally



lasts approximately 80ms, though values over 120ms are taken to be abnormal. Studies of 67,375 men in the United States Airforce have been used to generate normal values, and describe the frequency of variants such as right and left bundle branch block<sup>38,39,60</sup>.

None of the other techniques have been used in such large populations, but nevertheless, normal values have been published, frequently in the context of comparison with patients with cardiac disease, and these demonstrate that the normal timing of contraction is exquisitely well coordinated. A detailed review of all of these data is outside the purview of this thesis, but data for three-dimensional echocardiography is presented below.

Normal values for dyssynchrony and ejection fraction by 3D echocardiography have been generated by a number of groups, with varying numbers and ages of patients. The studies have varied as to those that have used normal volunteers, or patients referred for routine echocardiography that were deemed to be normal. Four studies have attempted to define normal ranges in adults by taking large samples of healthy subjects, but most studies have used a small sample as a control group against whom to compare the results from their patients. All the published values are summarised in table 5.2. Only a single study has published data in a paediatric population<sup>61</sup>. They examined 9 healthy children aged between 4.5 and 16 years old as controls to compare against children with LV dysfunction. In the healthy group the median SDI-16Q was 2.1%.

Kapetanakis et al studied 89 healthy adults and suggested that the upper limit of normal SDI-16 was 8.3% because this value was 3 standard deviations above the mean value of 3.5%<sup>54</sup>.

Gimenes et al investigated 131 subjects, 73 were male and the average age was  $46 \pm 14$  years<sup>62</sup>. These subjects did not have any structural cardiac

abnormalities, or history of cardiac disease, but had been referred for routine echocardiography. The mean SDI-16Q was  $1.59 \pm 0.99\%$ . The frequency distribution of SDI-16Q values are appreciably skewed to the left.

Conca et al published results of their investigation of 120 healthy subjects in an attempt to define normal ranges for 3D SDI-16Q, as well as tissue Doppler and radial strain imaging<sup>56</sup>. This study was powered to be able to define 90% confidence intervals around the mean value. Although they investigated 120 healthy subjects, they were only able to perform 3D assessment in 102 patients. They proposed a normal range for SDI-16Q of 1% to 4.8%, based on the 97.5% confidence intervals for their population. Interestingly, they found that there was little concordance between the two centres for tissue Doppler and radial strain imaging, but significant concordance in SDI-16Q.

De Castro et al studied 116 healthy volunteers and 20 elite athletes<sup>63</sup>. They validated their results by performing CMR on 20 of these subjects. In healthy volunteers the mean SDI-16 was  $2.37 \pm 0.8\%$ . They also describe the pattern of contraction seen in these subjects. The apex appears the most synchronous, and contracts earliest, whilst the basal segments are slightly less synchronous and contract later. Thus they describe a contraction time gradient from apex to base.

While the normal ranges for any test should be determined locally, most studies agree that the normal value of SDI-16 is approximately 3%, and that most healthy individuals have values below 6%. There do not appear to be significant differences in the normal range dependent upon the software used to generate SDI-16. There is an overlap between this normal range and the values seen in mild left ventricular dysfunction. However, values in the context of cardiac disease are discussed below.

## **1.5.2 Dyssynchrony due to right ventricular pacing.**

Dyssynchrony due to right ventricular pacing has been investigated for nearly as long as pacing therapy has existed. As pacing developed in the 1960's there was interest in the effects of pacing at different ventricular sites, but these early studies did not demonstrate significant differences at different sites and the right ventricular apex came to be the preferred site for ventricular pacing. In the 1980's interest in atrio-ventricular synchrony was generated by the advent of pacemakers that were capable of tracking atrial activity and thereby eliminate atrio-ventricular dissociation. From the 1990's onwards, attention was again focussed on intra-ventricular dyssynchrony as randomised controlled trials failed to demonstrate the expected benefits from dual chamber pacing and as bi-ventricular pacing was developed. These studies will be further explored below.

### **1.5.2.1 Atrioventricular dyssynchrony**

Complete atrioventricular dyssynchrony exists in complete heart block and this remains a feature in single chamber ventricular pacing. This can cause overt symptoms, which were first described in 1969 as pacemaker syndrome<sup>9</sup>. The ability to artificially synchronise atrial and ventricular pacing with a dual chamber pacemaker system allowed the investigation of the relative contribution of atrial contraction to cardiac output. Samet and others demonstrated that the atrial contribution to filling was greater than the effect of abnormal depolarisation caused by ventricular pacing, and indeed atrial sequential ventricular pacing did have a small detrimental effect on haemodynamics compared to intrinsic rhythm, but they suggested this might be explained by the shorter pr interval required to obviate intrinsic conduction<sup>64,65</sup>. A clinical correlate to this was a case report by Haas and others that described a severe case of pacemaker syndrome with falls in cardiac output seen with VVI pacing<sup>66</sup>. Comparison with single chamber pacing has demonstrated higher left ventricular end-diastolic

pressures, higher systolic and mean blood pressure, and lower right atrial and pulmonary capillary wedge pressures, as well as an increase in cardiac output with AV sequential pacing<sup>10</sup>.

#### **1.5.2.2 Intra-ventricular dyssynchrony, and the effect of pacing at different right ventricular sites.**

The first report of endocardial pacing by Furman and others included pacing at both the right ventricular apex and the right ventricular outflow tract<sup>7</sup>. In the subsequent decade there was a great deal of interest in determining the best place to pace the heart. Most studies were done in dogs, with conflicting results. Barold and others investigated 52 patients and paced both the RV inflow and outflow tract<sup>67</sup>. The inflow tract was defined as being just lateral to the spine, so therefore is similar to the position that would be termed the apex today. They found no significant differences in mean pulmonary or systemic pressures or in cardiac index when pacing at these locations.

One of the first studies using echocardiography to evaluate the effects of pacing at different RV sites was reported in 1974<sup>68</sup>. Abassi and others used M-mode echocardiography in patients with left bundle branch block as well as patients during right ventricular apical pacing. They found in left bundle branch block there was an early pre-ejection posterior motion of the inter-ventricular septum, together with paradoxical anterior motion during systole. During pacing, 7 of 10 patients exhibited a similar pattern of motion as those with left bundle branch block, 3 had apparently normal septal motion. These findings were expanded upon by Gomes and others who investigated patients with right ventricular pacing at the apex, outflow tract and inflow tract<sup>69</sup>. They selected patients because they had normal motion of the inter-ventricular septum in intrinsic rhythm. Pacing the inter-ventricular septum resulted in a biphasic motion with pre-ejection posterior motion of the IVS and then either anterior or posterior motion during the

ejection period. They found that pacing at inflow and outflow tracts resulted in abnormal motion in all patients, but during apical pacing there were a minority of patients that had normal septal motion. Furthermore they noted a delay between the septal motion and the posterior motion. Interestingly, in all locations, pacing resulted in a fall in end-diastolic dimensions, but not end-systolic dimensions, and this effect was seen with pacing in all sites.

Over the intervening 30 years these findings have been built on as newer echocardiography techniques have been developed. Xiao and others investigated 24 patients with RV apical pacing and 24 with left bundle branch block, with M-mode and Doppler echocardiography<sup>70</sup>. As in previous studies, they noted pre-ejection systolic motion of the inter-ventricular septum more frequently in left bundle branch block than during RV apical pacing. They also found that the isovolumic times were longer in LBBB than during RV pacing. They concluded that RV apical pacing was not a good experimental model for left bundle branch bloc.

Other modalities have been used to quantify the effects of pacing on left ventricular function. Leclercq and others performed haemodynamic and radionuclide studies on patients with normal intrinsic conduction and tested various pacing modes, including AAI, DDD and VVI<sup>71</sup>. They demonstrated that AAI pacing was better than the other 2 modalities in terms of cardiac output, pulmonary capillary wedge pressure, right atrial pressure, pulmonary artery pressure, LV stroke work index and LV ejection fraction. The differences were mainly due to the negative effects of right ventricular pacing on septal ejection fraction and on LV filling.

Schwaab and others also used this methodology to compare pacing the RV apex with pacing the RV septum<sup>72</sup>. They optimised the septal position of the electrode by assessing which position gave the narrowest paced QRS complex duration on the surface ECG. They also optimised the AV delay

for both positions. Again, by using radionuclide ventriculography they demonstrated that the decreased QRS duration associated with septal pacing correlates both with more synchronous left ventricular contraction and better systolic function.

Victor and others performed one of the first clinical trials of septal pacing<sup>73</sup>. In an elegantly designed clinical study they placed dual chamber pacemakers in 16 patients with atrial fibrillation who had undergone AV node ablation to induce complete heart block. Rather than using the atrial channel of the pacemaker for an atrial lead, they placed both leads in the right ventricle, one in the apex and the other in the right ventricular outflow tract. The patients were enrolled in a randomised cross-over protocol with pacing at the RVOT or apex for 3 months at a time. At the end of each period, they assessed NYHA class, left ventricular ejection fraction using radionuclide angiography, exercise time and maximal oxygen uptake. They did not demonstrate significant differences in any of these parameters, nor did they see any differences when the patients were stratified into 2 subgroups using a cut-off of a baseline ejection fraction of 40%. A similar study by Mera and others placed the leads in the RV apex or septum<sup>74</sup>. They found that septal pacing produced a shorter QRS duration and although it didn't lead to significant differences in LV dimensions as assessed by M-mode echocardiography, it did lead to a high fractional shortening, and a higher ejection fraction at rest measured by radionuclide angiography.

An invasive haemodynamic study by Kolettis and others showed no differences in systolic function between apical and RVOT pacing, but better indices of diastolic function with RVOT pacing<sup>75</sup>.

Deshmukh et al investigated His-bundle pacing after AV node ablation for permanent atrial fibrillation and dilated cardiomyopathy<sup>76</sup>. This population had a low mean ejection fraction at baseline of 20%. His-

bundle pacing was feasible in only 14 out of 18 patients, correct location of the pacing lead was challenging, and the mean threshold was relatively high at 2.4V at a 0.5ms pulse width. Nevertheless, echocardiographic improvement in heart function was demonstrated by a fall in left ventricular dimensions and an increase in fractional shortening at long term follow up. In contrast, Szili-Torok and others found that apical pacing in a similar cohort of patients with slightly better baseline ejection fraction (mean 47.5%) did not lead to any change in ventricular dimensions, but there was a significant fall in left ventricular ejection fraction to 43.2% at 3 months<sup>77</sup>.

Tantengco evaluated young patients with mostly congenital or acquired complete AV block, normal left ventricular morphology and function and no intracardiac shunts. After an average of 9.5 years of RV apical pacing, these patients had impaired 2D and Doppler echocardiographic measures of LV function when compared to normal controls<sup>78</sup>.

Tse and others provided evidence that longer-term remodelling resulted in adverse effects with RV apical pacing. They randomised 30 patients with complete heart block to apical or RVOT locations. The mean ejection fraction was 59% at baseline echocardiography. At 6 and 18 months the patients underwent dipyridamole stress thallium myocardial scintigraphy scans. RV apical pacing resulted in a broader QRS duration of 151ms vs 134 ms, and at 6 months there was a trend to increased myocardial perfusion defects and regional wall motion abnormalities but similar ejection fraction with apical pacing. By 18 months, the trend had become statistically significant and furthermore there was a significant fall in LV ejection fraction with pacing (47% vs 56%).

Nielsen and others investigated 177 patients with AAIR and DDDR pacing and followed them for a mean of 2.9 years<sup>79</sup>. Interestingly, they found that good echocardiographic follow up was challenging, with good quality paired apical 2 and 4 chamber views available in only 50 to 60% of

patients. Nevertheless, DDDR pacing led to an increase in left atrial dimensions whilst AAI pacing did not. Confirming the MOST findings, in those patients with a high proportion of right ventricular pacing there was a reduction in left ventricular ejection fraction.

The ROVA trial was a crossover trial of RVOT versus RV apical pacing in patients with heart failure, permanent atrial fibrillation and standard bradycardia indications for permanent pacemaker therapy<sup>80</sup>. They found that RVOT pacing shorten the QRS duration but after 3 months did not improve quality of life score, and indeed LVEF as assessed by 2D echocardiography was higher in the group assigned to apical pacing rather than RVOT pacing.

Nahlawi and others demonstrated using serial gated blood pool studies, that RV apical pacing results in deleterious effects on ejection fraction that persisted for at least 24 hours<sup>81</sup>.

Thambo and others show that dyssynchrony as measured by tissue Doppler calculation of delay longitudinal contraction is higher in patients who've been paced for a mean of 10 years for congenital complete heart block than in normal controls. Also, LV end diastolic dimension was higher and they had a lower cardiac output and exercise performance<sup>82</sup>.

A single study has used 3D echocardiography to evaluate dyssynchrony in 35 patients with sick sinus syndrome who had had dual chamber pacemakers implanted in the last 3 to 128 months<sup>83</sup>. They performed echocardiography when pacing the atrium, with intrinsic conduction, and when dual chamber pacing. With intrinsic conduction, the mean QRS duration was  $90\text{ms} \pm 14\text{ms}$ , not significantly different from control patients. The ventricular lead was in the RV apex. They measured myocardial performance index, tissue Doppler imaging of 12 segments, and 3D echocardiography SDI-17.



The myocardial performance index was significantly worse with apical pacing (with pacing  $0.42 \pm 0.18$  vs. without pacing  $0.31 \pm 0.14$ ;  $p = 0.004$ ), and LVEF derived by 3D echocardiography was significantly lower with apical pacing (with pacing  $54.4\% \pm 7.7\%$  vs. without pacing  $56.7 \pm 7.9\%$ ;  $p = 0.013$ ), indicating a deterioration of left ventricular function with apical pacing. The mean change in LVEF with apical pacing in an individual patient was 4.1%. There was also more dyssynchrony associated with apical pacing (SDI-17 with pacing  $7.00\% \pm 2.54\%$  vs. without pacing  $5.36\% \pm 2.17\%$ ;  $p = 0.0003$ ). Thus, RVA pacing induced 30.6% change in SDI-17 from baseline without RVA pacing.

However, the total pacing burden, or pacemaker programming of these patients is unknown, so it is unclear if there had been any chronic pacing induced change in left ventricular mechanics after implantation but before echocardiographic examination.

In summary therefore, these studies have demonstrated the deleterious effects of right ventricular apical pacing on global parameters of cardiac function and have suggested that this occurs due to increased intraventricular dyssynchrony. There is less data in the pacing of alternative right ventricular sites and these alternative sites include the His bundle, right ventricular outflow tract and right ventricular septum. These data are suggestive that alternative sites offer better ventricular function than right ventricular apical pacing, but there is conflicting evidence and insufficient data overall to draw a firm conclusion.

### **1.5.3 Dyssynchrony in left bundle branch block**

The investigation of left bundle branch block is potentially confounded by the fact that it is a very rare finding in patients without structural heart disease. Therefore most studies have necessarily involved patients with concomitant heart disease, though these have usually been compared to patients with heart failure and a normal QRS complex as well as normal

patients. Initially the focus was on the characteristics of left bundle branch block, but as CRT developed as a treatment, a great deal of interest was focussed on the assessment of dyssynchrony and the role that this could play in patient selection.

#### **1.5.3.1 Electrical mapping of left bundle branch block**

In 1984, endocardial electrical mapping of patients with left bundle branch block was reported<sup>84</sup> in 18 patients, 3 of whom had no other evidence of cardiac disease and were not on anti-arrhythmic medication. The other 15 were a heterogeneous group comprising patients with ischaemic heart disease, valvular disease or cardiomyopathies. The study was performed by placing intra-cardiac catheter electrodes and recording electrograms at multiple different points. This study demonstrated that left bundle branch block led to delayed activation of the left ventricle compared to the right ventricle, that the left ventricle was activated by right to left transeptal activation, and that the left ventricular endocardial activation sequence is heterogeneous amongst patients with different pathologies as the aetiology of left bundle branch block. Indeed later work with 3 dimensional electrical endocardial mapping has demonstrated that septal activation may also occur due to delayed conduction through the left bundle, rather than right to left trans-septal activation<sup>85</sup>. Right ventricular pacing has also been investigated using this technique which has demonstrated similar prolongation of timing of left ventricular activation as in left bundle branch block, but that the pattern of activation was markedly influenced by the site of previous myocardial infarction<sup>86</sup>.

### **1.5.3.2 Echocardiographic assessment of left bundle branch block and its utility in CRT**

#### **1.5.3.2.1 M-mode and 2D echocardiographic assessment**

Visual interpretation of 2D loops is perhaps the simplest method, and the abnormalities seen in left bundle branch block include multi-phasic motion of the inter-ventricular septum, rocking of the left ventricular apex and delay of the posterolateral wall. Unfortunately, these changes can be subtle<sup>87</sup> and the diagnostic specificity for dyssynchrony on one study was only moderate when compared with tissue Doppler imaging<sup>88</sup>.

#### **1.5.3.2.2 Doppler assessment**

Tissue Doppler imaging is attractive because of the very high temporal resolution. A number of parameters have been developed, from calculating the delay between the septum and the lateral wall in the 4 chamber apical view to more comprehensive assessments looking at the mid and basal segments of each wall in the 2, 3 and 4 chamber views. The standard deviation of the time to peak velocity in these 12 segments has become known as the Yu index<sup>89</sup>. These tissue Doppler assessments are highly angle dependent and whilst these indices have shown promise in single centre studies, Prospect, a multi-centre prospective trial looking at echo parameters as predictors of outcome from CRT failed to demonstrate good predictive ability. This was ascribed to relatively low yield and high variability in the tissue Doppler measures<sup>53</sup>.

The interest in Doppler assessments of dyssynchrony led to the investigation of patients with heart failure and without left bundle branch block. In a number of trials it has been demonstrated that QRS duration correlates poorly with dyssynchrony<sup>90,91</sup>, that dyssynchrony exists in patients with a normal QRS duration<sup>92</sup> and single and dual centre studies suggested benefit from CRT in patients without a prolonged QRS duration

but with Doppler evidence of dyssynchrony<sup>93,94</sup>. However, a multi-centre prospective study has failed to show beneficial effects of CRT on this population<sup>95</sup>, with other multi-centre trials in progress. How are these conflicting findings explained? Firstly, in studies looking at the correlation between QRS duration and dyssynchrony, the pattern of the QRS complex was not considered. It is likely that right and left bundle branch block or non-specific intraventricular conduction delay have differential effects on mechanical dyssynchrony. Furthermore, the variability in tissue Doppler measures may mean that in expert hands and single centre studies it is useful, but this doesn't translate into wider applicability. Finally, there is some evidence that the effect of CRT is not wholly mediated by dyssynchrony, but rather the amelioration of pericardial constraint on the left ventricle. Two studies from the same group have demonstrated acute haemodynamic benefits from CRT in patients with narrow QRS and no dyssynchrony on echocardiography,<sup>96</sup> and in patients with narrow QRS with no selection by echocardiography, longer term improvements in 6 minute hall walk distance, quality of life scores and New York Heart Association class.

#### **1.5.3.2.3 Speckle tracking**

Speckle tracking has also been used to assess dyssynchrony. Suffoletto and others demonstrated that this had good sensitivity and specificity to predict long term left ventricular remodelling after CRT<sup>97</sup>. They measured the time difference in peak septal wall to posterior wall radial strain on the basis that the computer algorithm appeared to track more reliably images from the parasternal short axis than apical acquisitions and the recognised effects of bundle branch block on septal motion. Interestingly, they did not find any significant differences in the measurements made using speckle tracking and using tissue Doppler to calculate radial strain. This group has subsequently prospectively demonstrated the value of speckle tracking dyssynchrony assessment in assessing CRT response, particularly with

regard to patients without broad left bundle branch block<sup>98</sup>. Other authors have confirmed this finding<sup>99</sup>, but have also demonstrated that other strain derived parameters such as longitudinal and circumferential strain appear to be less powerful as a predictor of response to CRT<sup>99-101</sup>. Further parameters have been investigated which include the standard deviation of the time to peak radial strain of the 6 segments in the mid ventricular short axis view, the standard deviation of time to peak longitudinal strain of the 12 basal and mid segments from the apical view, the strain delay index which was defined as the sum for 16 segments of the difference between longitudinal peak and end-systolic strain. Yet others have looked at LV twist and torsion at aortic valve closure, global longitudinal strain and holo-systolic shortening.

#### **1.5.3.2.4 3D echocardiography**

The studies in this area have focused on several heterogeneous groups of patients. These include patients with any form of cardiovascular disease, patients with heart failure and impaired ejection fraction, patients with left bundle branch block (LBBB) with and without symptoms, and patients who are candidates for cardiac resynchronisation therapy (CRT). The goal has been to describe the distribution of dyssynchrony in disease, as well as to see if 3D measures of dyssynchrony can help to better select patients who might benefit from CRT than the QRS duration alone.

Most groups that have looked at patients with cardiovascular disease and a range of cardiac function have demonstrated a strong negative correlation between ejection fraction and SDI-16<sup>54,102-104</sup>. This is illustrated in figure 5.10.

However, this correlation may be weaker in patients with drug-refractory symptomatic heart failure. In 40 patients referred to a heart failure clinic there was no significant difference in SDI-16 between patients with an EF < 30% ( $6.9 \pm 3\%$ ) as compared to patients with an EF > 30%

$(8.8 \pm 6.3\%)^{105}$ . The QRS width may be a confounding factor in this study as this cohort contained patients with both narrow and broad QRS and the distribution of broad QRS is unclear between the two groups with EF >30% and EF <30%.

It is difficult to separate dyssynchrony induced by LBBB alone with that seen in impaired left ventricular function, especially as LBBB is rare in healthy individuals. One group addressed this question by analysing the difference in dyssynchrony indices between healthy subjects, asymptomatic subjects with LBBB, and patients with heart failure and LBBB<sup>106</sup>. In the healthy subjects, mean LVEF was  $54 \pm 5\%$  and SDI-16 was  $5.6 \pm 3.6\%$ , in patients with asymptomatic LBBB the LVEF was  $50 \pm 9\%$ , and SDI-16  $7.3 \pm 3.2\%$  and in heart failure patients with LBBB the LVEF was  $29 \pm 9\%$  and SDI-16  $12.8 \pm 4.8\%$ . SDI-16 was significantly higher in HF patients than both other groups, but although the mean SDI-16 in subjects with asymptomatic LBBB was higher than healthy subjects, this difference did not reach statistical significance ( $p=0.08$ ). Also the mean QRS duration in the asymptomatic LBBB group was less than that of patients with HF and LBBB, this also did not quite reach statistical significance ( $p=0.052$ ). This suggests there may be a correlation between QRS width and SDI-16.

However, another study found this correlation between QRS width and SDI-16 in patients with heart failure to be weak. Soliman and others studied 84 patients with heart failure and either a narrow (mean QRS  $98 \pm 12$ ms, 30 patients) or wide QRS (mean QRS  $157 \pm 26$ ms, 54 patients) <sup>55</sup>. The SDI-16Q was significantly larger in the wide QRS group ( $15.0 \pm 7.9\%$ ) than in the narrow QRS group ( $10.5 \pm 7.7\%$ ,  $p < 0.01$ ). The correlation between the QRS duration and the SDI-16 was weak ( $r^2 = 0.07$ ,  $p < 0.05$ ), as was the correlation between the SDI-16 and the LVEF ( $r^2 = 0.12$ ,  $p < 0.01$ ). Out of this cohort 20% of the patients with HF with LVEF less than 35% had a narrow QRS and high SDI-16, and 14% of the patients with HF with LVEF greater than 35% had narrow QRS and high SDI-16. This is illustrated in figure 5.11.

#### *1.5.3.2.4.1 Patterns of dyssynchrony*

3D echocardiography has revealed some insights into the pattern of dyssynchrony in patients with left ventricular dysfunction. A comparative study of tissue Doppler and 3D dyssynchrony found that 3D echo was less sensitive than tissue Doppler at detecting significant dyssynchrony, and that the areas of maximum delay varied by tissue Doppler and 3D echo<sup>103</sup>. By 3D echo, the anteroseptal and septal walls were more frequently the most delayed, whilst by tissue Doppler it was the lateral and posterior walls. This is illustrated in figure 5.7, in which the lower left panel shows contraction front mapping and the septal wall to be red indicating delayed contraction. This variation occurred even in patients deemed to have good images. When 3D echo and TDI assessment of maximal delay was compared to delay by anatomical M-mode, the correlation was higher with 3D than TDI. In this population of patients, the average ejection fraction was 37% by 2D echo and average SDI-12 was 8.3%.

Furthermore, De Castro and others studied 39 patients with left ventricular dysfunction and narrow QRS (24 ischaemic heart disease, 15 DCM), and 90 patients with left ventricular dysfunction and LBBB<sup>63</sup>. They found that patients with left ventricular dysfunction had more dyssynchrony than normal and that patients with LBBB were more dyssynchronous than those with narrow QRS. The pattern of contraction also differed between the groups, with a time gradient from apical to basal contraction in patients with narrow QRS, but not in patients with LBBB in whom the mid segment often contracted before the apical segments. This emphasises the importance of assessing apical contraction and dyssynchrony, as many methods such as tissue Doppler imaging do not interrogate the apex. It is also important to realise that some 3D analysis software excludes the apical cap in their 16-segment model, though it still appears to have useful predictive value.

#### *1.5.3.2.4.2 SDI as a predictor of outcome of Cardiac Resynchronisation Therapy.*

CRT is a useful therapy in some patients with heart failure but it is acknowledged that up to a third of patients who meet current criteria for CRT implantation do not improve symptomatically<sup>107</sup>. A variety of techniques have been assessed to see if they can better predict outcome than current conventional criteria<sup>53</sup>. Several small studies with 3D echocardiography have shown that patients with high SDI-16 values do better with CRT than their counterparts with lower SDI-16. These studies have mainly used echocardiographic improvements in LV function as their endpoints.

Kapetanakis and others studied 26 patients who fulfilled standard criteria for cardiac resynchronisation therapy<sup>54</sup>. These patients had 3D echocardiography performed before and 10 months after CRT implantation. Clinical responders differed significantly in SDI-16 but not LVEF before implantation, with higher SDI-16 ( $16.6 \pm 1.1\%$  versus  $7.1 \pm 2\%$ ;  $p=0.0005$ )



but similar LVEF ( $18.6 \pm 2.8\%$  versus  $23.9 \pm 2.4\%$ ;  $p=0.4$ ) and NYHA class ( $3.4 \pm 1.8$  versus  $3.0 \pm 1.7$ ;  $p=0.09$ ).

Delgado and others studied 27 patients with DCM scheduled for CRT and performed echocardiography before, 24-48 hours after, and at 6 months<sup>108</sup>. Twenty-two patients had datasets that were adequate for analysis, and 11 patients were followed up at 6 months. The most delayed segment was the basal and mid inferoposterior segments. Pre CRT EF was  $26\% \pm 8\%$ , SDI-16 was  $14.3\% \pm 7.5\%$ , immediately post CRT EF was  $32\% \pm 7\%$ , SDI-16 was  $9.7 \pm 6.8\%$ , at 6 months EF  $39\% \pm 14\%$ , SDI-16  $4.9\% \pm 3.1\%$ . These improvements were statistically significant. They found that responders (as defined by a  $>10\%$  decrease in end-systolic volume) to CRT had a higher initial SDI-16 than non-responders but in their small cohort this was not statistically significant.

Marsan and others investigated 60 patients meeting standard criteria for CRT<sup>109</sup>. They performed 3D echocardiography before and within 48 hours of CRT and calculated the SDI-16. They excluded dyskinetic segments from their analysis. All patients were in sinus rhythm and most patients were in NYHA class III; 62% of patients had ischaemic cardiomyopathy. 3D echocardiography revealed severe LV dilation (mean LVEDV  $201 \pm 48$  mL), with depressed LV function (mean LVEF  $28 \pm 6\%$ ). The SDI-16 was significantly higher in responders, as compared with non-responders ( $9.7 \pm 4.1\%$  vs.  $3.4 \pm 1.8\%$ ,  $p < 0.0001$ ). Moreover, responders demonstrated a significant reduction in SDI-16 immediately after CRT (from  $9.7 \pm 4.1\%$  to  $3.6 \pm 1.8\%$ ,  $p < 0.0001$ ), whereas in non-responders SDI-16 remained unchanged (from  $3.4 \pm 1.8\%$  to  $3.1 \pm 1.1\%$ ,  $p=NS$ ). In addition, the posterolateral region (where the LV pacing lead is positioned) was latest activated in 74% of responders, as compared with 33% of non-responders ( $p = NS$ ). They performed receiver-operator characteristic to define a cut-off value of 5.6% for SDI-16Q, which had a sensitivity of 88% with a

specificity of 86% to predict an acute reduction >15% of LVESV (area under the curve = 0.96, 95% CI = 0.9–1.0,  $p < 0.0001$ ).

Van Dijk and others performed an acute study involving 17 patients who had severely impaired left ventricular function and NYHA class III or IV heart failure, but did not necessarily have a prolonged QRS duration<sup>110</sup>. They investigated the utility of baseline SDI-17 to predict change in LV dp/dt due to biventricular pacing. They measured LV dp/dt invasively during intrinsic rhythm, and after sequentially pacing the RA appendage, posterolateral branch of the coronary sinus and RV apex at a fixed AV delay of 100ms to ensure no intrinsic conduction. The mean SDI-17 was  $10.8 \pm 4.5\%$ . They found that SDI-17 correlated better with change in LV dp/dt than QRS duration.

Soliman and others studied 39 patients (age  $61 \pm 12$  years, 72% were male) with heart failure with LVEF <35%, QRS duration >120ms and on optimal medical therapy who underwent CRT<sup>55</sup>. At 12 months after CRT, 27 patients (69%) had more than 15% reduction in LVESV. These 27 volumetric responders had similar baseline characteristics except for a higher SDI-16 compared with non-responders ( $16.3\% \pm 3.3\%$  vs.  $8.8\% \pm 2.9\%$ ,  $p < 0.001$ ). The SDI-16 was significantly improved in CRT responders, reaching almost normal values ( $7.7\% \pm 2.4\%$ ,  $p < 0.001$ ). Conversely, the SDI-16 worsened in non-responders ( $8.8\% \pm 2.9\%$  to  $11.7\% \pm 3.8\%$ ,  $p < 0.01$ ). On the receiver operating characteristic curve, a value of SDI-16 greater than 10% best predicted reverse LV remodelling after 12 months of CRT with a sensitivity of 93%, a specificity of 91%, and an area under the curve of 0.91.

The same group confirmed these findings in a similar cohort of 90 patients undergoing CRT<sup>111</sup>. After 12 months of CRT, 68 patients (76%) were responders. Responders had larger differences in LVEDV ( $-21 \pm 7\%$  vs.  $-11 \pm 18\%$ ,  $p < 0.003$ ) LVESV ( $-33 \pm 8\%$  vs.  $-12 \pm 25\%$ ,  $p < 0.001$ ), LVEF

( $43 \pm 13\%$  vs.  $5 \pm 9\%$ ,  $p < 0.001$ ), and 6-minute walking distance ( $40 \pm 31\%$  vs.  $4 \pm 22\%$ ,  $p < 0.001$ ) compared with non-responders. An SDI-16Q  $> 10\%$  predicted CRT response with good sensitivity (96%) and specificity (88%).

More recently Kapetanakis and others reported data on 187 patients from two centres who underwent CRT<sup>112</sup>. They found excellent inter-institutional agreement in 3D assessment of left ventricular end-diastolic, end-systolic volumes, ejection fraction and SDI-16, with a variability of 2.9%, 1%, 7.1%, and 7.6%, respectively. SDI-16 had better predictive ability than QRS duration for symptomatic and echocardiographic outcome measures, and they suggested that a SDI-16 cutoff of 10.4% had the highest accuracy in predicting improvement following CRT.

These findings together suggest that SDI-16 may be a useful predictor of symptomatic benefit from CRT, that SDI-16 is a better predictor than QRS duration in determining acute response to CRT and long-term clinical outcomes. The cut-off value has varied between studies, and between software used to determine CRT, but further studies are warranted to confirm these findings in larger cohorts.

#### *1.5.3.2.4.3 3D assessment of dyssynchrony after CRT*

Porciani et al investigated 20 patients with CRT<sup>113</sup>. These patients had been implanted with an St Jude CRT device that was capable of optimising the delivery of CRT using an algorithm based upon intracardiac electrogram recordings. The patients underwent 3D echocardiography before and after optimisation, using this method to assess dyssynchrony at a mean interval of 9 months after device implantation. After optimisation, SDI-16 and SDI-12 significantly decreased from  $8.1 \pm 4.9\%$  to  $4.2 \pm 4.0\%$  ( $p < 0.001$ ) and from  $6.0 \pm 5.7\%$  to  $3.0 \pm 3.7\%$  ( $p = 0.01$ ) respectively, while SDI-6 did not show significant change. This improvement in LV synchrony was associated with improved LV systolic function as indicated by the

significant change in stroke volume from  $56 \pm 16$  mL to  $64 \pm 18$  mL ( $p=0.01$ ), and EF from  $29.3 \pm 11.1\%$  to  $32.3 \pm 10.9\%$  ( $p<0.001$ ). EF improved in all but two patients; the mean increase was 3.0% from 29.3% to 32.3%. Stroke volume improved in all but 2 patients; the mean increase was 8 mL. Somewhat surprisingly, given the improvements in stroke volume and EF, there were no significant changes in EDV or ESV.

Another factor in the delivery of CRT lies in the interplay between the latest contracting segment and left ventricular lead position. 3D echocardiography can demonstrate which segment contracts latest. It is not yet clear if this is useful information, but a study by Becker et al suggests that when the LV pacing site is close to the latest contracting segment, then a patient is more likely to benefit from CRT<sup>101</sup>. They demonstrated this by investigating 58 patients undergoing CRT and performed baseline echocardiography, and repeated echocardiography within a week and at 12 months after CRT. They determined the latest segment to reach minimum systolic volume (segment A), and they also determined the segment with the largest temporal difference between pre and postoperative minimum systolic volume (segment B). They suggest that segment B was where the LV lead tip was placed, and this did correlate well with lead position as determined by fluoroscopy. In those patients in whom segment B and segment A were the same or in close proximity (optimal patients), the outcome from CRT was better than when these segments were widely separated (non-optimal patients). Their outcome measures were echocardiographic volumes, ejection fraction and that of peak oxygen consumption on bicycle exercise which was performed at baseline and after 12 months.

For example the improvement in EF in optimal patients was  $10 \pm 2\%$ , whereas in non-optimal patients, the improvement was  $6 \pm 3\%$ ,  $p<0.01$ , and in VO<sub>2</sub> max the increase was  $2.4 \pm 0.3$  ml/kg/min, as compared to  $1.5 \pm 0.4$  ml/kg/min,  $p<0.01$ . There was 1 patient with an optimal LV lead

position and 3 patients with a non-optimal LV lead who were categorised as inadequate responders based on clinical information with no subjective clinical benefit and based on echocardiographic information with a decrease in LV end-systolic volume of <15%. This suggests that optimal LV lead position does identify a population of patients who might do better than non-optimal lead position, but that the population of patients with non-optimal lead position do still get some benefit from CRT.

## **1.6 Optimisation of pacing**

### **1.6.1 Why the interest in AV optimisation?**

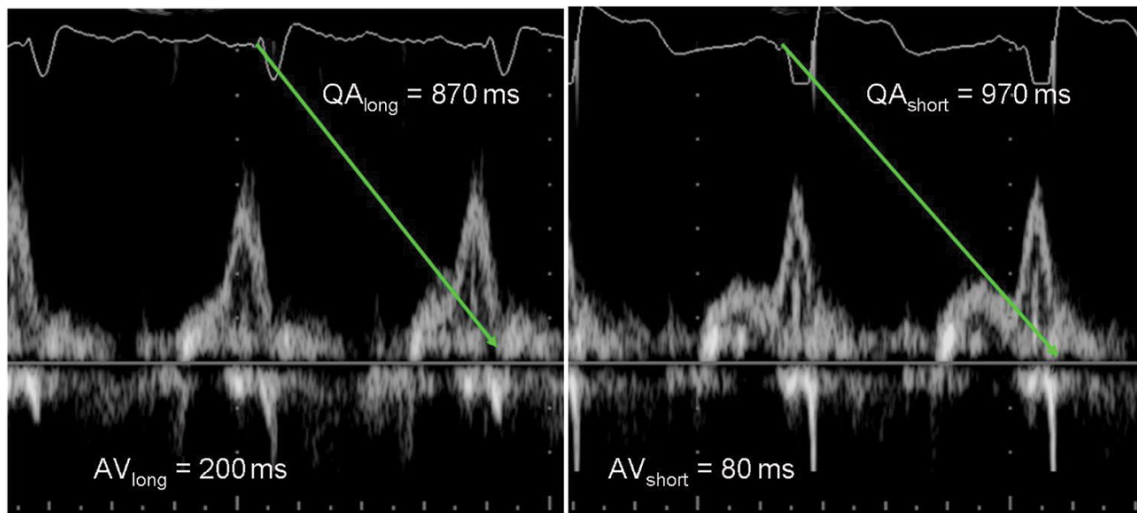
In the era of single chamber pacemakers, a constellation of symptoms and signs was described in 1969 by Mistui that later was named pacemaker syndrome<sup>9</sup>. Although not well defined, it can present with symptoms as severe as syncope, pre-syncope, oedema, dyspnoea, and chest pain, or more moderately and subtly as lethargy, palpitation, or an awareness of venous pulsations. These have been ascribed to the effects of atrio-ventricular dyssynchrony, most commonly when there is ventricular atrial conduction and thus atrial contraction against a closed mitral valve during ventricular systole, thus transmitting a greater pressure into the neck vessels, and reducing ventricular filling and cardiac output. These symptoms can also occur where there is competition between an intrinsic sinus rate and the paced ventricular rate, or indeed to a degree in patients with first degree heart block without a pacemaker, also known as a pseudo-pacemaker syndrome. These symptoms can be alleviated by dual chamber pacing which allows the maintenance of atrio-ventricular synchrony. However, the nominal settings of the device may not be optimal for an individual patient. This may be because patients often have abnormal atria - dilated due to hypertension or valve disease, or indeed have degenerative changes in atrial conduction tissue. If atrial conduction is slowed then despite a

nominally appropriate atrio-ventricular delay, atrial contraction may in fact be occurring late and resulting in pacemaker syndrome.

In the 1980's it was possible to program different atrio-ventricular delays and this was demonstrated to have an impact on cardiac output<sup>114</sup>. Echocardiography has been used to optimise AV delays in right ventricular pacing. Ritter et al conceived a simple method for calculating the appropriate AV delay in right ventricular pacing<sup>115</sup>.

However, because dual chamber pacing has virtually eliminated the problem of symptomatic pacemaker syndrome<sup>116</sup>, individual optimisation of the AV delay is infrequently performed in these patients.

Figure I.5 Example of the Ritter method for AV optimisation.<sup>117</sup>. This method programs two extreme AV intervals: a long AV interval with A wave attenuation (AVlong) and a short AV interval with A wave truncation (AVshort). For each AV interval, the time between the QRS complex onset to the completion of the A-wave is measured. The optimal AV interval is then calculated as below.



$$\text{Optimal AV interval} = \text{AV}_{\text{short}} + [(\text{AV}_{\text{long}} + \text{QA}_{\text{long}}) - (\text{AV}_{\text{short}} + \text{QA}_{\text{short}})]$$

$$\text{AV interval} = 80 + [(200 + 870) - (80 + 970)] = 100 \text{ ms}$$

In patients with heart failure, there was interest in the use of dual chamber pacemaker therapy as a treatment modality. Small initial studies did show some benefit and a mechanistic study by Nishimura et al

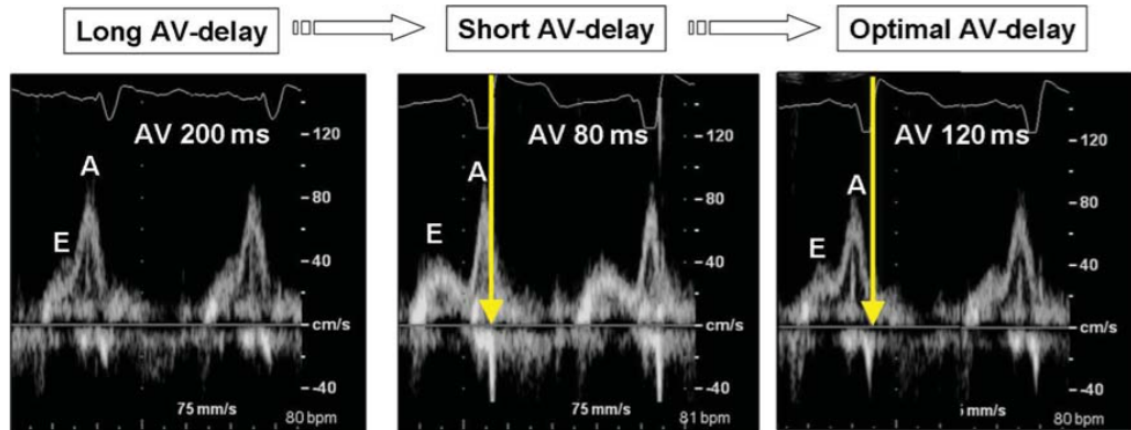
demonstrated in an acute human study that pacing with an optimum AV interval could improve cardiac output by up to 50%. This benefit was greatest in those patients in whom the PR interval was so prolonged that atrial contraction occurred during ventricular systole such that it could not contribute to ventricular filling. They also concluded that the optimal AV delay varied significantly between patients so that individual optimisation was necessary to realise the benefits of pacing<sup>118</sup>. A similar, but less profound benefit was demonstrated by Kinderman et al<sup>119</sup>.

Subsequent work demonstrated that the long-term effects of right ventricular pacing was deleterious in heart failure, and therefore this has been superseded by biventricular pacing (see other chapter).

### **1.6.2 Methods to optimise AV and VV delays.**

As described above, there are a number of methods that can be used to measure the change induced by altering the atrioventricular, and more recently for biventricular devices, the inter-ventricular delay. The majority of studies have used echocardiography because it is non-invasive, easily accessible to clinical departments and can directly measure left ventricular filling using pulsed wave Doppler placed at the tips of the mitral valve leaflets. The iterative method uses this method as described in figure 1.6.

Figure I.6. Iterative method. Initially a long AV delay is programmed and the mitral inflow interrogated. The AV delay is shortened in 20ms increments until truncation of the A wave occurs. It is then lengthened in 10ms increments until the A wave is no longer truncated<sup>117</sup>.



Echocardiography can also be used to measure stroke distance and thus estimate cardiac output. Although echocardiography is attractive, there is significant variability measured from beat to beat, partly due to true variation and partly due to variability in the placement of the sample volumes due to respiratory motion of the heart for example. Other methods which have been used are invasive measurements of left ventricular pressures utilising high-fidelity pressure transducers placed in the left ventricle. This allows the calculation of the rate of change in ventricular pressure, a surrogate for cardiac work. However, the practical use of this is limited by the invasive nature of the technique.

More recently, other non-invasive techniques have been described. These include beat to beat measurement of blood pressure using finger plethysmography, cardiac impedance to measure blood flow (a number of different techniques are available on the market). There has also been interest in intracardiac measurements which have the potential to be used in devices to provide optimisation at any time, including PEA and intracardiac impedance measurements. There has also been interest in optimisation using the surface ECG as well as intracardiac ECG's.



Comparison of these techniques is hampered by the fact that there is no gold standard. For example, one study defined the best setting as that which gave the greatest cardiac output by measurement of aortic stroke distance. Unsurprisingly when using this definition they found that measurement of aortic stroke distance was the best technique and performed better than determination of the best setting by mitral inflow Doppler sampling<sup>120</sup>! Furthermore, perfect concordance would not be expected in techniques with a degree of inherent variability, and where the change to be measured is small.

### **1.6.3 The role of AV optimisation in biventricular pacemakers**

Kass et al performed acute invasive haemodynamic measurements in 18 patients<sup>121</sup>. They found that biventricular pacing and left ventricular pacing improved LV dp/dt compared to RV pacing or intrinsic rhythm. They assessed different AV delays, and found that for most patients, the optimum value was around 120ms, with little change noted at different AV delays. If the AV delay was less than 90ms, however, this compromised LV filling and consequently LV dp/dt. Auricchio et al. also measured invasive haemodynamics in 25 patients during biventricular and univentricular pacing at different AV intervals and found that the best AV delay varied between individuals<sup>122</sup>. Gold et al performed invasive measurements in 28 patients at different AV delays<sup>123</sup>. Again, they found that there was again a spread of optimal AV delays and that the optimum delay was significantly longer for a paced AV delay than a sensed AV delay (i.e. delay after an atrial pacing stimulus rather than atrial sensed event). They also compared different methods of assessing the optimum AV delay against LV dp/dt as the reference standard. 2 echocardiographic optimisation methods were used - the Ritter method and the measurement of aortic VTI using continuous wave Doppler, as well as an algorithm using measurements derived from intracardiac electrograms from the pacing leads. They found

the mean difference in optimum AV delay from that determined by the reference standard was least using the intracardiac electrograms, followed by the Aortic VTI and then the Ritter method. Jansen et al also compared echo-guided optimisation methods against LV dp/dt in 30 patients<sup>124</sup>. They found that mitral inflow VTI most frequently gave concordant results, followed by left ventricular outflow tract (LVOT) VTI, then diastolic filling time and finally the Ritter method.

Stockburger et al. demonstrated that AV optimisation led to an improvement in echo-Doppler parameters including the myocardial performance index and left ventricular filling time fraction, over and above that offered by standard settings<sup>125</sup>.

In a longer term study, Sawhney et al. randomised 40 patients undergoing CRT to an empiric AV setting of 120 ms or AV delay optimisation using echo Doppler to measure aortic velocity time-integral<sup>126</sup>. They assessed 8 different AV delays and found a significant difference in individual optimal settings between patients, although the best setting for the majority was between 100 and 140 ms. This translated into a clinical improvement, with significantly more patients that improving by one or more NYHA class (75% in the optimised group vs. 40% in the empiric group,  $P < 0.03$ ) and a significantly larger improvement in quality of life score ( $23 \pm 13$  vs.  $13 \pm 11$  points respectively,  $P < 0.03$ ). However, these changes were not translated into an improved 6-min hall walk distance (6MHW).

Kedia et al published their experience with echo-guided AV optimisation<sup>127</sup>. In a retrospective cohort of 215 patients, most of whom were optimised using Ritter's method, they found that 40% of patients had an AV delay of  $>140$ ms - suggesting that a significant proportion of patients have an optimal AV delay significantly longer than nominal settings.

Hardt et al described the effects of echo-guided optimisation using LVOT VTI in 33 patients who were optimised on average 31 weeks after CRT implant<sup>128</sup>. Approximately 6 weeks after optimisation the patients underwent follow up echocardiography, NT pro-BNP measurements and 6MHW. They found that optimisation led to a small improvement in LVEF, a fall in NT pro-BNP and an increase in 6MHW. However, the lack of a control group makes it difficult to know what changes would be expected without optimisation.

Zhang et al. performed serial echo-Doppler guided AV delay optimisation on 31 consecutive patients receiving CRT for standard indications immediately after device implantation, at 3 months, and then at long-term follow up (at least 6 months after CRT) <sup>129</sup>. Not only did they find that the spread of optimal delays was wide, but also a significant number of patients (58%) required at least one change in their AV delay at 3 month or long-term follow up, suggesting that there may be a role for serial optimisations.

However, in Zhang's study, the agreement between the optimum AV delay as measured by echo-Doppler and by impedance cardiography was poor. This is an issue that bedevils CRT optimisation, namely what is the best technique to do this. Invasive studies might be the gold standard, but are not feasible for routine, multiple use. Echocardiography has some variability and is highly user dependent. Impedance cardiography, finger plethysmography are all also potentially useful and more reproducible techniques, but they require specialised equipment that may not be available in every centre.

Melzer et al examined whether dyssynchrony was the mechanism that underlies the benefit of AV optimisation<sup>130</sup>. In 11 patients, they optimised the AV delay using Ismer's method which utilises an oesophageal electrode to record left atrial electrograms, as well as concurrent echo-

Doppler sampling of mitral inflow. They measured dyssynchrony using tissue Doppler at the optimised delay and 50ms more or less than that optimum. They did not find any significant change in dyssynchrony at the different AV delays, implying that it is purely alterations in ventricular filling that underlie the haemodynamic benefits of AV optimisation.

Chawla et al published further on what appears to be the same cohort as the previous paper by Sawhney<sup>120,126</sup>. They compared the Ritter's method of optimisation versus the aortic VTI method. Interestingly, the correlation between the two methods was poor.

Whinnett et al have demonstrated that non-invasive blood pressure monitoring can be used to optimise the AV delay both at rest and on exercise<sup>131</sup>. Delnoy et al have demonstrated that an algorithm utilising peak endocardial acceleration signals from a specially designed lead can be used for optimisation as it correlates closely with invasive dp/dt across a series of AV delays{Delnoy:2008gq}.

Waggoner optimised 30 patients using continuous wave Doppler echocardiography for aortic VTI and stratified the response by the degree of diastolic dysfunction at baseline<sup>132</sup>. They found that optimisation had a significantly greater effect in patients with pseudo-normalised / restrictive filling at baseline.

Jones optimised 30 patient by echo-Doppler of mitral inflow, and compared this to the ECG<sup>133</sup>. They suggested that an AVD programmed to 30-40ms after the end of the p wave on the surface ECG would approximate the optimum delay found by echocardiography.

Valeur performed an observation study on 100 patients using a reference standard of the summed displacement of the 6 basal left ventricular segments measured using tissue Doppler echocardiography (DLV). They found that DLV correlated well with LVOT VTI, a lesser correlation with E/e' ratio and that it did not correlate with diastolic filling time.

One of the other issues in optimisation is that after making changes to the timing, there is an initial cardiac response which will affect haemodynamics, but compensatory peripheral vasculature changes can result in alterations in left ventricular filling and thus the steady state haemodynamics may not adequately reflect the magnitude of changes seen. This issue has not been considered by the echocardiographic community, but work by Whinnett and others elegantly demonstrates the changes in blood pressure seen on a beat to beat basis as measured by finger plethysmography<sup>134</sup>.

#### **1.6.4 The clinical basis for AV optimisation.**

Of the landmark studies demonstrating the effectiveness of CRT, the approach to optimisation differed widely. The MUSTIC investigators did not perform AV optimisation<sup>29</sup>, whereas the MIRACLE<sup>31</sup> and larger CARE-HF<sup>34</sup> studies performed echo-Doppler guided optimisation based on diastolic filling. The COMPANION study also used optimisation based on intracardiac electrograms<sup>33</sup>. Only one study thus far has been a randomised controlled trial of different AV delay strategies. The SMART delay study randomised 980 patients into a strategy of a fixed AV delay of 120ms, a single pre-discharge echo-Doppler guided optimisation, or optimisation pre discharge and at 3 months using an algorithm based on intracardiac electrograms<sup>135</sup>. The primary endpoint was LV end systolic volume measured by 2D echocardiography. They found no difference in the primary endpoint between the three groups. Neither were there any differences in the secondary endpoints which included functional measures such as change in 6MHW, change in quality of life scores or change in New York Heart Association class.

The FREEDOM trial<sup>136</sup> has yet to publish its findings, but preliminary results have been presented at Heart Rhythm 2010. This study is comparing QuickOpt optimisation with standard clinical care which may

or may not include AV or VV optimisation. They apparently have found no difference between the two groups.

### 1.6.5 The role of VV optimisation

Sogaard and others demonstrated that in some patients sequential biventricular (BiV) pacing has an additional benefit over simultaneous, and that the best settings varied significantly between individuals. They assessed 20 patients soon after device implantation using echocardiography and found that VV optimisation resulted in an average absolute improvement in left ventricular ejection fraction of 3.9%<sup>137</sup>. A number of studies have confirmed this acute benefit of sequential biventricular pacing using various techniques including invasive measurements of left ventricular dp/dt<sup>138,139</sup>, radionuclide ventriculography<sup>140</sup>, and echocardiography<sup>141</sup>.

These small scale studies were followed by data coming from larger scale trials. The InSync III investigators compared the effect of sequential biventricular pacing in 359 patients to that of patients enrolled in the MIRACLE study. VV optimisation was performed by measuring stroke distance after implant and before hospital discharge, at 3 and at 6 months. The optimal setting was different to simultaneous biventricular pacing in approximately 80% of patients at each time point. They found no difference in the NYHA functional class or quality of life between the optimised InSync III patients and the MIRACLE CRT patients, though the increase 6 minute hall walk distance was greater in the optimised group<sup>142</sup>. Boriani randomised 121 patients to echo-Doppler guided VV optimisation or simultaneous pacing but did not find any difference in 6 minute hall walk distance, NYHA functional class or quality of life<sup>143</sup>. Forty-eight of these patients were followed up with echocardiography at 6 months, but there was no difference in echocardiographic remodelling between the 2 groups<sup>144</sup>.

Vidal et al studied 31 patients and performed optimisation guided by tissue Doppler assessment of 2 opposing left ventricular walls. They assessed 3 VV delays and found a poor correlation between optimal settings determined by surface ECG QRS duration and echo. However, the correlation was better when measuring inter-ventricular delay on the surface ECG. A further study by the same group looked at compared tissue Doppler with LVOT VTI and found that they agreed in 81% of patients<sup>145</sup>.

Bertini et al however, studied 106 patients who had AV and then VV opt by echo<sup>146</sup>. They found that an optimisation strategy based on minimising the paced QRS duration on the surface ECG showed a good concordance with echo determined optimal VV settings.

Fischer et al looked at 47 patients referred to their optimisation clinic<sup>147</sup>. The optimised AV delay by mitral inflow, and VV delay by aortic VTI. They found no clinical characteristics that could predict optimal VV settings.

Sciariaffia used impedance cardiography and compared it to invasive dp/dt to determine optimum VV delays in 24 patients<sup>148</sup>. They found a poor concordance in the optimum settings by the two methods.

Marsan et al optimised 69 patients using echocardiography. They found that the effects of VV optimisation were greater in patients with ischaemic cardiomyopathy than in patients with dilated cardiomyopathy. Furthermore, there was a significant interaction with the extent of myocardial scar, with patient with more scar requiring earlier LV stimulation<sup>149</sup>.

Duvall et al reported on 74 consecutive patients referred for optimisation. These patients had had their device implanted a mean of 9.9 months prior to optimisation. They measured aortic VTI and 3D LVEF at 5 different VV delays. They found that these methods frequently did not agree on the optimum setting, and in the majority of patients (83% by aortic

VTI, 71% by 3D LVEF) the optimum setting was simultaneous stimulation<sup>150</sup>.

Herweg et al also performed late optimisation (mean 600 days post implant) in a consecutive series of 40 patients. They found that echo-guided optimisation using aortic VTI resulted in a QRS morphology on the surface ECG that was more suggestive of true biventricular pacing with a positive R wave in V1<sup>151</sup>.

Khan et al performed optimisation by echocardiography. They found that AV and VV optimisation provided an incremental improvement over AV optimisation alone, as assessed by non-invasive measurements of cardiac output. They also defined the site of the left ventricular lead in relation to the most delayed left ventricular myocardial segment defined by echo radial speckle tracking. They found that the benefit of VV optimisation existing in patients where the lead ventricular lead was sited adjacent to the most delayed segment rather than being directly over the segment or remote from it. This suggests that VV optimisation can be used to overcome a mildly sub-optimal LV lead location<sup>152</sup>.

Finally Tamborero randomised 156 consecutive patients to echo-Doppler guided AV optimisation and tissue Doppler VV optimisation against echo-Doppler guided AV optimisation and ECG guided VV optimisation. They found no difference in clinical endpoints between the two groups but a larger decrease in LVESV in the group whose VV delay was optimised by the ECG<sup>153</sup>.

### **1.6.6 AV & VV optimisation**

Valzania et al reported on their cohort of 37 patients who underwent serial echo-guided AV and VV optimisations. The Av delay was optimised based on diastolic filling and the VV interval by aortic VTI. They found that there were significant changes to the optimum settings over the course of 1



year follow up<sup>154</sup>. She also found that there were significant differences between optimal settings at rest and on exercise<sup>155</sup>.

Baker et al found that there was a good concordance correlation coefficient between QuickOpt and aortic VTI measurements in 58 patients<sup>61</sup>. However, Van Gelder et al compared QuickOpt at implant with invasive LV dp/dt measurements and found that there was a poor concordance in the optimum setting between the techniques<sup>156</sup>. Porciani examined the effect of QuickOpt settings on cardiac function in 20 patients using 3D echocardiography. Using Qlab, they found that optimisation led to an acute fall in dyssynchrony and an improvement in SV and LVEF<sup>113</sup>.

Zuber et al compared acoustic-cardiography against echo-guided optimisation in 43 patients. The iterative method was used for AV optimisation and LVOT VTI for VV optimisation. They found a good correlation between echo and acoustic cardiography for AV optimisation, but that the correlation was statistically significant, but less good for VV optimisation. They performed multiple measurements at different settings to evaluate the reproducibility of both techniques, and found that the signal to noise ratio of VTI was worse than that of acoustic cardiography<sup>157</sup>.

Khan validated non-invasive cardiac output monitoring against echocardiography for CRT optimisation<sup>158</sup>.

Turcott and others also compared cardiac impedance with echocardiography for optimisation in 20 patients. They looked at aortic VTI, mitral VTI, A wave truncation and septal-posterior wall motion delay. Measurements were made and averaged over 1 respiratory cycle. They found that impedance cardiography was the most reproducible and was able to give a statistically significant estimate of the optimum setting. The confidence interval was narrow. However, the echo measurements did not perform so well with only the Aortic VTI being able to give an estimate of the optimum AV interval and the confidence interval was wider than in

impedance cardiography. Some of the variability that they encountered may be explained by motion of the heart throughout the respiratory cycle which would inevitably result in motion of the sample volume.

Taha et al used a comprehensive echo-Doppler assessment to optimise AV and VV delays in 50 consecutive CRT patients referred for optimisation by the clinical cardiologist. The average time from CRT implant was 13.8 months and optimisation resulted in an acute improvement in echo systolic and diastolic characteristics as well as a longer term improvement in NYHA class and MLHFQ. However, 10 out of these patients had no net improvement post optimisation<sup>159</sup>.

Reinsch et al used inert gas rebreathing technique to measure cardiac output and performed AV and VV optimisation based on this. They found that this technique worked, but didn't compare it to other methods. Having said that the interesting thing about this paper is that they measured the effect of reprogramming the device 10 minutes after reprogramming to allow for equilibration<sup>160</sup>. This is the antithesis of Whinett's strategy.

Bogaard et al measured dp/dt during pacing at different LV epicardial sites in 16 patients. They found that optimisation could partially compensate for a sub-optimal lead position<sup>161</sup>.

Dizon et al used LIDCO to optimise 15 patients. They did a subgroup analysis which suggested that patients with an acute improvement in SV with optimisation did better at 6 week follow up in terms of LVEF, LVEDD and 6MHW distance. The subgroup analysis is probably meaningless though.

Bocchiardo et al compared dp/dt with intracardiac impedance measurements for optimisation of LV lead position, AV and VV delays. They found that variations in the LV lead location resulted in a mean optimal benefit of 18.1% in dp/dt. AV opt increased the benefit to 22.1%,

and VV delay opt also resulted in a benefit. Impedance was correlated well with the optimal values by  $dp/dt$ .

Pabari et al suggest that there needs to be an assessment of signal to noise ratio in the evaluation of techniques for CRT optimisation. This appears sensible, and she has given an elegant mathematical description to support her hypothesis. Unfortunately, there is no data on the signal to noise ratio for different techniques, nor indeed the recognition that for a given technique there is likely to be variation in this ratio between laboratories.

More recently Ginks et al demonstrate that intracardiac impedance can be used to estimate optimum AV and VV delays using invasive  $dp/dt$  as their reference standard<sup>162</sup>.

## 1.7 Summary

Dyssynchronous activation of the heart associated with left bundle branch block or ventricular pacing has been known about for nearly 100 years. The advent of echocardiography and improvements in pacing have resulted in the development of sensitive techniques to detect dyssynchrony and to ameliorate it using biventricular pacing. However, questions remain that this thesis will attempt to answer. Does pacing the right ventricle at a site other than the apex result in less dyssynchronous left ventricular contraction? Can 3D echo be used to assess optimal atrio-ventricular delays with pacing? Does everyone with a biventricular pacemaker require individual optimisation, or is the benefit limited to an identifiable sub-group of patients. Finally, can speckle tracking be applied to 3-D echo datasets to improve dyssynchrony assessment?

## Chapter 2 AdviseCRT

### 2.1 Abstract

The timing of atrioventricular (AV) delays may be adjusted in pacemakers. The optimisation of this delay has been demonstrated to alter cardiac output. We performed a clinical feasibility study to investigate the utility of cardiac impedance measurements to select the optimal AV delay. Measurements of impedance at different vectors were performed during implantation of a biventricular pacemaker through a specially designed pacemaker platform. This was referenced against invasive haemodynamic measurements at time of implant and echocardiographic measurements performed at a later time. There was poor correlation between impedance, invasive haemodynamics and echocardiographic measurements in selecting the optimal AV delay.

### 2.2 Introduction

The programming of artificial pacemakers requires the specification of the interval between atrial and ventricular pacing stimuli. Whilst this is true of dual-chamber pacemakers, it has come into focus more recently with the development of biventricular pacemakers. A number of different studies have demonstrated benefits in acute haemodynamics, surrogates of cardiac output and also echocardiographic parameters (see section 1.6.3). A number of methods can be used to select the best interval in a given patient, but these methods are time consuming and only assess the patient at one moment in time.

The ability for a pacemaker to self-optimize is an attractive concept as it might allow automatic and frequent optimisation of the pacemaker timing. One potential method is the measurement of electrical impedance. This

method is currently used within pacemakers as a means to monitor the water content of the lungs as a surrogate for heart failure control (Optivol)<sup>163</sup>. However, beat to beat changes in impedance may be a surrogate of cardiac function<sup>164</sup>.

We therefore performed a clinical feasibility study to determine whether different methods of measuring cardiac function might ultimately be used to optimise pacemaker timing. As a necessary precursor, we compared invasive measurements of left ventricular pressure, measurements of cardiac impedance and 2-dimensional and 3-dimensional echocardiographic assessments. Therefore the null hypothesis was that there was no concordance of these methods for selecting the optimum AV delay.

## **2.3 Methods**

### **2.3.1 Study Objectives**

The objective of this study was to determine whether the measurement of cardiac impedance through implanted pacemaker leads could be performed and might ultimately be used to optimise the atrioventricular delay. As a necessary precursor we performed measurements of impedance, invasive haemodynamics and echocardiography and correlated these.

### **2.3.2 Study design**

The study was a prospective, non-randomised clinical feasibility study, sponsored by Medtronic Inc. Patients were recruited at Kings College Hospital, London and the University of Pittsburgh Medical Center, Pennsylvania, USA. Both centres collected impedance data measured through the implanted pacemaker leads and performed Doppler and 2-dimensional echocardiography after pacemaker implant. The atrioventricular delay was varied and impedance measurements through the

pacemaker leads were compared to simultaneous pressure and volume measurements, as well as to subsequent 2-dimensional and 3-dimensional echocardiographic measurements with the same programmed intervals. An additional sub-study was performed only at Kings College Hospital that gathered invasive left ventricular pressure and volume measurements and 3-dimensional echocardiographic data after pacemaker implant. This sub-study was designed by the author and colleagues, the data acquired and analysed by the author as part of this thesis. Offline echocardiographic measurements were performed by the author on all patients from both centres. The analysis of cardiac impedance data was performed by Dr Todd Zielinski of Medtronic Inc. Only data pertaining to the patients in this sub-study are presented here.

The study was approved by the hospital ethics committee.

### **2.3.3 Patient eligibility criteria**

Inclusion criteria were:

1. Patients scheduled for a new biventricular pacemaker / defibrillator (CRT-D) implant or CRT-D generator replacement
2. Patients greater than 18 years old.
3. Patients able and willing to give informed consent.

Exclusion criteria were:

1. Patients with persistent or permanent atrial fibrillation
2. Patients who were pacemaker dependent.
3. Patients with an integrated bipolar defibrillation lead (as 2 RV pacing electrodes distinct from the defibrillation coil electrode were necessary for the impedance measurements).
4. Patients with hypertrophic cardiomyopathy.

5. Patients enrolled in a concurrent study that might confound this study.

6. Patients who were pregnant.

7. Patients unable or unwilling to participate in study procedures.

8. Patients with acute cardiac ischaemia

Withdrawal criteria:

1. If the patient wished to terminate study participation.

2. The Investigator, at his or her own discretion, could withdraw a patient from the study at any time if the patient's well being could be jeopardised by continuation of the study.

### **2.3.4 Implant set-up**

Immediately before CRT-D implant or replacement, a respiratory belt transducer (Biopac Systems Inc, CA, USA) was placed around the patient's thorax and the transducer amplifier module was connected. The respiratory belt transducer measured the change in thoracic circumference that occurred as the subject breathes, without any electrical connection to the patient. The respiratory belt was contained outside the sterile field and therefore did not require sterilisation prior to use. The patient was then cleaned and draped for implant. The leads used for the clinical implant were placed transvenously in the right atrial appendage (CapsureFix Novus 5076, Medtronic Inc), right ventricular apex (Sprint Quattro Secure, Medtronic, UK) and over the left ventricle using the coronary sinus to access a posterolateral or true lateral branch vein. These were commercially available leads from Medtronic, Inc and the choice of left ventricular lead was at the discretion of the implanting physician. The pacemaker pocket was created subcutaneously below the left clavicle and a Medtronic model # 5719 Active Can Emulator was temporarily placed

inside the pocket; this pocket was subsequently used for the patient's device implant. The study protocol was performed after implantation of the clinical leads, but before connection to the clinical device. The Active Can Emulator (ACE) mimics the electrical and dimensional characteristics of the final patient implanted device in order to collect impedance vector data from the RV lead electrodes to the ACE electrode. The transvenous leads and Active Can Emulator were connected via a Medtronic Header Kit model 5460 to the investigational Continuous Impedance Module Model 19051 (cZm) via two patient cables (Medtronic Models 5420 & 5436). The cZm allowed atrial and ventricular pacing together with simultaneous impedance measurements from specified poles of the leads. The cZm and respiratory band were connected to a data acquisition module (MP150, Biopac Systems Inc, CA, USA) and respiratory transducer amplifier respectively (RSP100, Biopac Systems, Inc, CA, USA).

Pressure volume measurements were performed using a 7 French conductance catheter (CA-71103-PL, CD Leycom, Netherlands). Before implant the conductance catheter was calibrated against a 100mmHg standard and against atmospheric pressure. A 7 French arterial sheath was placed in the femoral artery. An Emerald 150cm J-tipped diagnostic 0.035" guide-wire (502-521, Cordis, UK) was used to place a Judkins Right Coronary JR4 catheter (Cordis, UK) into the left ventricle. A 300cm ChoiCE extra support 0.014" wire (Boston Scientific, UK) had a J-shape formed at its tip and the Emerald J wire was exchanged for this. The JR4 catheter was then exchanged for the conductance catheter. The catheter was connected to a monitor for set-up and data acquisition (CFL-512, CD Leycom, Netherlands). The conductance catheter measures impedance between 10mm spaced electrodes on the catheter shaft. This is proportional to left ventricular volume, and was calibrated using 3-dimensional echocardiographic measurement of left ventricular volume acquired just before the start of the procedure. The measurement of impedance requires



injection of an electrical current. Simultaneous measurements by the conductance catheter and the pacemaker leads were therefore physically impossible as the two devices simultaneously injected currents that interfered with one another. The pacing interventions and impedance measurements from the pacemaker leads were performed as described below, with simultaneous pressure measurements from the conductance catheter whilst the catheter electrodes were deactivated. To acquire pressure-volume loops, the pacing intervention had to be repeated with the conductance catheter active. Pressure-volume data were analysed using software (ConductNT v3.18, CD Leycom, Netherlands).

After the first 3 patients, the acquisition of pressure-volume data was deemed to add excessive time to the procedure. This increased the risk of infection to the patient and therefore the collection of this data was abandoned and replaced with pressure only measurements that could be performed simultaneously to the impedance measurements.

Pressure only measurements were performed using a high fidelity pressure transducer (Pressure wire Certus, St Jude Medical, UK). This was placed via a right radial 6Fr sheath. Again an Emerald J-wire and JR4 catheter were placed in the left ventricle and the J-wire exchanged for the pressure-wire. The JR4 catheter was then removed. The pressure-wire was then connected via the RadiAnalyzer Xpress measurement system to the data acquisition module.

In both scenarios 5,000 international units of heparin were administered intravenously to prevent thrombus formation on the wire. The pressure signals were routed via the catheter laboratory monitoring equipment (Axiom Sensis, Siemens Healthcare, UK) to the applicable analog input channel on the data acquisition module. After the procedure, haemostasis was achieved by use of an Angioseal (St Jude Medical, UK) if femoral arterial access, or a TR band (Terumo, UK) if radial arterial access was used.

The calibrated BioPac unit sampled the analog electrical output of the cZM, respiratory band and the pressure transducer at 2000Hz. BIOPAC Acknowledge Data Acquisition Software was used to collect and store these real time signals using a laptop computer. Real- time impedance waveform data was collected in four electrode configurations using conventional pacing leads for a minimum duration of two respiratory cycles.

After measurements, the external pacemaker generator was disconnected, a Medtronic Protecta CRT-D device attached and the implant procedure completed in the standard method of the operator.

### **2.3.5 Implant measurements**

The cZm was programmed to pace the atrium 10 beats per minute faster than the intrinsic sinus rate to ensure reliable capture. The delay between atrial pacing and the subsequent ventricular sensed event on the right ventricular lead was measured through the pacemaker generator. In order to achieve a completely paced beat (as opposed to one arising from fusion of pacemaker stimuli and intrinsic conduction) 10 ms was subtracted from this delay and this value was defined as 100% of the paced AV interval.

Atrial and ventricular pacing was performed in DDD mode, sequentially at atrioventricular delays calculated to be 100%, 80%, 60%, 40% and 20% of the AV interval rounded to the nearest 10ms. The second protocol added baseline (unpaced) and 30ms atrioventricular delay measurements (30ms delay was chosen as this was the smallest programmable value).

Simultaneous impedance and pressure measurements were performed for approximately 20-30 seconds for each impedance configuration tested, to allow for 2 normal breath cycles of the patient. Impedance measurements were performed with 4 different electrode configurations. Each configuration was determined by a pair of electrodes to inject current, and a sensing pair of electrodes. The configurations are defined in table 2.1.

Offline pressure-volume loop analysis was performed using ConductNT

3.18 (CD Leycom, Netherlands). Offline impedance and simultaneous pressure analysis was performed using AcqKnowledge 3.9 (Biopac Systems, CA, USA). Three consecutive stable cardiac cycles were chosen for analysis and results averaged.

**Table 2.1 – Table of impedance vectors**

Configuration	Injection electrodes	Sensing electrodes
1 - left ventricle	RV ring & LV ring	RV tip & LV tip
2 - right ventricle	RV tip & RV coil	RV ring & RV coil
3 - right atrium to right ventricle	RA tip & RV tip	RA ring & RV ring
4 - RV to can	RV tip & can	RV ring & can

The cZm was based on a pacing platform that allowed pacing from a single ventricular electrode during impedance measurements. Initially this was engineered to pace the right ventricle. This is not consistent with the clinical use of CRT-D devices which are predicated on pacing both ventricles simultaneously. The cZm was re-engineered during the study, but was unable to allow biventricular pacing simultaneously with impedance measurements. As left ventricular pacing may improve left ventricular function similarly to biventricular pacing and maybe programmed in a clinical device, the cZm was re-engineered to deliver left ventricular pacing rather than right ventricular pacing.

### **2.3.6 Post Procedure echocardiogram**

Within 3 days of the procedure, the patient underwent echocardiographic assessment of cardiac performance to replicate the peri-implant impedance protocol. The pacemaker was programmed to DDD,

pacing the same chamber and at the same lower rate as used during impedance measurements. The AV interval was varied to include 80%, 60%, 40% and 20% of the intrinsic AV conduction; identical to those used during impedance measurements at device implant. Measurements were performed at least 20 seconds after adjustment of AV interval.

Echocardiographic assessment included pulsed wave Doppler of mitral inflow, left ventricular outflow, 2-dimensional echocardiography with apical windows optimised for the left ventricle along the three standard cut-planes, as well as 3-dimensional acquisitions of the left ventricle. This was performed using a Philips ie33 system with S5 and x3 transducers (Philips, UK).

Doppler measurements were performed at a fast sweep speed of 100mm per second and optimised scale to maximise measurement accuracy. Mitral inflow was interrogated using pulsed wave Doppler. The E to A time was measured at least 3 times. Mitral regurgitation was interrogated using continuous wave Doppler to measure LV dp/dt, at least 3 times. Left ventricular outflow tract blood flow was assessed using pulsed wave Doppler. The velocity time integral (LVOT VTI) and the ejection time was measured on 3 beats. The aortic flow was assessed using continuous wave Doppler. Again the velocity time integral (Ao VTI) was measured 3 times.

Apical 4 chamber and 2 chamber and 3 chamber views were recorded, with depth and sector width optimised for the left ventricle. At least 3 consecutive beats were recorded.

3-dimensional acquisitions with depth and sector width optimised for the left ventricle were performed. These acquisitions were gated over 4 or 7 consecutive cardiac cycles depending on the frequency of ventricular ectopy and patient tolerance during breath-holding in the phase of respiration that afforded the best image quality.

The myocardial performance index was calculated as –

[time that mitral valve is closed – ejection time] / ejection time

The time that the mitral valve is closed is measured as the time between the end of the A wave to the beginning of the E wave on mitral Doppler. The ejection time is measured on continuous wave Doppler through the aortic valve.

Offline image analysis was performed using Xcelera 4.0, Philips and LV analysis 2.7, TomTec GmbH Germany. Results were analysed using Excel 2008 for Mac, Microsoft, WA, USA, Prism 5.0 for Mac OS X, GraphPad CA, USA and SPSS 19.0, IBM, USA.

## **2.4 Results**

### **2.4.1 Patients**

In total 13 patients were recruited into the study, however 1 patient, K008, subsequently was withdrawn as the implant procedure was prolonged and it was felt that study measurements would add excessive time to the procedure and increase the risk of wound infection.

The first patient underwent the procedure and measurements as planned, however, echocardiography was mistakenly performed during biventricular pacing as it was not appreciated that the cZm could only pace from a single ventricular lead. Therefore impedance data is not available for comparison. Three-dimensional echocardiography was not performed at the shortest AV delay at the patients request.

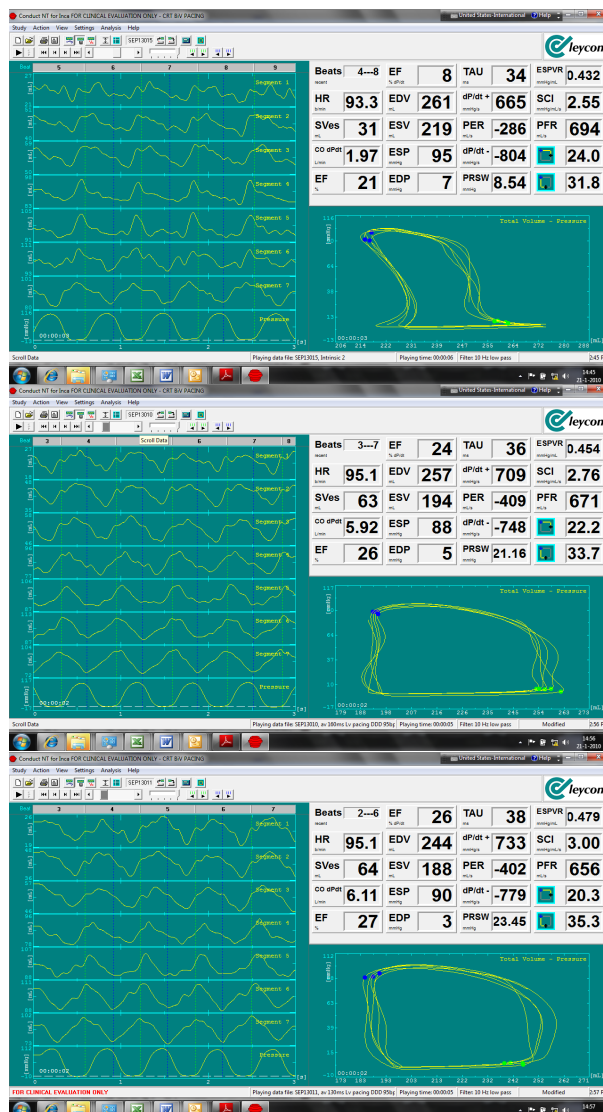
The subsequent 6 patients, K002 to K007 were all performed during right ventricular pacing.

After re-engineering the cZm, the protocol was changed such that the subsequent 5 patients, K009 to K013 were all assessed during left ventricular pacing.

Of the 6 patients who underwent measurements during right ventricular pacing, 2 of these had 3D echocardiograms that were not analysable. One patient, K005, had such frequent ventricular ectopy that a gated 3D left ventricular acquisition was impossible. Doppler and 2-dimensional assessments were acquired with difficulty and all measurements were performed on the second cycle after a ventricular ectopic beat. Patient K007 had echocardiographic windows that were too poor to allow 3D analysis.

Example pressure volume loops are shown in figure 2.1. Whilst excellent loops were obtained in some patients, this was time consuming and abandoned as it was thought to add excess time and risk to the patient.

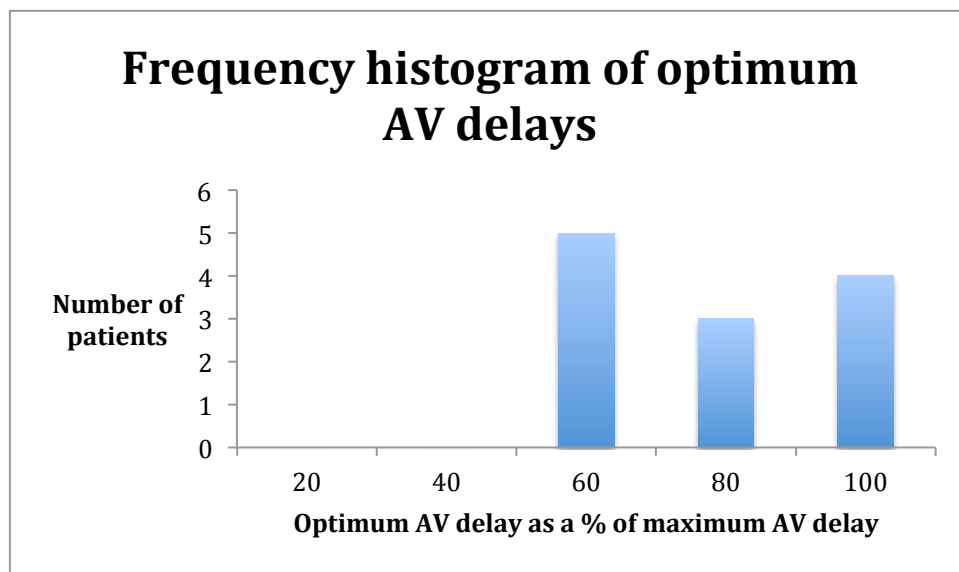
Figure 2.1 Pressure volume loops. An example patient during intrinsic rhythm (upper panel), LV pacing with an AV delay of 160ms (middle panel) and 120ms (lower panel). The segmental loops are on the left, the global LV loop is bottom right and summary data in the upper right. In intrinsic rhythm the cardiac function is poor with a stroke volume of 31 ml and the shape of the loop indicates inefficient cardiac work. During LV pacing there is a “square” shaped loop indicating efficient cardiac function and much better haemodynamics with a stroke volume of 63 ml. There is little difference between the AV delays shown.



### 2.4.2 Optimum AV delay

The mean optimum AV delay as ascertained by dp/dt was 78% of the maximum paced AV delay with a standard deviation of 18%, and a range of 60-100%. No patients had an optimum AV delay below 60% of the maximum AV delay. Figure 2.2 shows a frequency histogram of the optimum AV delays.

Figure 2.2 – Frequency histogram of optimum AV delays.

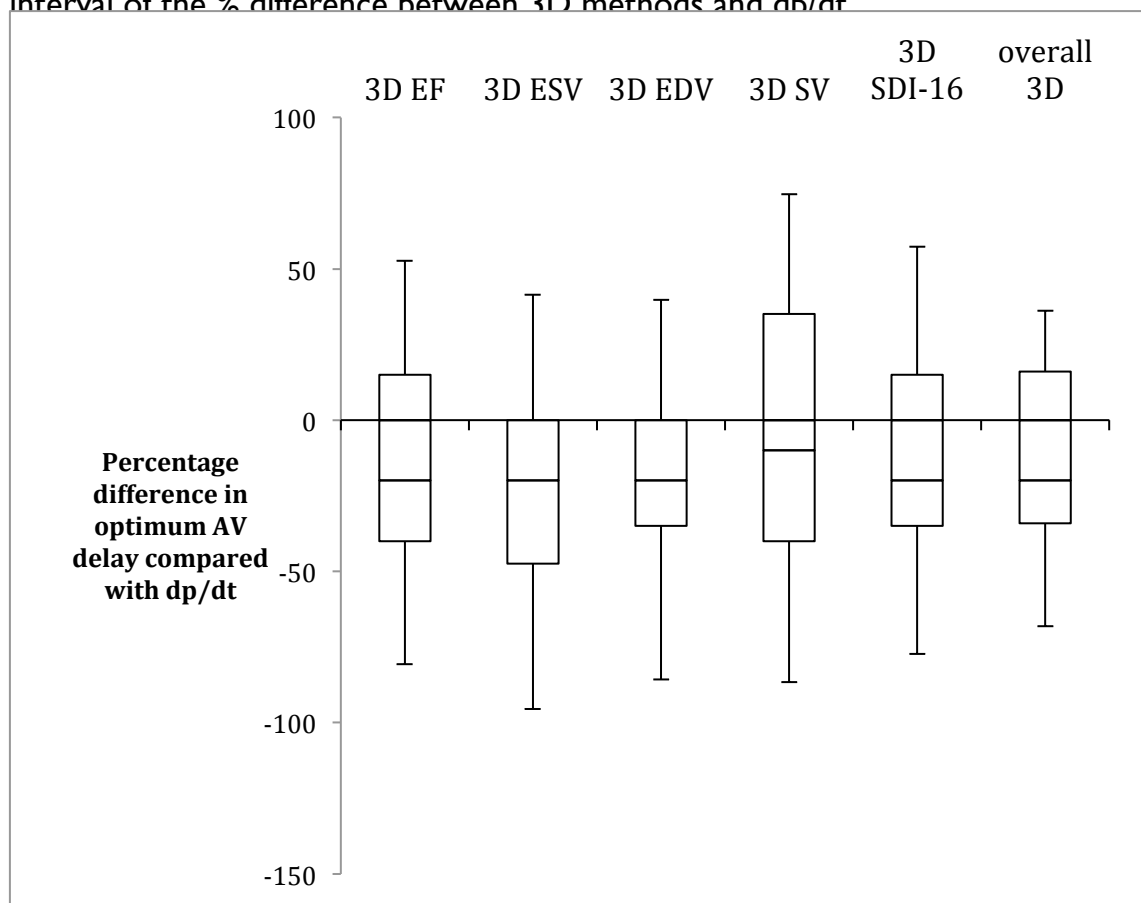


### 2.4.3 3-Dimensional echocardiography to determine optimum AV delay

The utility of 3-dimensional echocardiographic methods was determined by comparing the optimum selected AV delay with that determined by dp/dt. The mean optimum AV delay was shorter with all 3D methods than dp/dt by 16%, though this was not significant ( $p>0.05$ ). The ranges were wide suggesting a poor concordance in selecting the same AV delay as that by dp/dt. Figure 2.3 is a box plot showing the median, interquartile ranges and 95% confidence interval of the % difference between the methods.



Figure 2.3 – Box plot showing median, interquartile ranges and 95% confidence interval of the % difference between 3D methods and dp/dt



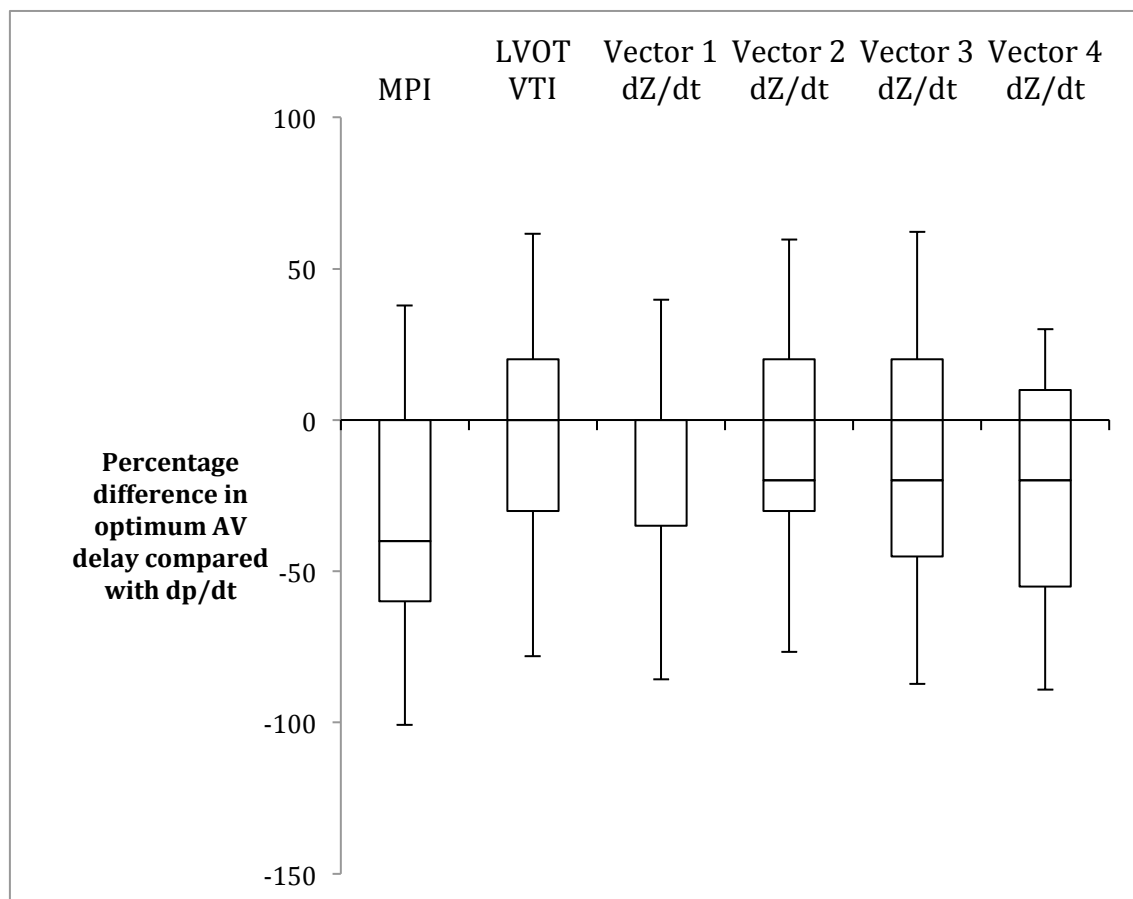
#### 2.4.4 Doppler echocardiography and Cardiac Impedance to determine optimum AV delay

The utility of Doppler and Cardiac Impedance methods was determined by comparing the optimum selected AV delay with that determined by dp/dt. The mean optimum AV delay was shorter with myocardial performance index (32%) and LVOT VTI (7%), though these were not significant ( $p>0.05$ ).

Similarly, all cardiac impedance vectors selected a shorter AV delay than dp/dt, though these were not significant ( $p>0.05$ ). Wide ranges for all measures suggest a poor concordance in selecting the same AV delay as that by dp/dt. Figure 2.4 is a box plot showing the median, interquartile

ranges and 95% confidence interval of the % difference between the methods..

Figure 2.4 – Box plot of difference in AV delay for each method against dp/dt. The box indicates the median difference and the interquartile range. The whiskers indicate the 95% confidence interval.



## 2.5 Conclusions

Simultaneous pressure-volume and cardiac impedance measurements were physically impossible using these techniques as intracardiac volume assessments are performed using impedance which physically interfered with simultaneous impedance measurements from the pacing system.

The agreement between pressure and cardiac impedance measurements in choosing the best atrioventricular delay was poor for right ventricular

and left ventricular pacing. Furthermore the agreement between these methods and echocardiographic methods was also poor. Finally, even within the modality of echocardiography there were discrepancies in the best atrioventricular delay between different measurements.

This study was not designed to investigate the reasons behind these findings. However, a number of different issues can be considered which may have been responsible for the variability seen.

Firstly, the role of homeostatic mechanisms governing cardiac filling. Alterations to the atrioventricular delay results in acute effects on cardiac filling and output, but compensatory mechanisms exist influencing venous return which may have an impact on cardiac output. Although Gold and colleagues have demonstrated the utility of  $dp/dt$  in selecting atrioventricular delays<sup>123</sup>, other studies by Whinnett and others have demonstrated that it is easier to select the best atrioventricular delay when making many measurements immediately following changes to the atrioventricular interval<sup>165</sup>.

Secondly, alteration of the atrioventricular delay was not performed in a randomized manner. The sequential assessment of AV delays from long to short may have influenced homeostatic mechanisms and is a limitation of the study.

Thirdly, the inherent variability of the methods used to assess the atrioventricular delay. If the variability is significant in comparison to the differences being measured, then chance alone might account for the different atrioventricular delays measured. Reproducibility of measurements such as LV  $dp/dt$  assessed by echocardiography was not performed in this study.

Thirdly, comparison of echocardiographic data acquired 3 days after implantation may be affected by loading conditions. Patients were fasted before their procedure and therefore likely to be intravascularly deplete.

Patients were not fasted for their echocardiogram so their intravascular volume is likely to have been different. Patients also found echocardiography after CRT implant uncomfortable. The wound remained tender and they were being asked to lie in a left decubitus position. This may have had an impact on the patients sympathetic tone. Furthermore, the alteration from sinus rhythm to biventricular pacing for three days prior to echocardiography may have had an impact on cardiac remodelling already and response to single ventricular chamber pacing.

Finally, the fact that the intervention was performed during atrial and ventricular pacing may be significant. Pacing 10 beats above the intrinsic sinus rate at time of implant means that many patients were paced at 70-90 beats per minute. The pattern of ventricular filling is strongly influenced by the heart rate and length of the diastolic interval. E and A wave fusion occurs at higher heart rates. The heart rates used here were physiological but significantly above that of the target resting heart rate and indeed actual resting heart rate in this cohort of patients.

## Chapter 3 RV mid-septal or apical pacing

### 3.1 Abstract

Right ventricular apical pacing leads to left ventricular dyssynchrony. Using real-time 3-dimensional echocardiography, we compared the effects of right ventricular apical and mid septal pacing on left ventricular contraction.

An observational cohort study was performed on 64 patients scheduled for pacemaker or defibrillator implant. Real time 3 dimensional echocardiography was performed both in intrinsic rhythm and during pacing.

Overall, pacing led to an increase in dyssynchrony and a fall in ejection fraction in both groups, though this was greater with apical pacing than with mid-septal pacing. Stratification by left ventricular function indicated that in patients with normal left ventricular function there was no difference between apical and septal pacing, whereas in patients with left ventricular dysfunction there was a greater increase in dyssynchrony and fall in ejection fraction with apical versus mid-septal pacing.

Real time 3-dimensional echocardiography enables the accurate assessment of left ventricular volumes, ejection fraction and dyssynchrony in patients with pacemakers. Apical pacing causes acutely increased dyssynchrony and lower ejection fraction than mid-septal pacing, though this appears to be limited to those patients with left ventricular dysfunction.

### 3.2 Introduction

Endocardial right ventricular apical pacing is the conventional method of delivering pacemaker therapy. However, this pacing has been demonstrated to lead to impaired cardiac output, left ventricular systolic

dysfunction<sup>71</sup>, long term structural changes as seen by histology<sup>166</sup> as well as increased morbidity and mortality<sup>25</sup>. Furthermore biventricular pacing has recently been demonstrated to improve outcomes compared to right ventricular apical pacing in patients with pre-existing left ventricular systolic dysfunction<sup>167</sup>.

These detrimental effects may be the results of dyssynchronous left ventricular contraction. Alternative locations for right ventricular pacing have been sought which may obviate some of these detrimental effects. The other locations that have been investigated include the right ventricular outflow tract, mid-septum, upper septum and septal-his bundle. The existing literature is conflicting with several studies indicating that right ventricular outflow tract pacing leads to better haemodynamics and less dyssynchrony<sup>72</sup>, though other studies have been unable to reproduce this<sup>80</sup> and there is no conclusive evidence of clinical benefit from alternate site pacing<sup>168,169</sup>. Three-dimensional and tissue Doppler echocardiographic dyssynchrony assessment has indicated that both right ventricular apical and outflow tract pacing leads to greater dyssynchrony than sinus rhythm<sup>83,170</sup>.

There are fewer data regarding mid-septal pacing and dyssynchrony. Cano and others investigated the effects of mid septal and apical pacing in patients with normal left ventricular ejection fraction after the first week of implant and at 6 and 12 months using tissue Doppler echocardiography<sup>171</sup>. Septal pacing was associated with less dyssynchrony than apical pacing at 12 months, though there were no changes in left ventricular ejection fraction or in clinical parameters. However Ng and others found increased circumferential strain dyssynchrony with chronic septal pacing compared to apical pacing and lower ejection fraction<sup>172</sup>. Part of this discrepancy may be accounted for by the heterogeneity in the site of pacing.

We hypothesised that pacing the right ventricular mid-septum would produce less dyssynchrony and greater left ventricular ejection fraction than right ventricular apical pacing as determined using real-time 3-dimensional echocardiography.

### 3.3 Methods

An observational parallel cohort study was performed on patients undergoing pacemaker or defibrillator implant. Patients were eligible for inclusion if they were over 18 and were scheduled for pacemaker or defibrillator implant. Patients who were pacing dependent were excluded.

Pacemakers or defibrillators were implanted using standard techniques, at the usual site preferred by the operator. Lead position was adjudicated by researchers after implant by reviewing fluoroscopy in both right anterior oblique 30 degree and left anterior oblique 40 degree projections, as well as post procedure radiographs.

The apical location was recorded if the tip of the lead was pointing downwards in an area within 2 cm distance from the apical border of the heart. The mid septal location was recorded if the lead tip was approximately at the level of the superior aspect of the tricuspid valve in the right anterior oblique projection, and was pointing toward the left ventricle in the left anterior oblique position, with an angle between 0 and 80 degrees<sup>173</sup> to ensure that the septum was being paced rather than the free wall or the anterior aspect of the right ventricle. Patients with leads outside these areas were excluded from the analysis.

In patients in sinus rhythm, the sensed atrio-ventricular delay was reduced to the minimum value to determine the ECG morphology of a completely paced beat, and then the sensed AV delay was increased to the either the longest value that allowed complete pacing without getting fusion, or to the nominal sensed atrio-ventricular delay was programmed

where this resulted in a completely paced beat. In patients in atrial fibrillation, the lower rate of the device was set to 10 beats per minute higher than the mean intrinsic rate. It is assumed that this eliminated fusion beats.

Echocardiography was performed during intrinsic rhythm and during pacing in all patients within 72 hours of implant. Philips iE 33 machines were used together with S5 and X3 transducers (Philips Healthcare, Guildford, Surrey, UK). Three-dimensional datasets were acquired over 4 or 7 consecutive beats during breath holding, depending on the ability of the patient to hold their breath. Image acquisition was optimised by adjusting depth to include the mitral valve annulus and exclude the left atrium, as well as adjusting the density of the scanning sector. Datasets were inspected for quality and stitching artefacts before storing. Datasets were stored on line and imported into Research Arena platform (TomTec Imaging Systems GmbH, Munich, Germany). Analysis was performed using LV analysis 2.7 (TomTec Imaging Systems GmbH, Munich, Germany). This software did not display the electrocardiogram enabling analysis to be performed by an operator blinded as to whether a dataset was acquired during intrinsic or paced rhythm. Furthermore, patients were excluded if the image quality of the dataset was inadequate. This was defined as datasets with stitch artefact, echocardiographic dropout of 4 or more segments, or poor endocardial definition of 4 or more segments.

Electrocardiography was performed during intrinsic and paced rhythm.

Results were recorded into a database created using Bento 2.0 (Filemaker, Inc, Santa Clara, California, USA) and analysed using Excel 2008 (Microsoft, Seattle, Oregon, USA), SPSS 19 (IBM Armonk, New York, USA) and GraphPad Prism 5.0 (GraphPad, La Jolla, California, USA)

Based on pilot data, a power calculation was performed to estimate the sample size required. Based on a mean baseline ejection fraction of 50%



and a standard deviation of 9%, it was estimated that 28 patients were required in a group to detect an absolute change in ejection fraction of 5% due to pacing with a power of 81% using a paired two-tailed Student's t-test. Adjustment for the variability of echocardiographic results was not made.

The results were analysed using two-tailed paired Student's t-tests within groups and unpaired Student's t-tests between groups.

### 3.4 Results

A total of 64 patients were recruited into the study. Six of these (9.4%) were excluded due to image quality. A further 3 patients were excluded because the right ventricular lead was sited at the right ventricular outflow tract. Baseline characteristics are listed in Table 3.1. The mean age of patients was 73 years in both groups  $p=0.49$ , with a similar prevalence between the groups of hypertension (36% and 37% in apex and mid-septal groups respectively  $p=0.92$ ), duration of the electrocardiographic QRS complex (109 vs. 117ms,  $p=0.41$ ), ischaemic heart disease (43% vs. 33%  $p=0.47$ ), valvular disease (7% vs. 26%  $p=0.06$ ) and high degree AV block (21% vs. 37%  $p=0.2$ ) as an indication for their device. Patients with apical leads were more likely to have diabetes mellitus (21% vs. 4%  $p=0.05$ ) and implantation of defibrillators (39% vs 7%  $p=0.01$ ) compared to patients in the mid-septal group.

There were no significant differences in procedure time or screening time between the groups. Mean implant duration and standard deviation was 92 +/- 29 minutes in the apical group compared to 90 +/- 28 minutes in the mid-septal group  $p=0.79$ . Similarly, fluoroscopy times were 7.3 +/- 4.0 minutes in the apical group and 9.5 +/- 7.1 minutes in the mid-septal group  $p=0.17$ .

Table 3.1 - Baseline characteristics. Asterix indicates p value <0.05

	Apex	Mid-septum
Total	28	27
ICD	39%(11)*	7% (2)
EF>50	54%(15)	48% (13)
High degree AV block	21% (6)	37% (10)
Mean age (years +/- SD)	72.8 +/- 12.3	73 +/- 13.2
IHD	43% (12)	33% (9)
DM	21% (6)*	4% (1)
Hypertension	36%(10)	37% (10)
Valve disease	7%(2)	26% (7)
Intrinsic QRS (msec +/- SD)	109 +/- 39	117 +/- 29

In intrinsic rhythm, there was no significant difference between the groups for end-diastolic and end-systolic volumes, ejection fraction or systolic dyssynchrony index, as listed in Table 3.2. With pacing, the end-diastolic volume fell by 6ml in the apical group and 7ml in the mid-septal group. However, there was a differential response in the end-systolic volumes between the groups with the end-systolic volume increasing with pacing in the apical group by 4ml, but falling by 2ml in the mid-septal group. The cumulative effect of these changes in volumes resulted in a significant fall in ejection fraction in both groups (paired t-test for change in EF  $p<0.001$  for both groups) as shown in figure 3.5, the magnitude of which was significantly greater in the apex group (absolute fall of 9% in apex group vs. 5% in mid-septal group,  $p=0.02$ ) as demonstrated in figure 3.2.

Apical pacing also led to a significantly higher SDI than mid-septal pacing (6.7 vs. 5.2,  $p=0.03$ ) as seen in figure 3.6. There was no difference in QRS duration with apical pacing than mid-septal pacing (156ms vs. 140ms,  $p=0.61$ ).

Table 3.2 - Effects of pacing at different locations. Asterix indicates P value <0.05

	Apex		Mid-Septal	
	Intrinsic	With pacing	Intrinsic	With pacing
EDV (ml +/-SD)	99 +/- 31	93 +/- 28	99 +/- 49	92 +/- 43
ESV (ml +/-SD)	52 +/- 22	56 +/- 22	53 +/- 40	51 +/- 34
EF (% +/- SD)	48 +/- 11	39 +/- 13*	50 +/- 10	45 +/- 10*
SDI (% +/- SD)	4.2 +/- 2.4	6.7 +/- 5.2*	4.9 +/- 3.0	5.2 +/- 2.7
QRS (ms +/-SD)	109 +/- 39	156 +/- 21	117 +/- 29	140 +/- 29

Figure 3.1 3D analysis of a patient in baseline rhythm. The upper left panel shows a short axis cut of the endocardial cast. The upper right panel shows the 4ch cut, and the lower left panel shows a bullseye plot. The volume graphs for each of 16 segments is shown in the lower right panel. There is very little dispersion in the time to minimum volume across the segments, indicating synchronous contraction. Ejection fraction was 47%, SDI 1.9%

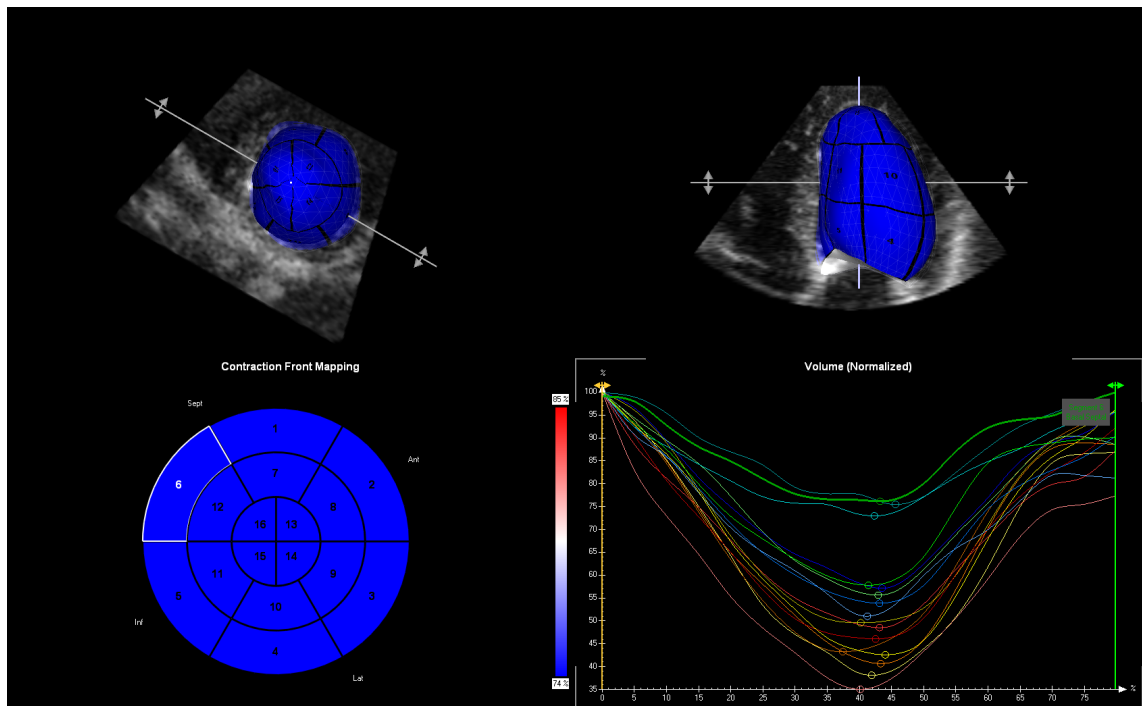


Figure 3.2. The same patient with apical RV pacing. There is now more dispersion seen in the time to minimum volume in the lower right panel. The EF was 39%, SDI 5.8%.

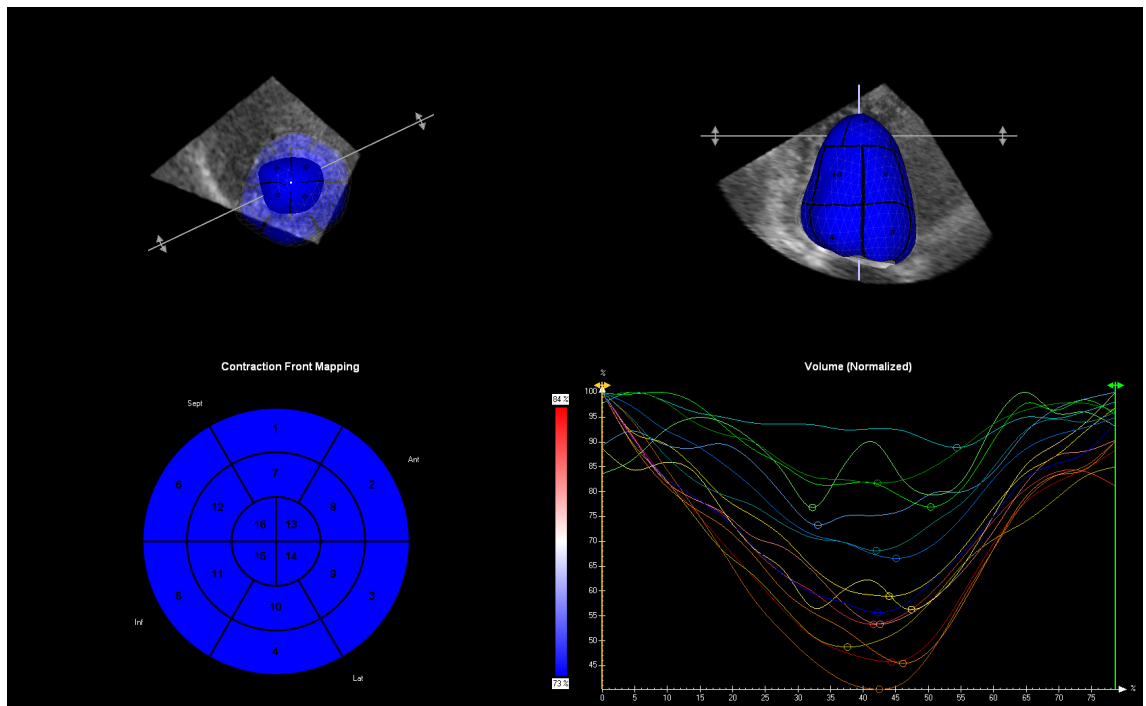


Figure 3.3 Another patient at baseline. EF is 63%, SDI 2.7%

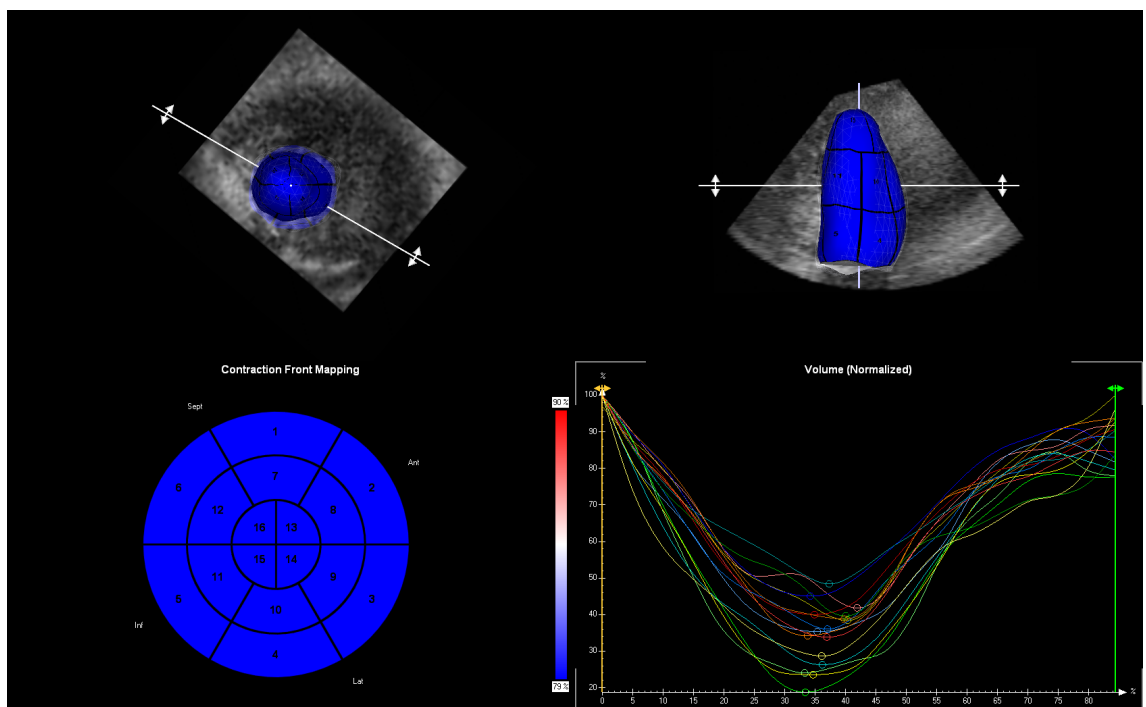
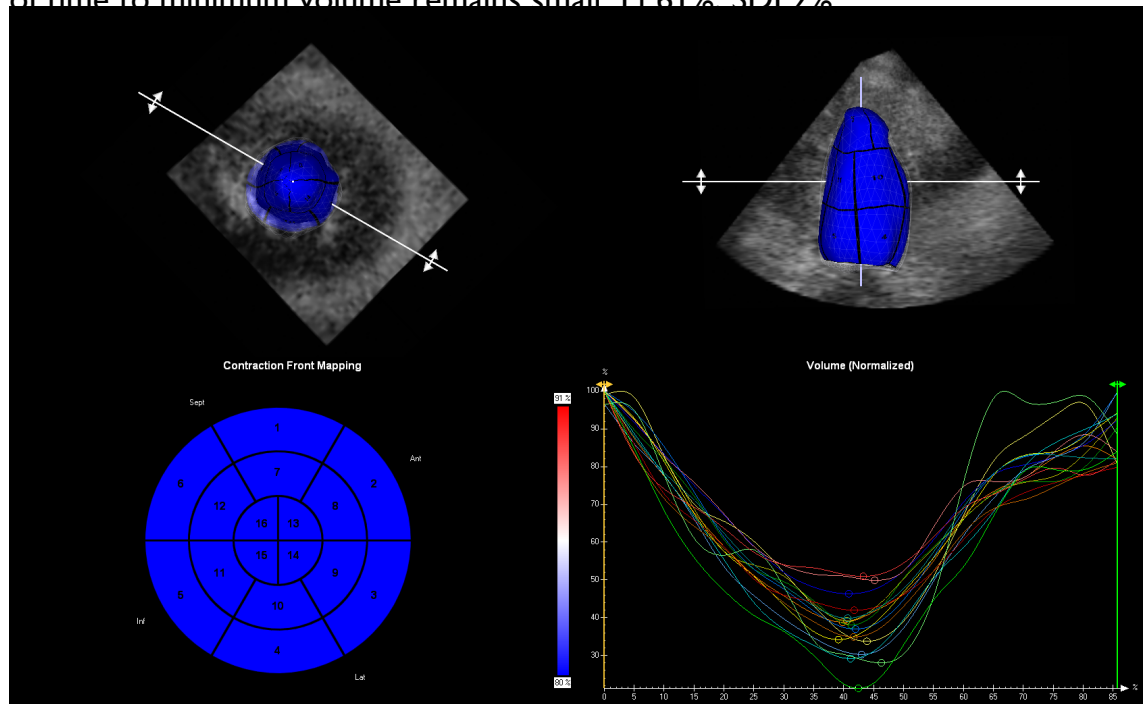


Figure 3.4. The same patient as 3.3 during mid-septal RV pacing. The dispersion of time to minimum volume remains small. Ef 61% SDI 2%



Both groups were further stratified by baseline ejection fraction, as summarised in tables 3.3 and 3.4. In 28 patients with a baseline ejection fraction of  $>50\%$ , both apical and mid-septal pacing led to a similar fall in end-diastolic volumes (8ml vs. 9ml), but no significant change in end-systolic volumes (3ml vs. 1ml). There was a significant fall in ejection fraction seen in both groups due to pacing (9% in apical group,  $p<0.001$ , 6% in mid-septal group  $p=0.008$ ), with no significant difference between the groups ( $p=0.19$ ). Apical pacing was associated with a mean SDI of 4.6, whereas mid-septal pacing led to an SDI of 4.3,  $p=0.29$ .

However, in 27 patients with a baseline ejection fraction  $<50\%$ , pacing from either apex or mid-septum did not appear to alter end-diastolic volumes (0 vs -5ml respectively  $p=0.39$ ), but apical pacing caused an increase in end-systolic volume, which was not seen with mid-septal pacing (6ml vs -1ml  $p<0.01$ ). Cumulatively this resulted in a significant fall in ejection fraction with apical pacing (9%,  $p=0.01$  paired t-test), but not

mid-septal pacing (4%,  $p=0.29$  paired t-test) but with no significant difference between the groups in ejection fraction (9% with apical pacing vs. 4% with mid-septal pacing,  $p=0.06$ ) or SDI (3.3% with apical pacing vs. 0.1% with mid-septal pacing,  $p=0.07$ ). Relative changes were statistically significant, with apical pacing resulting in a 23% relative fall in ejection fraction vs 6% in mid-septal pacing ( $p=0.03$ ) and the relative rise in SDI being 74% vs 15% ( $p = 0.03$ ).

Table 3.3 - Effects of pacing in patients with normal ejection fraction. Asterisk indicates  $p<0.01$

EF > 50%	Apex (n=14)		Mid- Septal (n=14)	
	Intrinsic	With pacing	Intrinsic	With pacing
EDV (ml +/-SD)	90 +/- 32	82 +/- 28	86 +/- 43	77 +/- 35
ESV (ml +/-SD)	40 +/- 17	43 +/- 17	37 +/- 19	36 +/- 17
EF (% +/- SD)	57 +/- 5	48 +/- 7*	57 +/- 3	52 +/- 6*
SDI (% +/- SD)	2.9 +/- 1	4.6 +/- 2.7	3.8 +/- 2.1	4.3 +/- 2.0
QRS (ms +/- SD)	100 +/- 28	155 +/- 23	111 +/- 30	126 +/- 23

Table 3.4 - effects of pacing in patients with low ejection fraction

EF < 50%	Apex (n=14)		Mid- Septal (n=13)	
	Intrinsic	With pacing	Intrinsic	With pacing
EDV (ml +/- SD)	108 +/- 29	108 +/- 23	112 +/- 53	107 +/- 47
ESV (ml +/- SD)	64 +/- 19	72 +/- 17*	68 +/- 49	67 +/- 39
EF (% +/- SD)	39 +/- 8	30 +/- 10*	42 +/- 10	38 +/- 9
SDI (% +/- SD)	5.5 +/- 2.7	8.8 +/- 6.2	6.1 +/- 3.4	6.2 +/- 3.1
QRS (ms +/- SD)	122 +/- 50	159 +/- 18	123 +/- 28	152 +/- 29



Figure 3.5 - Figure 1. Box and whisker plot showing LV ejection fraction during intrinsic rhythm and pacing in apex and mid-septal regions. Paired t-test indicates a significant fall in ejection fraction in both groups,  $p < 0.01$

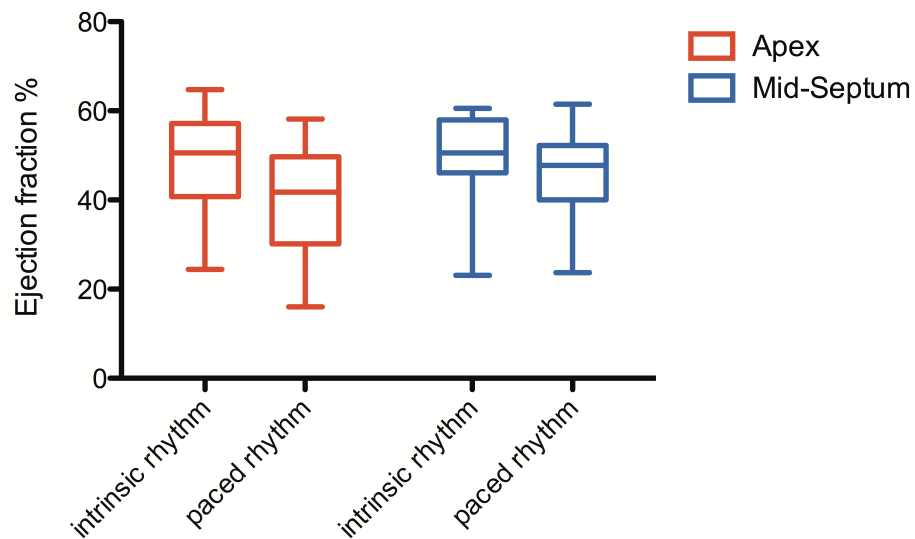


Figure 3.6 - Box and Whisker plot showing change in LV ejection fraction due to pacing in apex and mid-septal regions. Box indicates 25th and 75th percentiles with whiskers indicating 5th and 95th percentiles. P value for difference = 0.02.

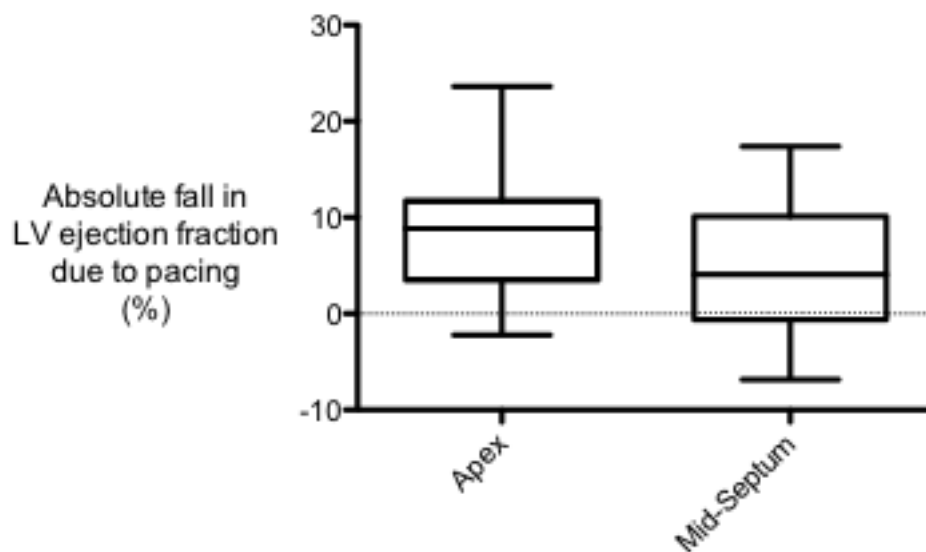


Figure 3.7 - Box and Whisker plot showing change in SDI due to pacing in apex and mid-septal regions. Box indicates 25th and 75th percentiles with whiskers indicating 5th and 95th percentiles. P value for difference between apex and mid-septum = 0.03.

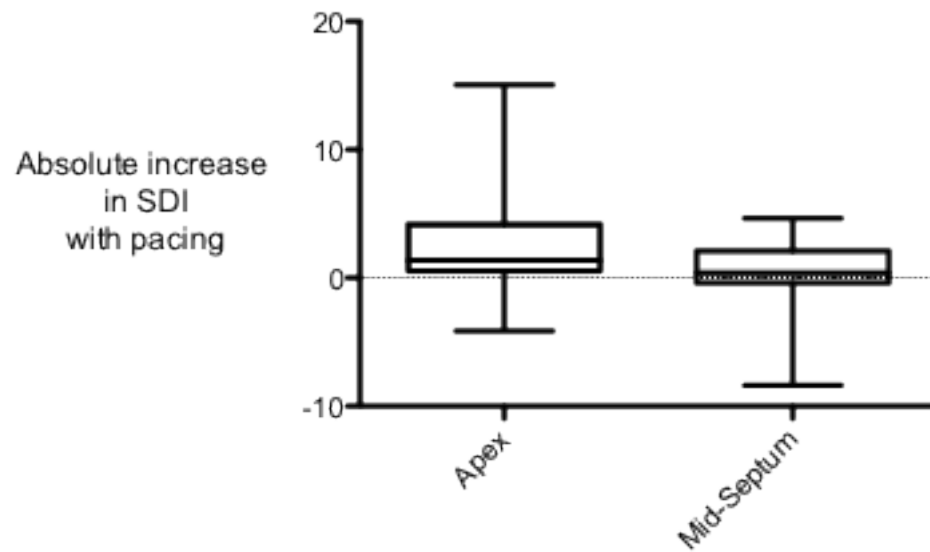
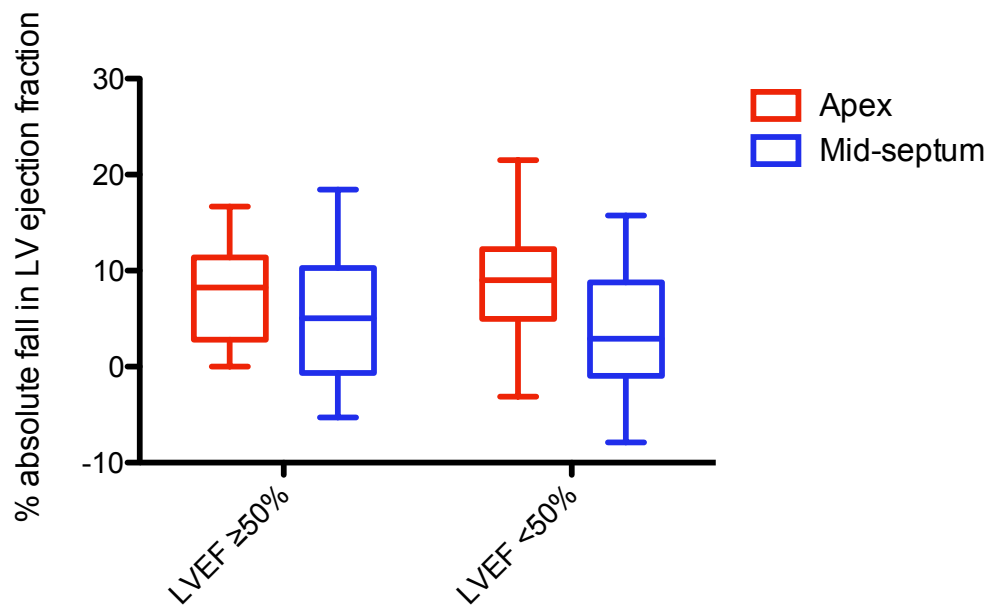


Figure 3.8 - Box and Whisker plot showing absolute change in LV ejection fraction due to pacing in apex and mid-septal regions, stratified by baseline LV ejection fraction. Box indicates 25th and 75th percentiles with whiskers indicating 5th and 95th percentiles. P value for difference between apex and mid septum in patients with low baseline LV ejection fraction = 0.03.



### 3.5 Conclusions

These data demonstrate that pacing causes an acute fall in left ventricular ejection fraction when measured using real-time 3-dimensional echocardiography. This appears to be due to falls in the end-diastolic volume as well as changes in the end-systolic volume. The magnitude of change is greater in patients who are paced from the right ventricular apex than the right ventricular aspect of the mid inter-ventricular septum. Furthermore, this acute difference appears more pronounced in patients with a low baseline ejection fraction of <50%. These alterations in volume and ejection fraction are accompanied by a corresponding increase in the systolic dyssynchrony index, suggesting that increased dyssynchrony may be a cause of the alterations in volume and ejection fraction seen.

Another technical explanation that might account for part of the alterations in volumes observed is that pacing may alter the triggering of the echocardiographic acquisition. Multi-beat acquisition requires the scanning matrix to be repositioned before the start of the next beat resulting in loss of part of diastole. Normally, acquisition is performed by triggering the acquisition on the peak of the electrocardiographic R wave. However, during pacing, triggering frequently occurs on the pacing spike, before the R wave. This will bring forward the acquired part of the cardiac cycle, and therefore true end-diastole may be missed. This might account for the smaller end-diastolic volumes seen with pacing in both groups, however, it is unlikely to have had a significantly different effect between the two groups and is therefore unlikely to be the sole reason for the observed changes in volumes and ejection fraction.

This study is limited in that although dataset analysis was blinded, patients were not randomly assigned to either group. The baseline characteristics indicate that there was a greater prevalence of diabetes and implantable defibrillators in the apical group, indicating that the groups are different. The rationale behind lead site selection for defibrillator leads may be different to that for pacing leads. Defibrillator leads are not expected to pace the heart frequently, and they are required not only to sense and pace the heart but also allow a good vector for defibrillation energy delivery to the ventricular myocardium. Furthermore, there is little published data regarding the placement of defibrillator leads outside the apical site. However, the fact that this was an acute study means that long-term differences in the frequency of pacing is unlikely to have impacted on the results.

The subgroup analysis suggests that patients with impaired left ventricular function are more sensitive to the effects of pacing, particularly from the apex. This study cannot elucidate the mechanism for this, but it generates a hypothesis to be tested in future studies. For clinical care, it is

important that the group of patients with mild to moderately impaired left ventricular function continue to be studied to determine the optimal pacemaker therapy for them. The recent Block-HF trial indicates that biventricular pacing is superior to right ventricular apical pacing in patients with impaired LV function<sup>167</sup>. Septal pacing is less complex than biventricular pacing and requires a similar implant time as conventional apical pacing. It therefore would be an interesting comparator against biventricular pacing in patients with impaired LV function.

Follow-up of our cohort might demonstrate longer term differences in LV function, but would be confounded by differences in the percentage of ventricular pacing between patients as well as the effects of revascularisation or changes in valvular function.

This study has demonstrated that it is feasible to assess left ventricular function before and after pacing using real-time 3 dimensional echocardiography. This technique has a great deal to offer in the long-term follow up of patients with pacemakers as it is accurate, non-invasive, does not require radiation, is becoming widely available and is safe. Whilst pacemakers have now been developed which allow MRI scans to be performed, they are not yet universally available from all manufacturers and have a cost implication so this modality will not be routinely available in pacemaker patients for some years to come. In the interim, 3-dimensional echocardiography offers the best technique to follow and study pacemaker patients.

## Chapter 4 Do we need to optimise?

### 4.1 Abstract

Cardiac resynchronisation therapy has entered clinical practice with the routine use of echocardiography guided optimisation of pacemaker stimuli.

An observational cohort study was performed of 145 patients scheduled for cardiac resynchronisation therapy. Real time 3 dimensional echocardiography was performed at baseline, early after cardiac resynchronisation therapy and before and after Doppler echocardiographic optimisation.

There was improvement in LV systolic function after CRT. The SDI at baseline and the change in SDI with CRT were statistically significant predictors of echocardiographic response. There was no good correlation between any parameters and the response to optimisation, though the frequency of echocardiographic response to optimisation was higher in those patients who remained dyssynchronous after CRT.

### 4.2 Introduction

Cardiac resynchronisation therapy has been demonstrated to be an effective treatment in selected patients with heart failure. Nevertheless, a clinical response is not seen in approximately 30% of patients. Strategies to improve response rates are therefore attractive. The initial trials of CRT implantation such as CARE-HF required optimisation of atrioventricular delays, and this has therefore entered clinical practice<sup>34</sup>. Numerous small clinical trials have demonstrated that optimisation of atrio-ventricular and, to a lesser degree, inter-ventricular delays can acutely improve cardiac output<sup>120,126,137,139,174</sup>. However, a larger scale trial SMART-AV which randomised patients to an empirical AV delay, echocardiographically

optimised AV delay or intracardiac electrogram optimised AV delay did not show significant benefits of optimised delays over an empirically programmed delay<sup>135</sup>. This has cast doubt on the clinical utility of atrioventricular optimisation.

There are a number of reasons why CRT optimisation may not be clinically useful. Firstly, the increment in cardiac output achieved by optimisation may be clinically negligible. Secondly, methods of optimisation may not be reliable enough to be reproducible. Finally, the optimised setting may change over time and in different patient situations such as exercise or volume status.

We hypothesised that CRT optimisation was of greater benefit in the sub-group of patients who remained dyssynchronous after CRT implantation, rather than in those patients in whom CRT had restored synchronous left ventricular contraction. We sought to identify this group by performing an observational cohort study where all patients underwent echocardiographic CRT optimisation. Stratification of echocardiographic response to optimisation was performed on the basis of real-time 3D echocardiographic dyssynchrony assessment early after CRT implantation.

## **4.3 Methods**

### **4.3.1 Patients**

Patients scheduled for CRT implant between 2008 and 2012 were recruited into this study. All patients were eligible and gave permission for their clinical records and the data acquired during clinical echocardiography to be analysed for research purposes. Demographic information, prior medical history, medication use and the results of functional assessment and quality of life questionnaires were gathered from the patient records. Approval for this study was obtained from the institutional review committee.

### 4.3.2 Study Procedures

Baseline testing of patients included clinical assessment to determine the New York Heart Association Class of heart failure severity. A 12 lead ECG was performed together the completion of the Minnesota Living with Heart failure questionnaire and measurement of the six minute hall walk distance. The definition of left bundle branch block was as described by the World Health Organisation

Patients underwent 3-dimensional echocardiography as previously described<sup>54</sup>, as part of their work-up for CRT. CRT was implanted using conventional transvenous methods. After implantation, 3-dimensional echocardiography was performed within 72 hours prior to hospital discharge. All patients were offered CRT optimisation at a median of 3 months after implantation. This time period was chosen clinically to allow a degree of remodelling to have occurred prior to optimisation and therefore that the settings determined at implant were likely to be appropriate for a longer future period. Subsequent optimisations were scheduled at the discretion of the clinicians, but were not included in this study. Patients were assessed at every visit to the hospital for device follow up and long term follow up was determined at the latest contact before May 2014.

Optimisation was performed using a standard protocol as described below. Before optimisation 3-dimensional left ventricular volumes were acquired. Subsequently atrioventricular optimisation was performed using pulsed wave Doppler echocardiography. The CRT device was interrogated to determine if the device was predominantly sensing atrial activity or pacing the atrium, and therefore determine if the sensed atrioventricular delay or the paced atrio-ventricular delay were to be optimised. If the patient was in atrial fibrillation, the optimisation of the atrio-ventricular interval was impossible. The longest atrioventricular interval that allowed



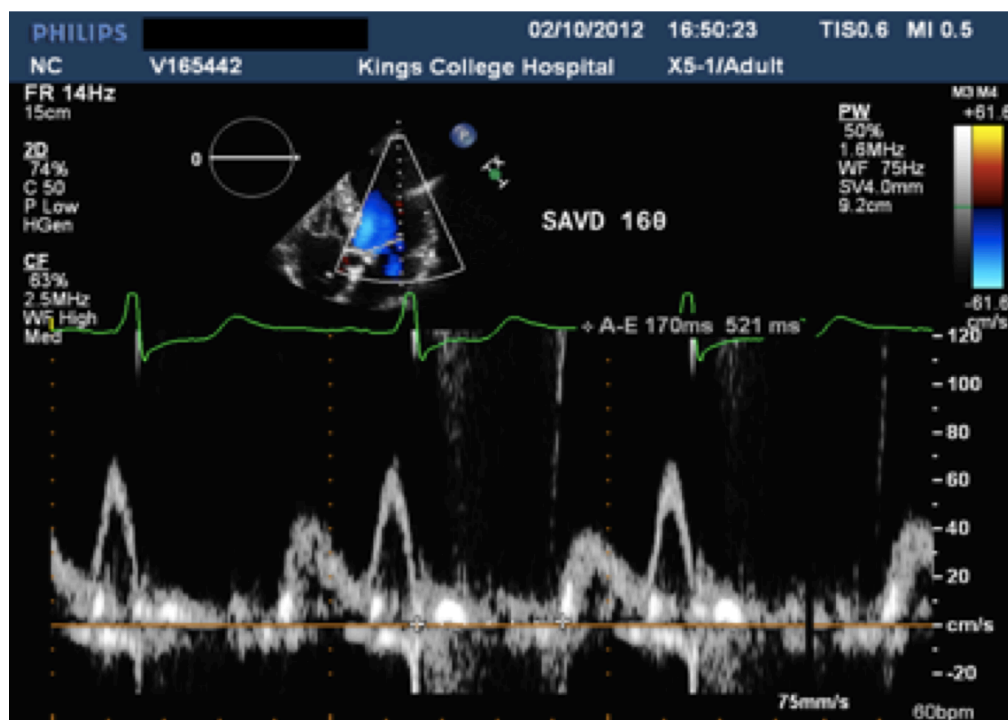
capture of the ventricle was determined on the basis of the surface ECG. This atrioventricular interval was programmed and measurements were performed. The interval was subsequently decreased in 20 millisecond steps and measurements were performed at each of these intervals.

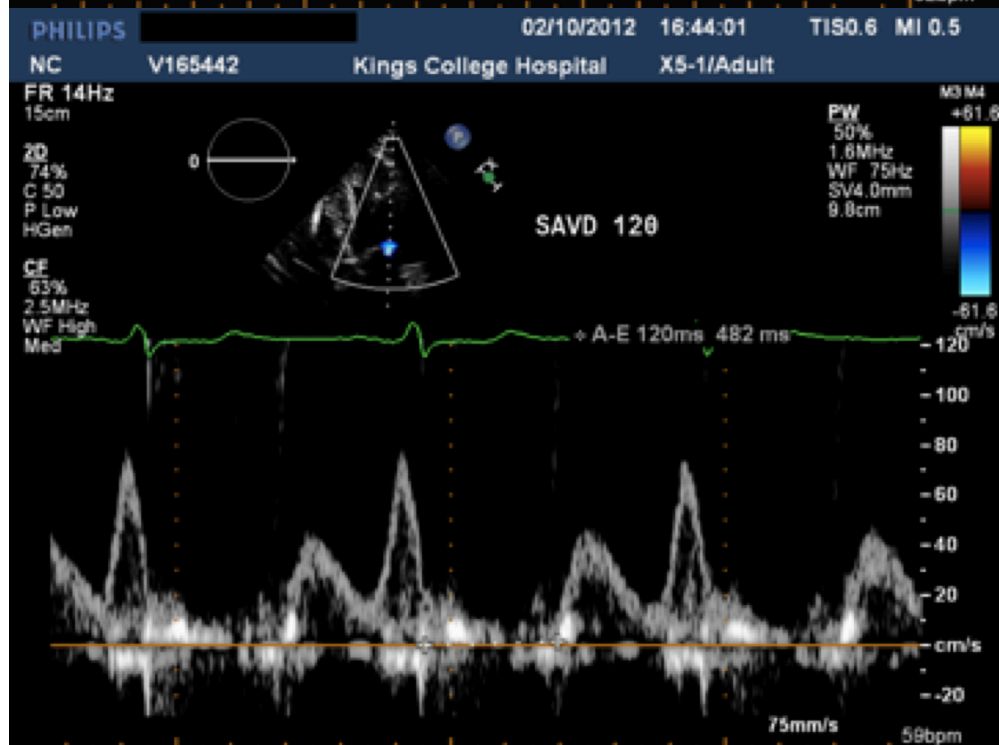
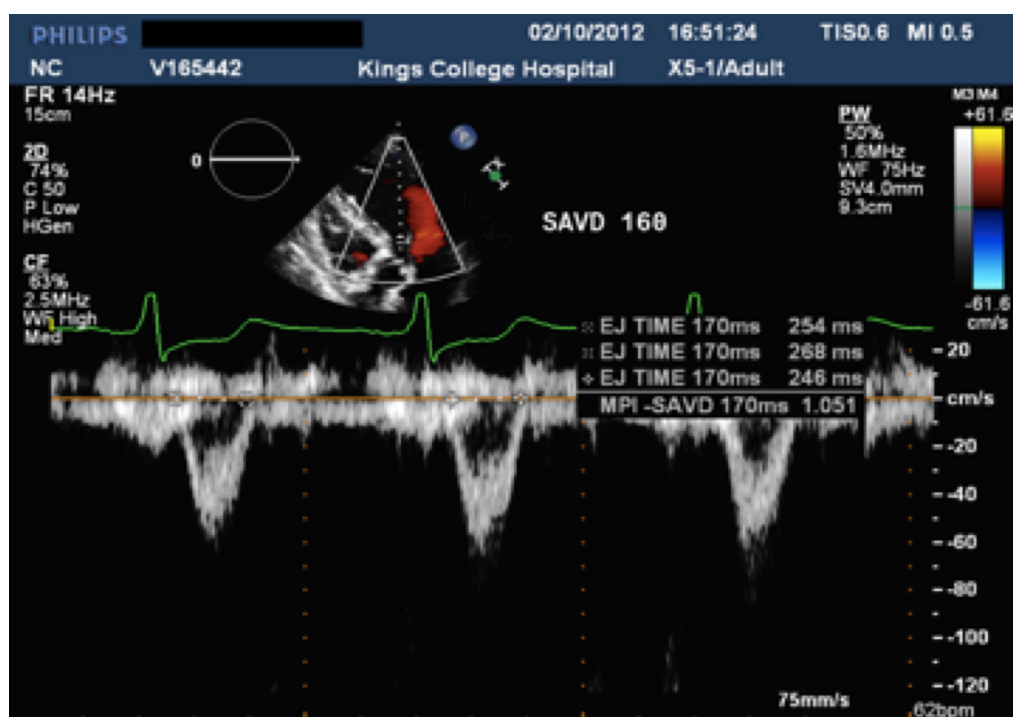
Pulsed wave Doppler was used to interrogate mitral inflow just below the level of the mitral valve leaflet tips. Because of the dilatation of the mitral annulus that is frequently seen in CRT patients, which results in the direction of peak flow being at an angle to the cardiac axis, care was taken to align the signal as parallel to the direction of flow as possible, as determined by colour flow imaging. The mitral valve leaflet closure artefacts were avoided as these may occur prior to true valve closure if the anterior mitral valve leaflet crosses the sample volume prior to leaflet closure. Similarly pulsed wave Doppler was performed in the left ventricular outflow tract, just below the aortic valve. At least 3 waveforms were recorded, during the same phase of respiration that afforded the best image quality. Ventricular or atrial ectopic beats and the 2 subsequent beats were excluded because of the effects of the ectopic beats on ventricular filling. Changes to the atrioventricular interval were made, and subsequent cardiac cycles acquired before manual measurement of the waveforms was performed. This minimised the time taken to acquire the waveforms and to minimise variation due to differences in location of the pulsed volume sample.

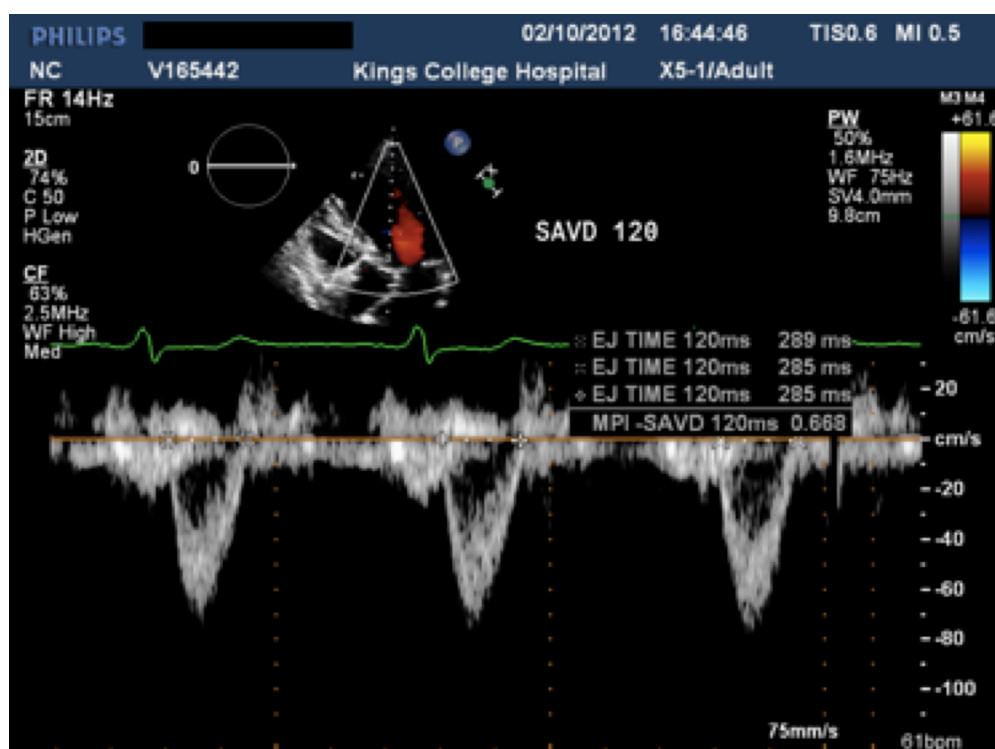
Measurements were made to calculate the myocardial performance index (MPI). This is a measure that is independent of heart rate and is a measure of cardiac efficiency. The index is the ratio of the duration of the isovolumic time to the ejection time, with a lower number indicating more efficient cardiac contraction. This measure takes into account alterations in the ejection phase that occur as the atrioventricular interval is manipulated. This is calculated by the measurement of the time interval between the end of the A wave and the beginning of the E wave (A-E time) using mitral

inflow pulsed wave Doppler. This interval is the time period when the ventricle is not filling. The time for ejection was also measured (Ej time) using left ventricular outflow tract pulsed wave Doppler. The Ej time was subtracted from the A-E time to give the isovolumic time, and divided by the Ej time, giving the MPI. The echocardiography machine was programmed with this formula to calculate the MPI. The MPI was calculated for each interval using averages of 3 measured cardiac cycles. The lowest figure was taken to reflect the optimum atrioventricular interval and this was therefore programmed<sup>175</sup>.

Figure 4.1 Four images demonstrating the calculation of the Myocardial performance index. The A-E time is measured at least 3 times. The Ejection time is also measured at least 3 times. The echo machine has been programmed to automatically calculate the average MPI. The panels show a measurement at 2 example sensed AV delays of 160ms and 120ms. 120ms is determined to be the optimum setting with an MPI of 0.67, as compared to 160ms which has a higher MPI of 1.05







Subsequently, inter-ventricular optimisation was performed. The CRT device was programmed to an inter-ventricular delay of 0ms, and the delay was varied in 15ms increments up to 60ms. If the CRT device was unable to program these intervals, the closest programmable interval to these settings was used. The atrio-ventricular delay was kept at the value determined in the previous step, but was defined as the time between the atrial event and the first subsequent ventricular pacing stimulus. CRT devices from different manufacturers calculate the atrio-ventricular delay differently - for example, Boston Scientific devices define the atrio-ventricular delay with respect to the timing of the right ventricular pacing stimulus, not the first ventricular stimulus, so the programming of the device took this into account where applicable. Blood flow through the left ventricular outflow tract was measured using pulsed wave Doppler. Again, acquisition of at least 3 cardiac cycles during the same phase of respiration was performed, with serial acquisitions at different inter-ventricular delays being performed before the waveforms were traced to minimise the

potential for changes in the pulse volume location. An observer identified several individual points on the waveform with the software joining these points with a straight line to trace the borders of the waveforms. The area of the waveform is the integral of velocity over time and gives the stroke distance. The best inter-ventricular delay was taken to be the delay with the maximum average stroke distance. To mitigate against variability, subsequently further acquisitions were performed at an inter-ventricular delay of 0ms and at the best inter-ventricular delay in the previous step. The best inter-ventricular delay was accepted as the optimum inter-ventricular delay if the stroke distance was again measured to be greater than that at an inter-ventricular delay of 0ms. 3-dimensional echo left ventricular volumes were acquired at the optimum inter-ventricular delay.

Analysis of 3-dimensional volumes was performed off line using TomTec LV analysis software V2.7. Furthermore, the observer subjectively graded the image quality of the volumes into categories of good, fair or poor. Datasets were deemed not analysable if 4 or more segments were not visualised throughout the cardiac cycle or if there was significant stitch artifact. Twelve datasets were further analysed by another operator to assess inter-observer variability.

Data was collected on aetiology of heart failure, New York Heart Association functional class, 6 minute hall walk distance and Minnesota Living with heart failure questionnaire.

### **4.3.3 Outcome measures**

Left ventricular ejection fraction was assessed using 3D echocardiography prior to optimisation. The change from baseline was used as a medium term response to CRT therapy. Immediately after optimisation left ventricular function was assessed using 3D echocardiography. This allowed the immediate change due to optimisation to be measured. Long term symptomatic response was assessed using New

York Heart association functional class and the Minnesota living with heart failure questionnaire prior to CRT implantation, at optimisation and at long term follow up. Six minute hall walk distance was also measured prior to implant and at optimisation. Data was collected regarding death and hospitalisation.

#### **4.3.4 Statistical analysis**

Inter-observer variability was assessed by initially using the Shapiro Wilkins test to verify the normality of distribution of each variable. Where the variable was not normally distributed a square root transformation was performed to restore normality. The single measures intraclass correlation coefficient (ICC) was calculated. A Bland-Altman analysis was also performed to assess the mean difference between observers and the limits of agreement.

The response to cardiac resynchronisation therapy was assessed using a repeated measures analysis of variance with Maunchly's Test of sphericity and correction with Greenhouse-Geisser estimates where appropriate. Individual determinants of response were investigated using a univariate analysis of variance.

To investigate the utility of post CRT SDI measures to predict the outcome of CRT optimisation it was decided that the best echocardiographic outcome metric was the 3D assessment of left ventricular function. Alternative metrics such as a change in device settings such as AV and VV delay was deemed inappropriate as it does not quantify the effect of altering the settings. Furthermore Doppler echocardiographic indices were deemed inappropriate because these indices were used to determine optimum device settings.

The production of a receiver operating characteristic curve for the outcome of CRT optimisation was considered, but this requires

dichotomising the outcome into response or non-response. As the outcome measure has a degree of noise in the signal, dichotomising the outcome measure may be incorrect and also loses the magnitude of change elicited.

Therefore the best method was deemed to be the use a cut-off determined from previous work. Kapetanakis et al demonstrated the likelihood of response to CRT was low in patients who had an SDI value of less than 7.5 prior to CRT<sup>112</sup>. This value was therefore investigated as a cut-off for response to CRT optimisation. The cohort was dichotomised on this basis and the mean change in ejection fraction after optimisation compared. Levene's test for equality of variances was used followed by a two tailed homoscedastic Students T-test

The Shapiro-Wilk test was used to verify if residuals obtained on analysis of variance did approximate a normal distribution. If the distribution was not normal, the variables were mathematically transformed to restore normality before analysis. Categorical variables were compared using Chi squared or Fisher's exact tests, as appropriate. Paired continuous variables were compared using paired Student's t tests. Where more than 2 repeated measures were available a repeated measures ANOVA was performed together with Maunchly's test of sphericity and correction with Greenhouse-Geisser estimates as appropriate. Survival curves were plotted using the Kaplan-Meier method and compared using a log-rank test. The mean duration of follow-up was computed using the reverse Kaplan-Meier method. Statistical analyses and figures were obtained using PASW version 19.0 (IBM, Bois-Colombes, France) and GraphPad Prism (GraphPad Software, La Jolla, CA).

## 4.4 Results

Of 145 consecutive patients undergoing CRT, 3D echocardiography was attempted in 129 and successful in 96. Twelve patients were excluded because of software incompatibility. A total of 84 patients therefore entered

the study. Full echocardiographic data was available in 74 because 7 died before optimization, 1 patient refused post procedure echocardiography and 2 patients did not attend optimization despite repeated invitations.

#### 4.4.1 Baseline Characteristics

Table 4.1 Baseline Characteristics

Male sex no (%)	63 (76)
Age – yr	71.1 +/- 10.8
Left ventricular ejection fraction - %	24.0 +/- 8.4
Sinus Rhythm – no (%)	59 (71)
QRS duration – msec	160 +/- 23.8
QRS pattern	
LBBB – no (%)	69 (83)
RBBB – no (%)	7 (8)
NSIVD – no (%)	4 (5)
NYHA class – no (%)	
I	4 (5)
II	14 (17)
III	56 (67)
IV	7 (8)
Cardiomyopathy – no (%)	
Ischaemic	42 (51)
Dilated Cardiomyopathy	34 (41)
Other	6 (6)
Minnesota Living with Heart Failure Questionnaire score	39.5 +/- 23.2
Betablocker use – no (%)	66 (80)
ACE or ARB use – no (%)	78 (94)
MRA use – no (%)	42 (51)



#### 4.4.2 Inter-observer variability.

Twelve patients were randomly selected for repeat analysis of 3D echocardiographic datasets by another operator. Single measures Intraclass correlation coefficients (ICC) for ejection fraction, end systolic volume and systolic dyssynchrony index were calculated. The ICC for ejection fraction was 0.870 with a 95% confidence interval of 0.611 to 0.961. The ICC for end systolic volume was 0.894 with a 95% confidence interval between 0.684 to 0.968. The Shapiro Wilkins test demonstrated that SDI was not normally distributed ( $p=0.033$ ) and therefore a square root transformation of the values was performed to restore normality. The single measures ICC for SDI (square root transformed) was 0.927. A Bland Altman analysis was also performed to calculate the mean difference between operators. For SDI the mean difference was -0.1.

#### 4.4.3 Response to CRT

Ejection fraction was measured at baseline, within 72 hours of CRT and before and after optimisation at a median of 105 days post CRT. There was an increase in ejection fraction seen at each time point. This is illustrated in Graph 4.1. The series of figures 4.2 to 4.5 demonstrate a single patient at baseline, early after CRT and before and after optimisation. The Ejection fraction was normally distributed and the serial change in ejection fraction was statistically significant with a  $p$  value of  $<0.001$  (repeated measures ANOVA test with Greenhouse-Geisser correction).

Figure 4.2 3D assessment of a single patient at baseline. The upper left panel shows a short axis view of the endocardial case, the upper right a long axis view. The lower left panel is a bulls eye plot of all 16 segments. The activation wavefront is seen over the endocardial casts. Individual segmental motion is plotted in the lower right panel. The ejection fraction was 16% and SDI 14.0%

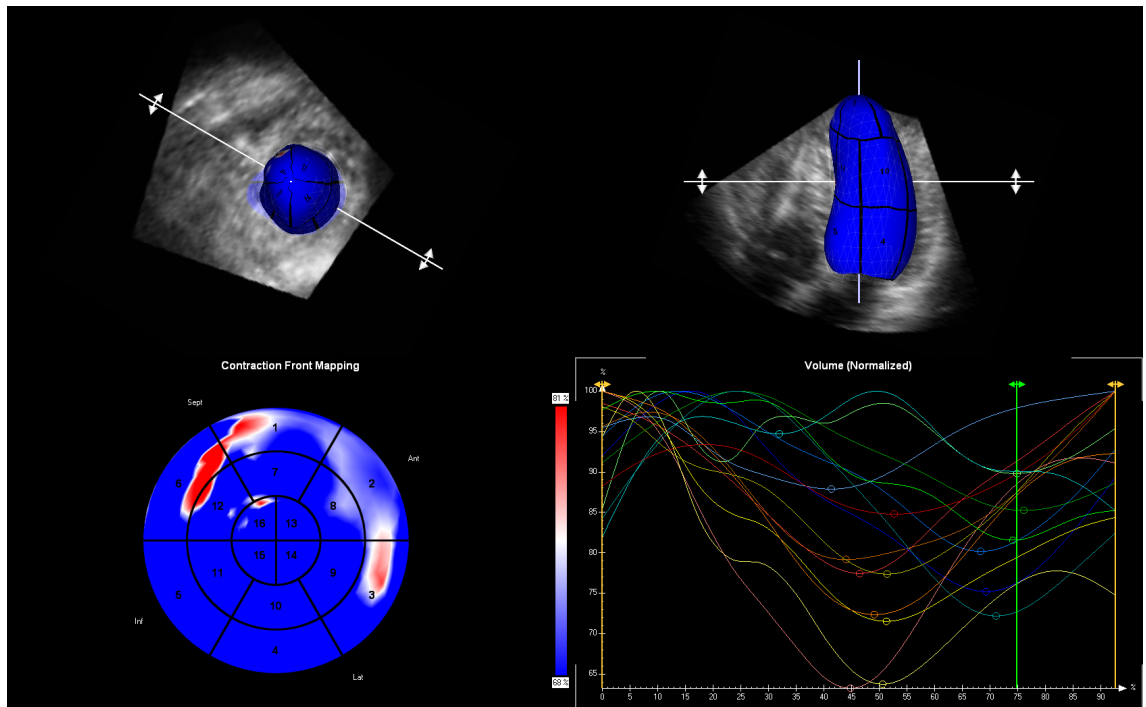


Figure 4.3 3D assessment of the same patient after CRT. The panels are in the same order as Figure 4.2. The graph indicates some improvement in dyssynchrony. The EF was 26% and SDI 7.7%.

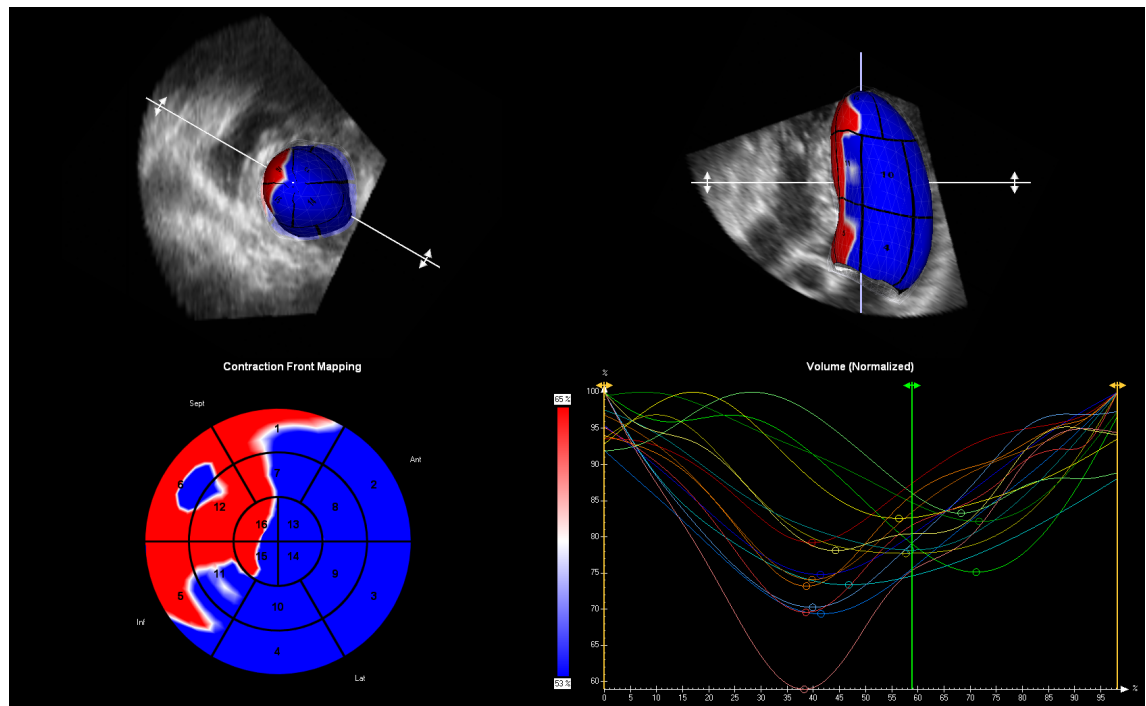


Figure 4.4 The same patient before optimisation. In this figure the lower right panel gives the numerical results.

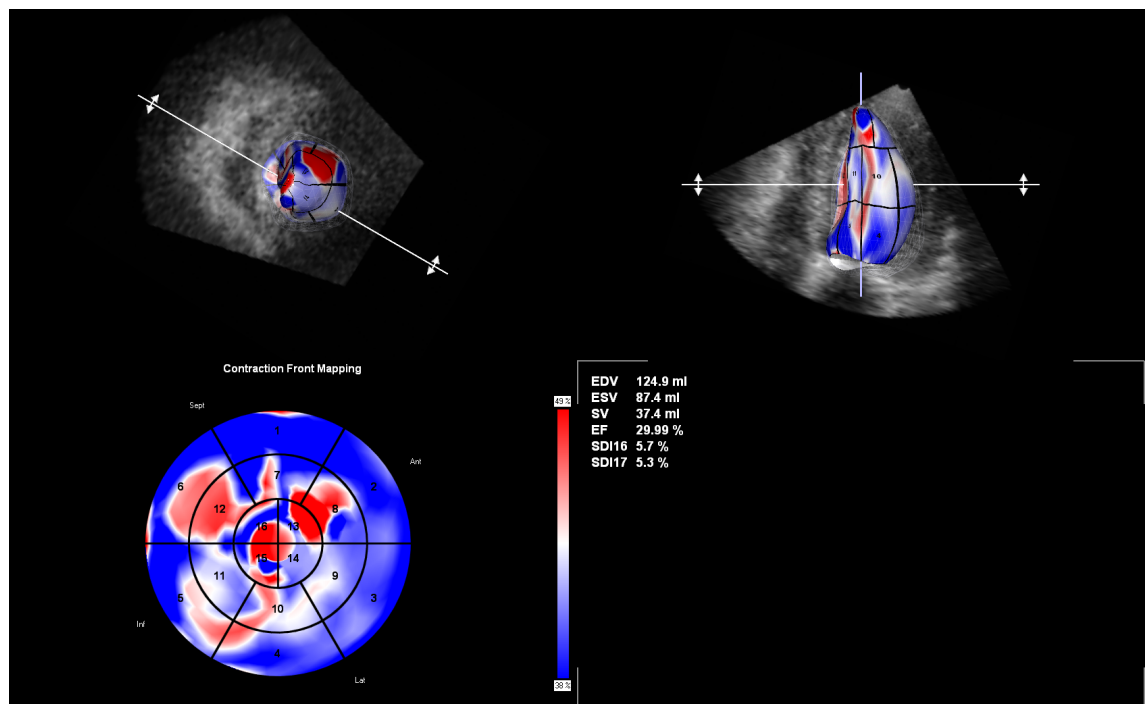
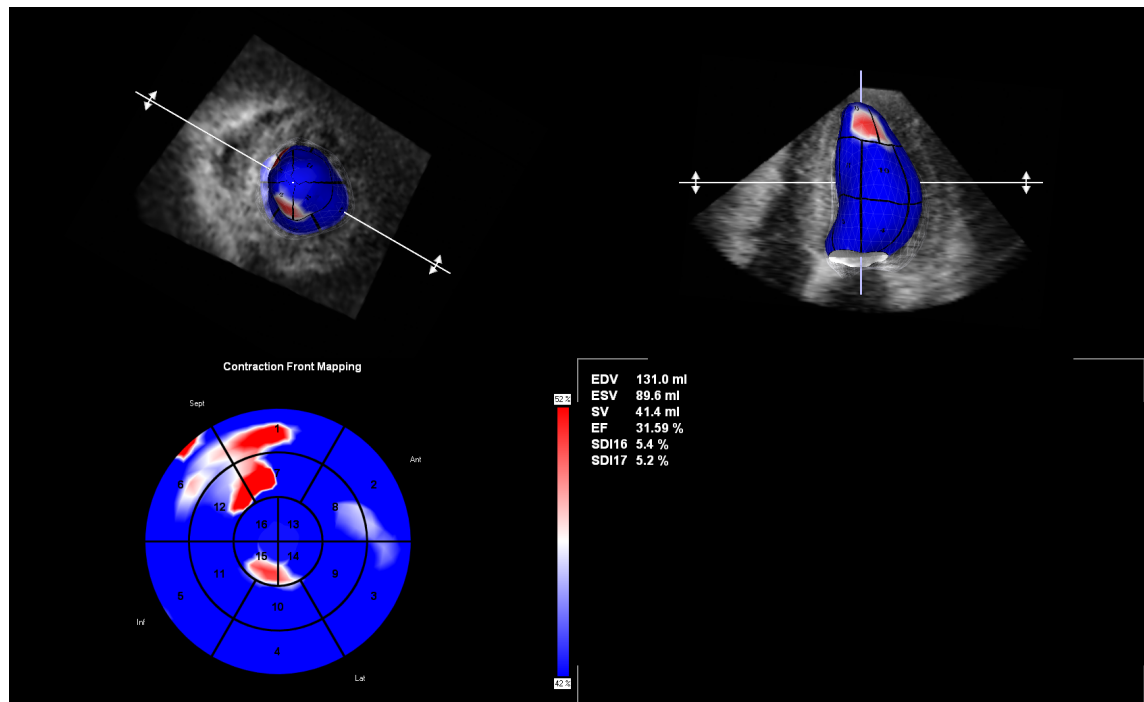
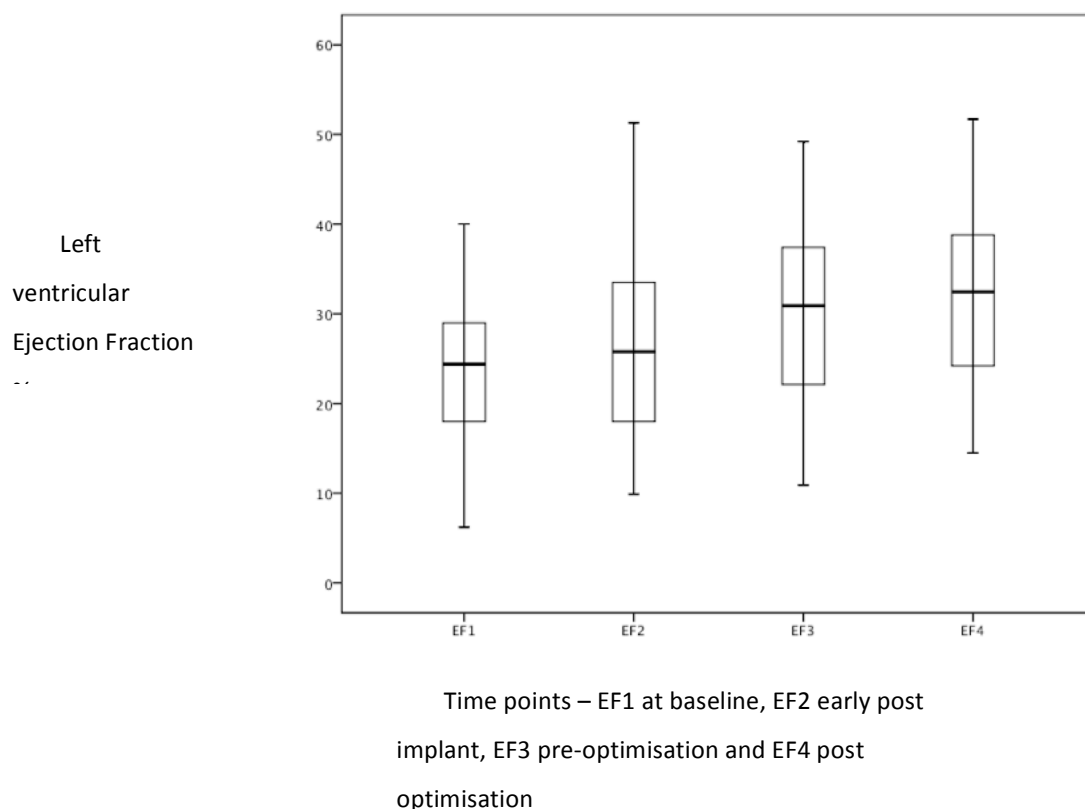


Figure 4.5. After optimisation (AV and VV). The ejection fraction has increased from 30 to 32% with a small drop in SDI from 5.7 to 5.4.



Graph 4.1 This graph shows a box plot of ejection fraction at baseline (EF 1), within 72 hours of CRT implant (EF 2), before optimisation (EF 3) and immediately after optimisation. The horizontal line indicates the median ejection fraction at each time point, the boxes enclose the 25th to 75th percentiles of the range and the whiskers enclose approximately 95% of the range. When assessed with a repeated measures ANOVA test, the serial change in ejection fraction over the 4 time points was statistically significant  $p<0.001$



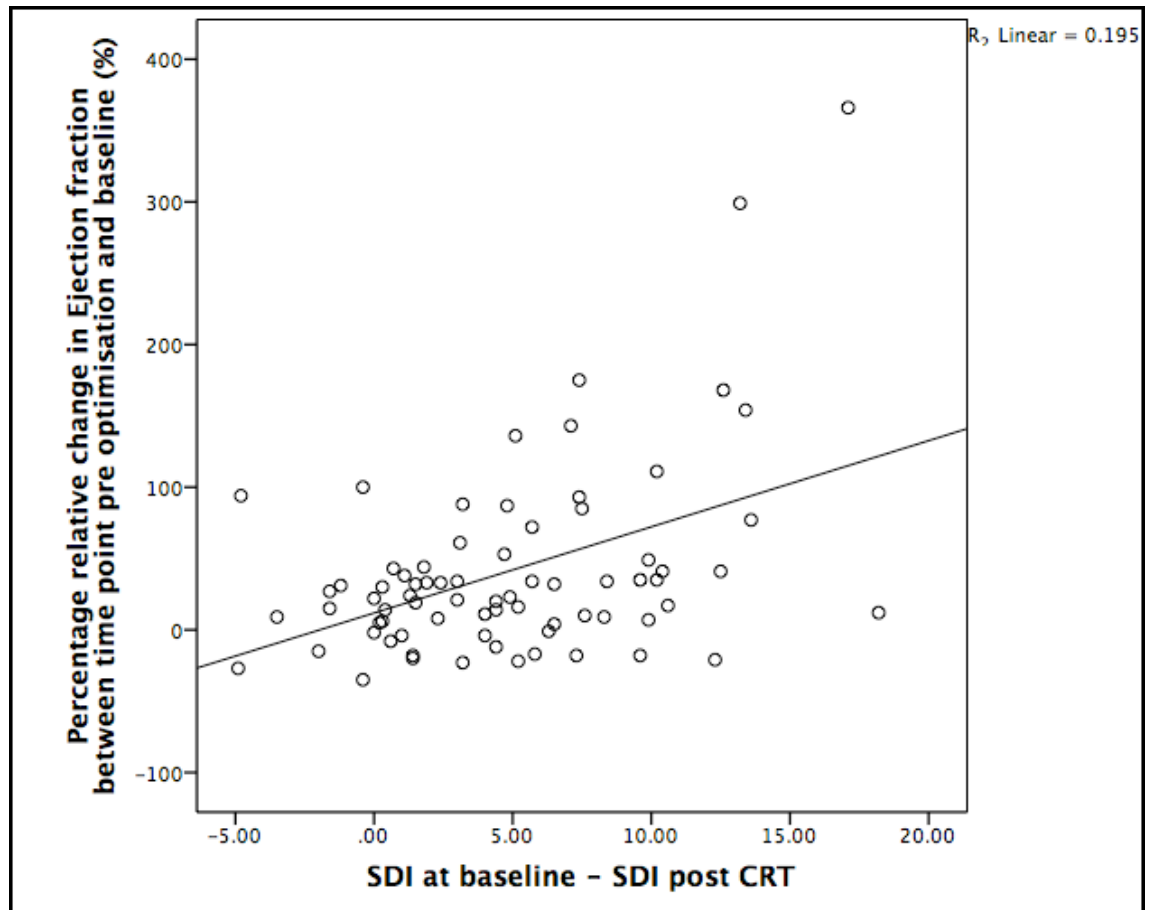
#### 4.4.4 Determinants of response

The determinants of response were investigated using univariate analysis of variance. The relative change in ejection fraction between baseline and before optimization was used as the dependent variable; rhythm, QRS morphology, sex and aetiology as factors and EF1, SDI1, SDI1-SDI2, EF2, 6MHW at baseline, Minnesota living with heart failure questionnaire at baseline and before optimization as covariates. This model indicated that

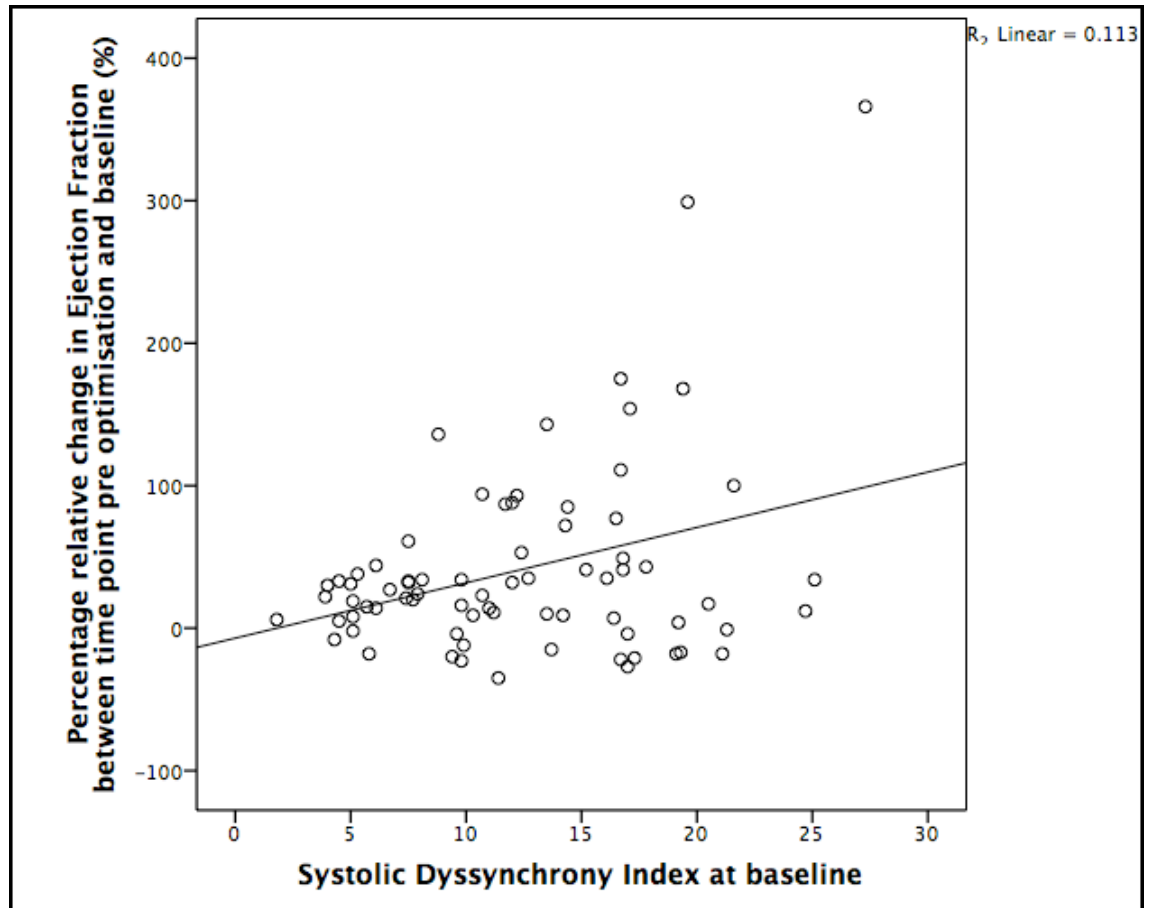
SDI1 ( $p=0.018$ ) and SDI 1-2 ( $p=0.001$ ) were significant predictors of relative change in ejection fraction. Graphical representation in figures 4.2 to 4.4 indicate the spread and the R squared value reflects the degree of response variable variation due to SDI 1-2 (19.5%), SDI 1 (11%) and QRS duration (5%) in the linear model.

Assessing the effect of factors, the estimated marginal means after correcting for covariates indicated that the relative change in ejection fraction was greater in patients in sinus rhythm than those with atrial fibrillation; with Left Bundle Branch block as compared to Right bundle branch block, women more than men, and patients with dilated cardiomyopathy or valvular disease compared with patients with ischaemic heart disease.

Graph 4.2 A plot of relative change in ejection fraction against change in SDI post CRT. A Linear regression line is plotted and the  $R^2$  value of 0.195.

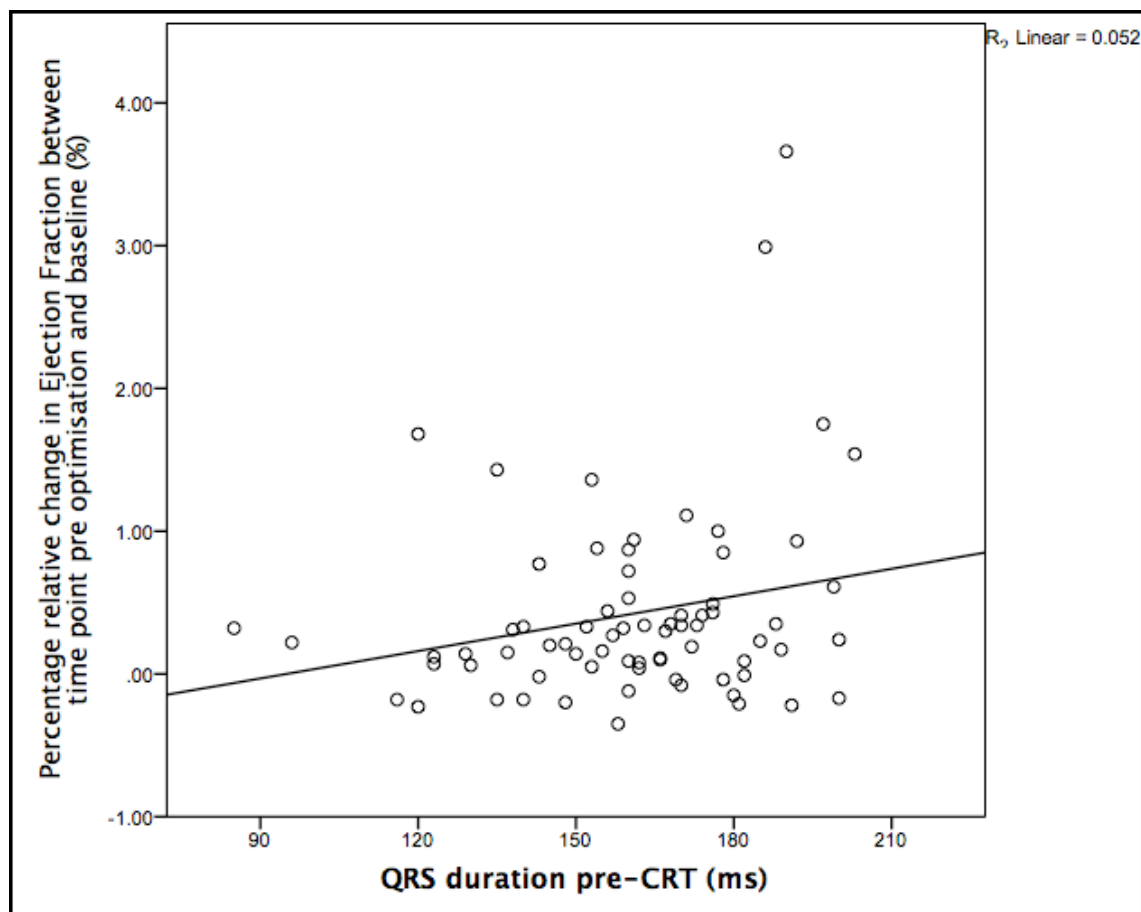


Graph 4.3 Relative change in Ejection fraction plotted against Systolic Dyssynchrony Index at baseline. A linear regression line is plotted. The  $R^2$  value of 0.113.

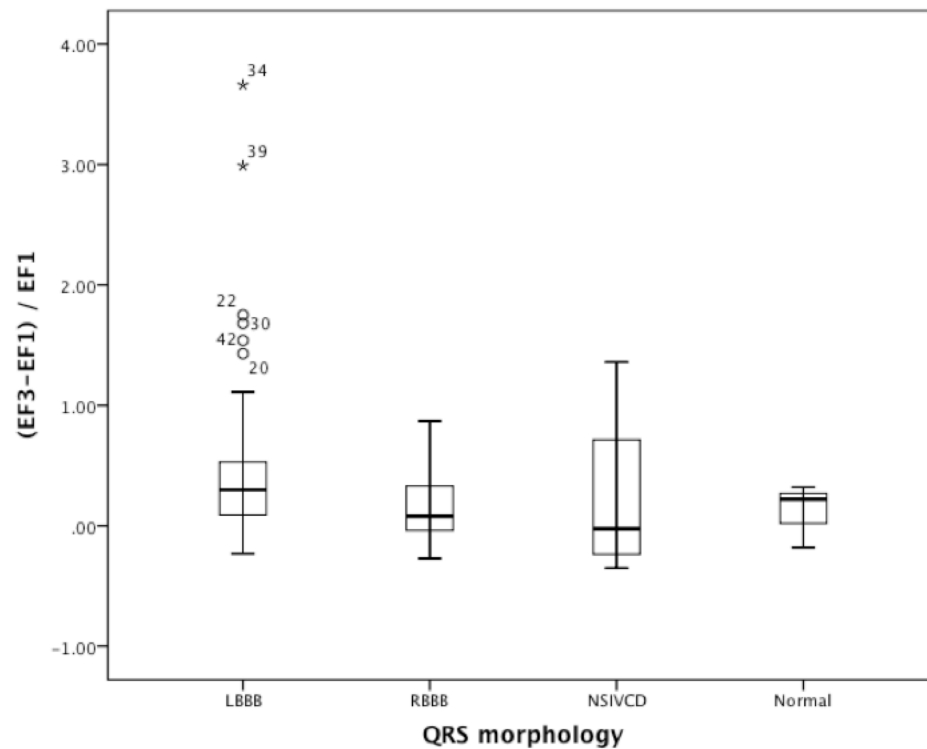




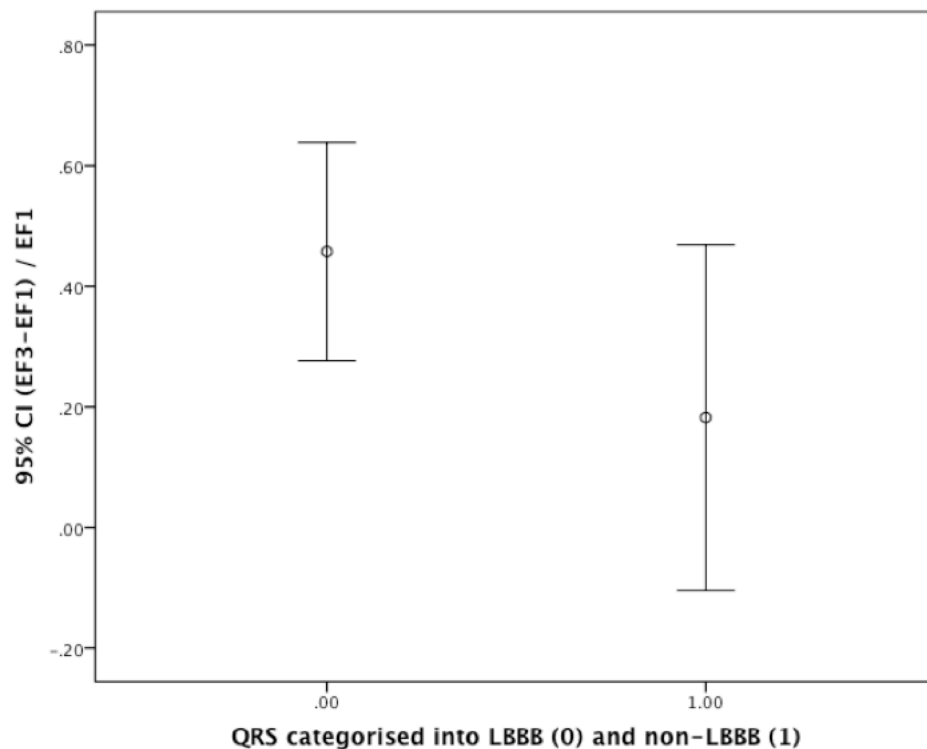
Graph 4.4 Relative change in Ejection Fraction plotted against QRS. A linear regression line is shown. The  $R^2$  value of 0.052.



Graph 4.5 Box-plot demonstrating the relative change in ejection fraction between baseline and before optimisation categorised by QRS morphology. Normal refers to a QRS of  $\leq 120$ ms. NSIVCD refers to a QRS of  $>120$ ms that did not meet WHO criteria for left or right bundle branch block.



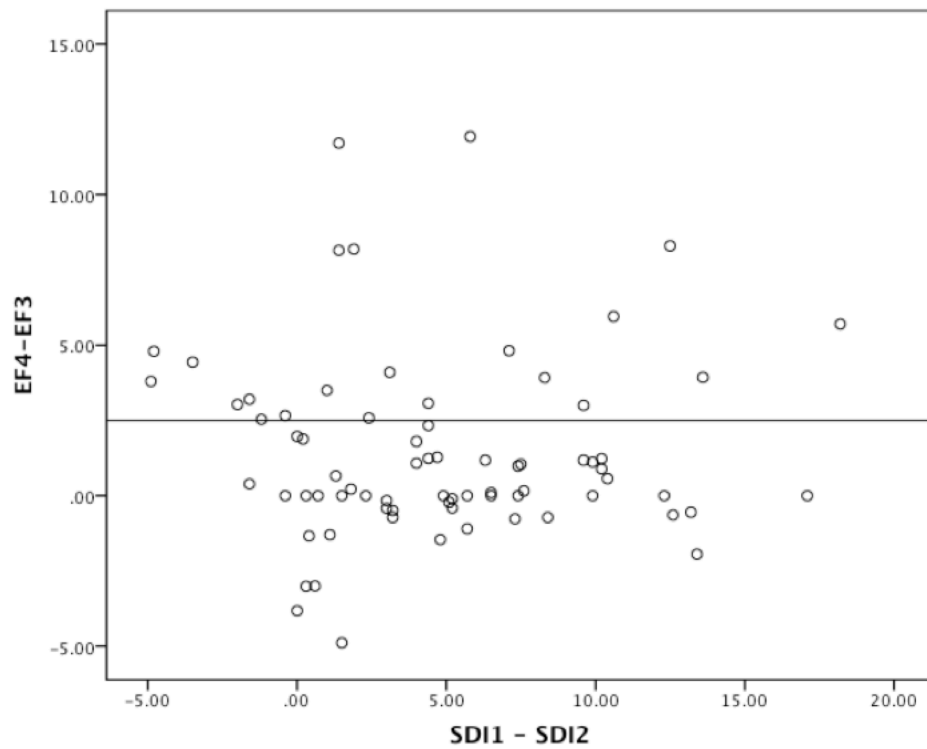
Graph 4.6 Graph showing mean and 95% confidence intervals for the relative change in ejection fraction between baseline and before optimisation as categorised by QRS morphology. P value for comparison <0.05



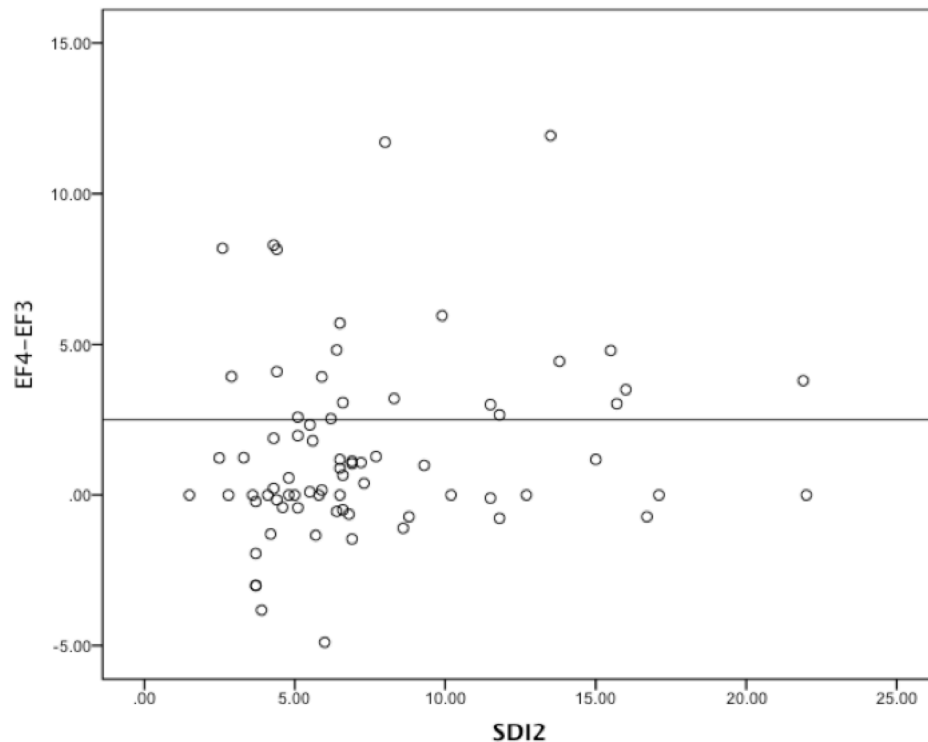
#### 4.4.5 Effect of optimisation

Further exploratory analysis was performed on the ability to predict change in ejection fraction due to optimisation. Graph 4.7 plots the absolute change in ejection fraction peri-optimisation against absolute change in SDI before and after CRT implantation. A horizontal line at an increase in absolute ejection fraction of 2.5% has been superimposed. We suggest this value empirically as a marker of the acute response to optimisation. The graph suggests that there is no clear relationship between the two variables. This is confirmed on univariate analysis.

Graph 4.7 Absolute change in ejection fraction peri-optimisation plotted against absolute change in SDI before and after CRT implantation. Regression confirms no statistical correlation between change in ejection fraction and change in SDI (R square 0.01)



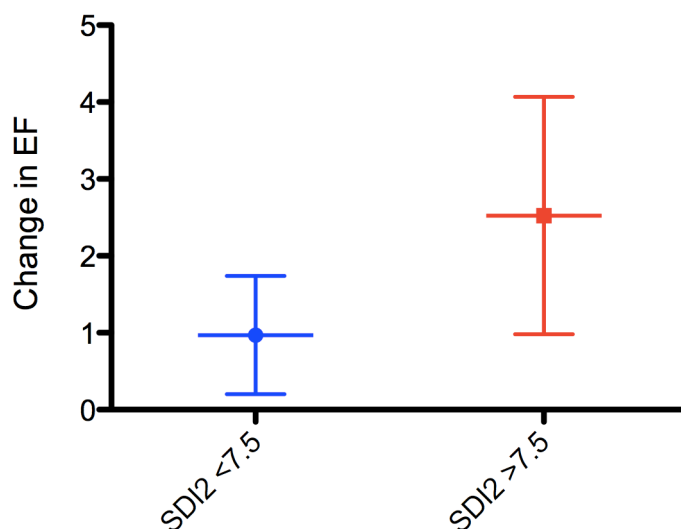
Graph 4.8 plots absolute change in ejection fraction due to optimisation against SDI2. Regression confirms no statistical correlation between change in ejection fraction and SDI2 (R square 0.14)



This again indicates no linear relationship between the two variables. However, the proportion of patients who have a benefit from optimization is greater in patients with a higher SDI after optimization.

Previously, an SDI of 7.5% has been suggested to be a lower limit for response to CRT<sup>112</sup>. We found 51 (69%) patients had an SDI of <7.5% and in this group of patients the mean benefit of optimisation was 0.97% increase in absolute ejection fraction. In the 23 patients with an SDI of >7.5% the benefit from optimisation was significantly larger at 2.52% absolute increase in ejection fraction (p value = 0.044).

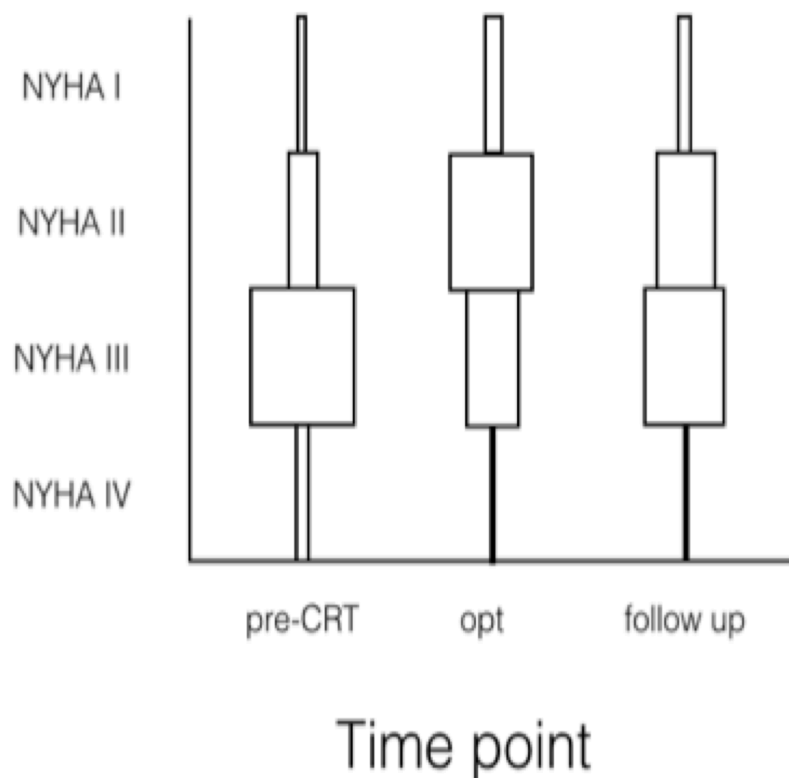
Graph 4.9 Change in Mean Ejection fraction due to optimisation stratified by SDI2 Graph shows mean  $\pm$  95% confidence intervals. P value  $<0.05$



#### 4.4.6 Clinical outcome of CRT

The mean NYHA class at baseline was 2.8, 2.3 at optimisation and 2.5 at long term follow up. The frequency of NYHA class is shown in Graph 10. The distribution of patients changed with a greater proportion of patients improving into NYHA class I to II. Minnesota living with heart failure questionnaire (MLHFQ) at baseline was 37.3, at optimisation 33.7 and 33.1 at follow up.

Graph 4.10 Plot of patients stratified according to NYHA functional class pre CRT implantation, at optimisation and at follow up. The width of the boxes indicates the proportion of patients in each class.



At baseline the mean 6MHW distance was 322.1m with a standard deviation of 119.8 and at optimisation this had increased to 378.9m with a standard deviation of 109.2, with the mean change being 56.8m. A paired t-test had a 95% confidence interval in the change in 6MHW distance to be between 34.2m and 79.4m with a p value of less than 0.001. Six minute hall walk distance was not recorded at long term follow up.

The MHLFQ was used to assess symptoms of heart failure. At baseline, the mean score was 42.2 with a standard deviation of 24.1. At optimisation the mean score had fallen to 32.4 with a standard deviation of 25. At long term follow up the mean score was 32.9 with a standard deviation of 19.8.

A paired t-test indicated that the difference between baseline and optimisation was statistically significant with a p value of 0.005.

Thirteen patients died during follow up. Eleven patients were hospitalised for any reason.

## 4.5 Conclusions

These data demonstrate that serial real-time 3 dimensional echocardiography can be successfully performed in the majority of patients undergoing CRT.

They confirm prior studies that 3D assessment of mechanical dyssynchrony prior to CRT can predict medium term echocardiographic response<sup>54,112</sup>. They also indicate that modulation of dyssynchrony by CRT is a statistically significant predictor of medium term echocardiographic response. However, these variables account for 30% of the variation in response.

It is not surprising that dyssynchrony does not account for more of the variation in response, as there are many factors that can modulate response to CRT, not least the presence of scar and the location of left ventricular pacing. The treatment may be able to influence some of these but not others.

We hypothesized that the assessment of dyssynchrony immediately after CRT may be useful in the prediction of outcome from CRT optimization. All patients were optimized using a standardized Doppler echocardiography protocol, and immediately after optimization, the effect was assessed using an independent criterion namely 3D echocardiography

Overall, a minority of patients had an improvement in ejection fraction following optimisation. These patients are heterogeneous, with some patients being super-responders who have little to gain from optimisation,



whereas other patients do not respond and cannot be made to respond by altering the timing of pacing stimuli. The group in whom altering the timing of pacing stimuli does make a difference is small.

Nevertheless, those patients who remained dyssynchronous post CRT had a greater benefit from optimisation than those who had a lower SDI. Sixty nine percent of the cohort had a low SDI following CRT, so concentrating optimisation efforts on the remaining 31% would significantly reduce the number of optimisations performed.

Despite a careful protocol, some patients appeared to have a decrease in ejection fraction following CRT optimization and this may reflect the inherent variability of both optimization and the technique used to measure it. The variability informed the decision to analyse these patients as a group rather than perform a receiver operating characteristic curve using an empirical cut-off for response that would be close to the noise due to variability.

# Chapter 5 Three-dimensional echocardiographic Speckle tracking

## 5.1 Abstract

The ability to track specular patterns seen in echocardiographic imaging of myocardial tissue has been demonstrated in 2D echocardiography. It is attractive to extend this method into 3 dimensions. In this study we used novel software to analyse 3 dimensional datasets and explored the inter-observer variability of the measurements obtained. Further work to minimise this variability was performed. Whilst agreement for volumes and ejection fraction was good, agreement was less good for measures of dyssynchrony, global longitudinal strain, twist and torsion. Further work needs to be done to improve the reproducibility of these measurements before their clinical utility can be investigated.

## 5.2 Introduction

Speckle tracking has been developed in 2 dimensional echocardiography as a method to quantify directional strain and displacement. It relies on tracking the grey-scale pattern produced by reflection and refraction of ultrasound by the myocardium throughout the cardiac cycle. There are limitations to speckle tracking related to the fact that the pattern of speckles must be stable enough through the cardiac cycle so that tracking can occur. This means that image quality must be good, but also that the pattern must be stable enough despite the fact that myocardial movement occurs in three dimensions and thus can go out of the 2 dimensional imaging plane. There is therefore a great deal of interest in extending speckle tracking techniques into three dimensions.

Three dimensional speckle tracking echocardiography may also have advantages compared to border detection algorithms. Border detection algorithms may incorrectly track in regions with significant trabeculation and especially with left ventricular papillary muscles. Automation of the border detection process is frequently inaccurate and requires manual editing. Speckle tracking based algorithms should be less affected by papillary muscle, can generate information on strain that cannot be obtained by border detection algorithms as well as giving directional information that may be particularly relevant to dyssynchrony assessment.

We therefore evaluated the feasibility and reliability of novel 3 dimensional speckle tracking software in the assessment of volumes, ejection fraction, dyssynchrony assessment and strain values within observers, between observers and between 2 institutions. This basic validation work is necessary before exploring the research and clinical utility of these tools.

## **5.3 Methods**

This work was a collaboration between Kings College Hospital, the University of Chicago and TomTec imaging systems who produced the software.

Echocardiography was performed on both sites, using Philips ie33 systems, with a either x3 and x5 probes. Full volume datasets were acquired over 4 cardiac cycles during breath-holding as previously reported. Where possible, the depth, width and elevation of the volume was minimised to focus on the left ventricle alone.

Datasets were analysed from 10 healthy subjects, 10 patients who had left bundle branch block (LBBB), but no other cardiac or medical diagnoses (normal & LBBB), 10 patients with dilated cardiomyopathy (DCM) and left bundle branch block, and 10 patients who had dilated cardiomyopathy and

no evidence of bundle branch block or intra-ventricular conduction delay on the surface ECG. These datasets had previously been acquired for another research study on conventional 3 dimensional echocardiographic analysis. Subsequently further datasets were acquired both in Chicago and at Kings and added to this cohort in order to replace those deemed to have insufficient image quality.

Off-line echocardiographic analysis was performed using TomTec Research Arena platform version and module LV analysis 3.0 for conventional border detection analysis, as well as TomTec Image Arena platform and modules 4D cartesian export, LV analysis 4.0. A specially constructed MatLab tool was also used for the exclusion of segments and calculation of dyssynchrony and strain parameters. The method for using module LV analysis 3.0 is covered earlier in this thesis. 4D cartesian export and the LV analysis version 4 have a different workflow. The workflow in 4D cartesian export is based on LV analysis 3.0. After opening the dataset in the module, the dataset is oriented so that the central axis intersects the apex of the left ventricle and the middle of the mitral valve in the apical 4 chamber, 2 chamber and 3 chamber views. The end systolic and diastolic frames are then defined. The border is manually traced at end-diastole. This provides the starting points for speckle tracking strain analysis, but this module can also produce conventional 3-dimensional parameters if the border is subsequently traced at end-systole too. At the next stage, border tracking is checked frame-by-frame border and edited if necessary as in LV analysis 3.0. This editing does not alter the output of the speckle tracking module, but does alter the conventional 3-dimensional parameter output. After this stage, the conventional parameters are output. Data is then exported before analysis using TomTec tracking modules. This module processes the data and exports movie files of long and short axis cuts throughout the cardiac cycle. The baseline speckle pattern is indicated by a green dot and red dots indicate that location as it moves through the

cardiac cycle. This allows a visual analysis of the quality of the tracking. Darker points indicate areas outside the ultrasound sector that are not tracked, but are interpolated from the surrounding segments. The module also output numerical parameters, strain, velocity, integrated displacement which is the 3-dimensional distance from the end-diastolic point as well as left ventricular volumes for every time-point. Strain and velocity parameters have 3 components, circumferential, longitudinal and radial. Integrated displacement also has a further angular component that is calculated.

The module LV analysis 4.0 has a more automated workflow. After importing a dataset, the orientation of the left ventricle is adjusted and the reference frame defined. The software then produces a border which is displayed in the 4 chamber, 2 chamber and 4 chamber views as well as the short axis. If, as is usually necessary, the border requires editing, it can be selected and dragged to the correct area. When the operator is satisfied with this starting point, progressing to the next step generates a border that is tracked throughout the cardiac cycle. This can be inspected simultaneously in 3 longitudinal and 3 short axis cut-planes and edited if necessary. Editing the borders in this step results in recalculation of the speckle tracking. This editing step was thought to perform relatively poorly and therefore operators were encouraged to go back and edit the initial border in preference to editing after tracking. The final step delivered parameters in summary and graphical format as well as allowing export in a format compatible with Microsoft Excel. This output could also be imported into a bespoke MatLab tool that allowed individual segments to be included or excluded from the overall analysis as well as calculating standard deviations for any of the displacement or strain parameters. As this was a simpler workflow than the previous version, all datasets were reanalysed using this version. Revision builds were provided by TomTec as they were finalized.

The dyssynchrony parameters produced by the software included the measure SDI-I which was analogous to SDI-16 from the contour detection method. This measure was the standard deviation of time to peak strain of each of the 16 segments. It also generated a novel measure SDI-II which incorporated apical rocking into the measurement. There were measures of Global Longitudinal Strain, twist and torsion also.

Figure 5.1 Aligned volume. The volume has been opened in LV analysis 4.0. The volume has been rotated along the axes to that the axis goes through the apex and the mitral valve. The aortic valve has been marked in the short axis view (SAX, upper left panel) to aid the software in recognizing the standard 2,3 and 4 chamber long axis cuts (3Ch upper right, 2Ch lower left and 4Ch lower right respectively).

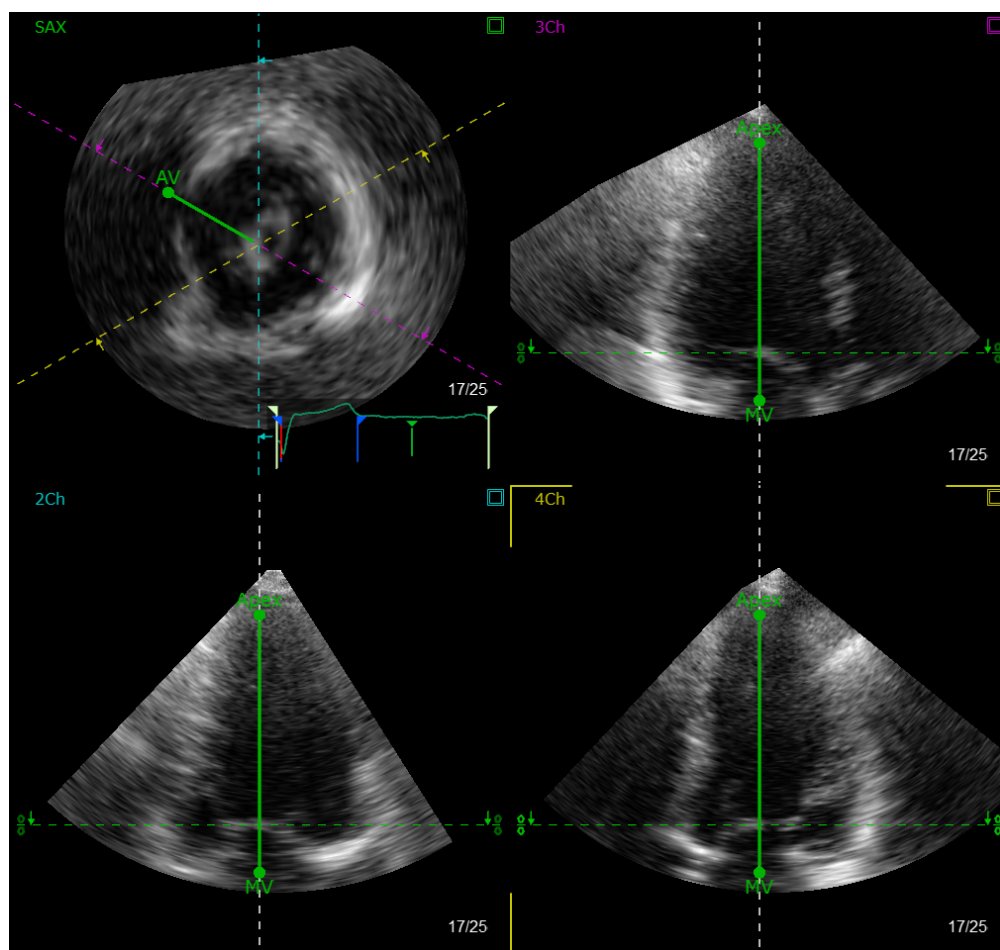


Figure 5.2. The software generates an endocardial border at a single timepoint in the cardiac cycle. This is visible next to the moving image and can be manipulated to ensure accurate placement of the border. After this step the software tracks the border and generates the moving endocardial cast. This can then be visualised throughout the cardiac cycle to ensure a good fit

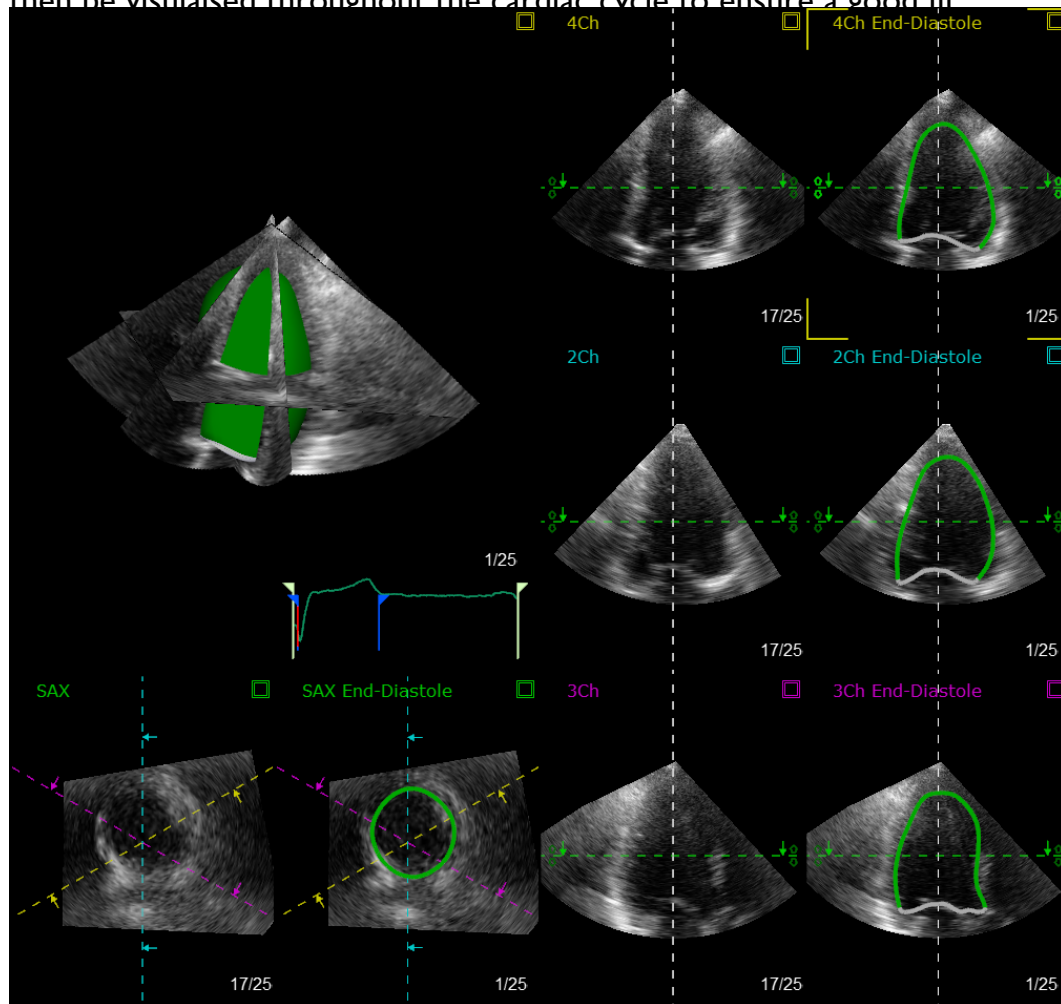
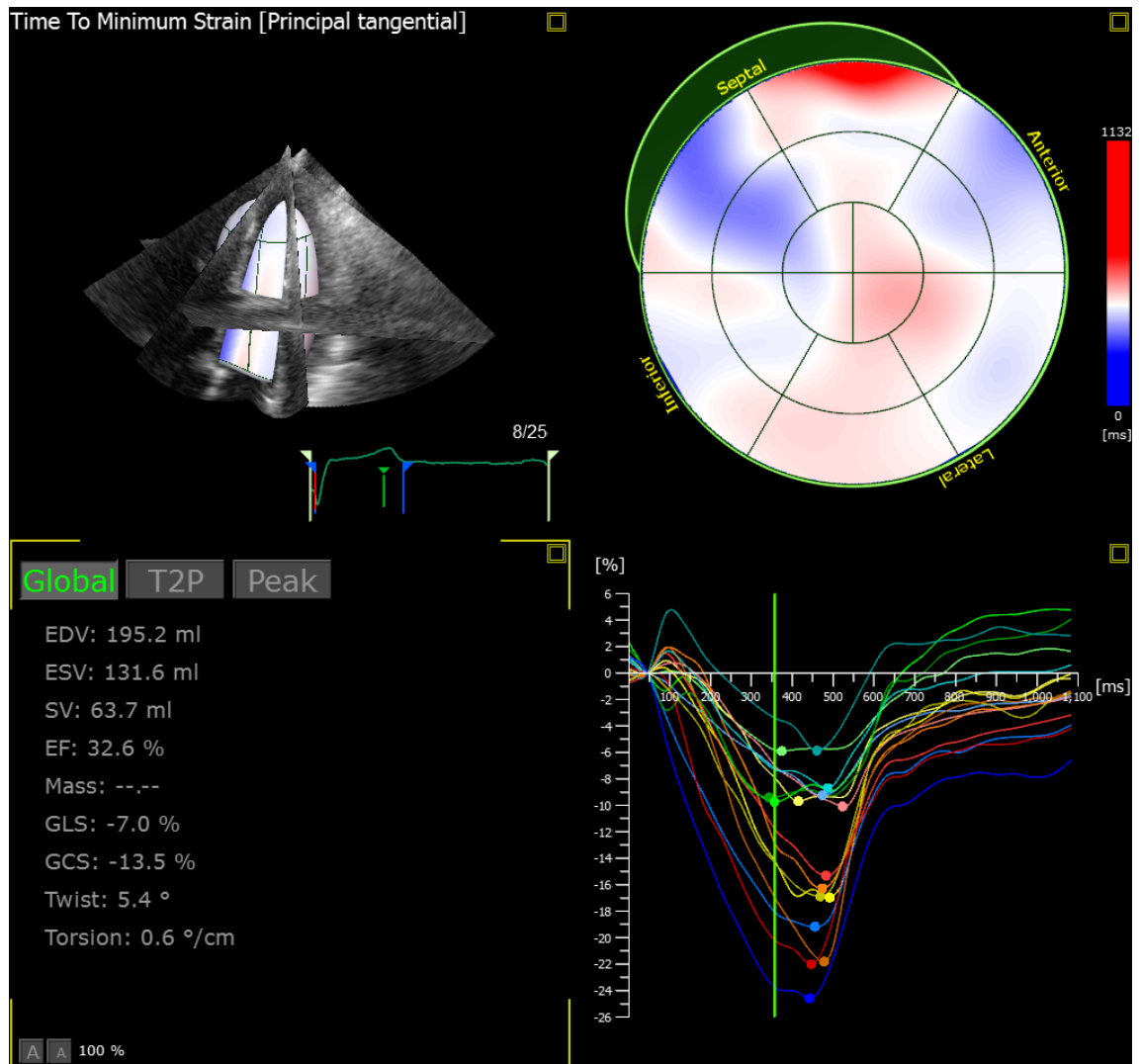


Figure 5.3 Output of LV analysis 4.0. This figure shows the 3D cast in the upper right panel, bullseye plot upper left panel, numerical results lower left panel and graph of 3D strain against time in lower right panel.



### 5.3.1 Statistics

Bland – Altman plots were used as the primary method for visual analysis of reproducibility<sup>57</sup>. These plot the difference between observers against the mean value for an individual data point. This highlights systematic bias, any trends in this bias across the range of mean values, as well as allows the calculation of the limits of agreement, defined as  $\pm 1.96 \times \text{standard deviation of the differences between observers}$ . The limits of



agreement are likely to be wide in a pilot study involving limited numbers of datasets, and therefore the intraclass correlation coefficients were calculated<sup>58</sup>. Analysis was performed using Excel 2008 for Mac.

## 5.4 Results

Initially, 2 datasets were exchanged between the centres and analysis performed. This revealed similar values for ejection fraction, a bias in volumes, a reasonable correlation for SDI-I and a less good correlation for SDI-II. We then proceeded to blinded analysis of the rest of the cohort. The mean values for each group, as well as the mean differences are shown in Table 5.1. In the normal group, 8 out of 14 patients had to be excluded for a number of reasons, including stitch artefact (2 patients), missing datasets (3 patients), volume acquisition optimised for RV rather than LV volume (1 patient), insufficient frame rate to open (3 patients). The mean difference for end diastolic and end systolic volumes was 12.5 and 9.6 ml respectively, which gives a smaller mean difference of 2.8ml for stroke volume and 4.2% for ejection fraction. The bias was for the Chicago group to generate smaller volumes in this cohort. Proportionally there was a greater difference for SDI-I, with a mean value of 6.5%, but the mean difference between groups being 3% i.e. nearly half of the value being measured. The mean SDI-II was 5.5%, with a mean difference of 1.3% which is better than that of SDI-I.

Table 5.1. P values for bias between Chicago and Kings are all non significant (>0.05)

Group	Total pts	Pts included	Mean EDV (ml)	Mean n Difference	Mean an ESV (ml)	Mean Difference (ml)	Mean SV (ml)	Mean Difference (ml)	Mean EF (%)	Mean Difference (%)	Mean SDI-I	Mean Difference	Mean SDI-II	Mean Difference	Mean GLS	Mean Difference
Healthy	14	6	95.1	-13	42	-9.6	52.8	-2.8	56.4	4.2	6.5	3.0	5.5	1.3	-17.2	1.8
DCM	12	8	227.8	7.3	180	7.8	48.0	-0.5	22.2	-0.6	12.1	10.4	13.5	9.6	-5.3	-0.5
Healthy & LBBB	7	4	123.6	-41	71	-36.7	51.4	-4.5	43.2	11.8	8.4	-1.7	8.0	0.7	n/a	n/a
DCM & LBBB	12	12	282.0	-6.0	235	-5.8	47.0	-0.2	17.7	-0.3	12.2	5.7	15.5	2.4	-5.9	0.3

Of the DCM patients, 4 were excluded, 2 because of stitching artefacts and 2 because the author deemed the tracking to be too poor for the results to be meaningful. The mean end diastolic and systolic volumes were much larger than the normal group at 227.8ml and 180.2 ml respectively. The mean differences were proportionately lower than the normal patients at 7.3ml and 7.8ml respectively. The ejection fraction in these patients was also much lower than the normal patients at 22.2%, with a mean difference of 0.6%. SDI-I and SDI-II values were higher than the normal patients at 12.1% and 13.5% respectively, but the mean differences in SDI were high at 10.4% for SDI-I and 9.6% for SDI-II.

Of the patients with left bundle branch block, there were clear differences between the two groups in the analysis of those deemed otherwise to be normal. Only 4 patients were analysed at both sites, yet there were large differences in the volumes obtained. The mean EDV was 123.6ml, with a mean difference of 41.3ml, and the mean ESV was 71.2ml with a mean difference of 36.7ml. However the stroke volumes were similar with a mean of 51.4ml and a mean difference of 4.5ml. Ejection fraction differed between the groups with a mean of 43.2%, but a mean difference of 11.8%. SDI-I and SDI-II values were better than others groups with a mean SDI-I and SDI-II of 8.4% and 8.0 %, with mean difference of 1.7% and 0.7 % respectively. Those patients with left bundle branch block and a dilated cardiomyopathy had much larger volumes with a mean EDV of 282 ml, and a mean difference of only 6ml, a mean ESV of 235.1ml and a mean difference of 5.8ml. Consequently ejection fraction was also lower than other groups at 17.7%, but a mean difference of only 0.3%. Again SDI-I and SDI-II had marked differences between the two sites, with mean values of 12.2% and 15.5%, but mean differences of 5.7% and 2.4% respectively.

Bland-Altman plots for individual patients are plotted (see Figures 5.4 to 5.9) and these confirm the above impressions - that the author generated significantly larger volumes and lower ejection fraction in normal ventricles, though in abnormal ventricles the mean values for volume and ejection fraction were very good. However, there was significant divergence in the values for dyssynchrony between the groups.

Figure 5.4 Bland Altman plot for End Diastolic Volume. Solid line indicates bias and dashed lines indicate 95% confidence intervals.

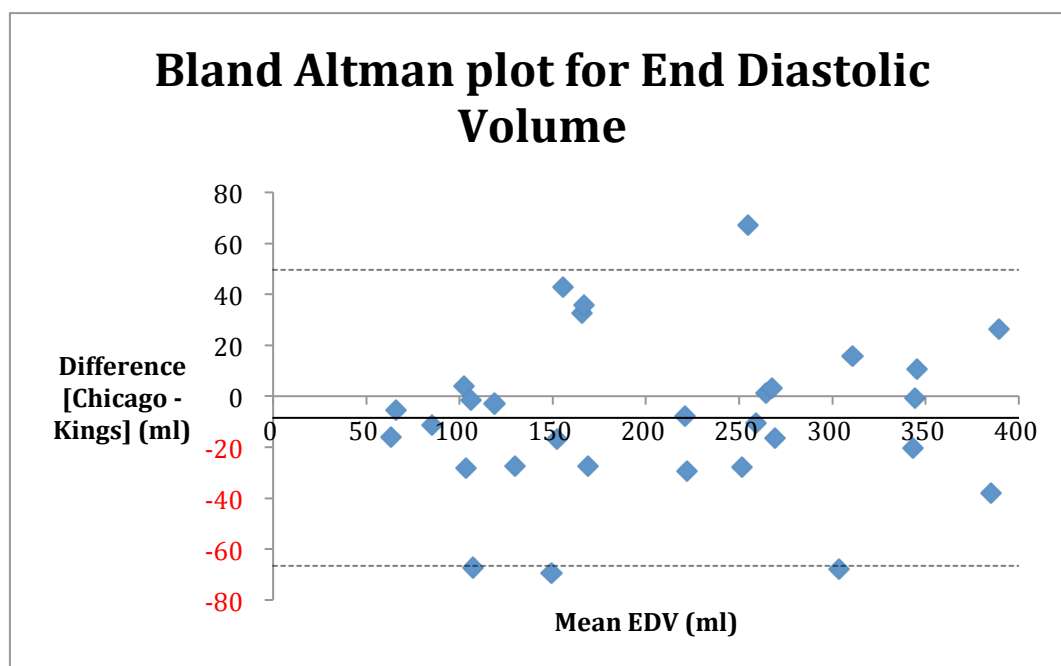


Figure 5.5 Bland Altman plot for End Systolic Volume. Solid line indicates bias and dashed lines indicate 95% confidence intervals.

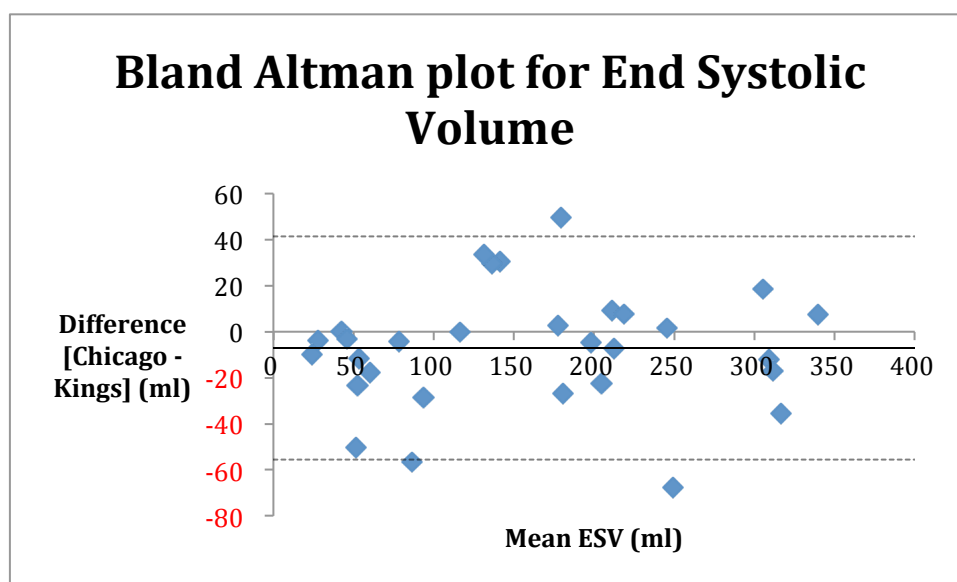


Figure 5.6 Bland Altman plot for Stroke Volume. Solid line indicates bias (-1.4 ml), dashed lines indicate 95% confidence intervals (+/- 19ml)

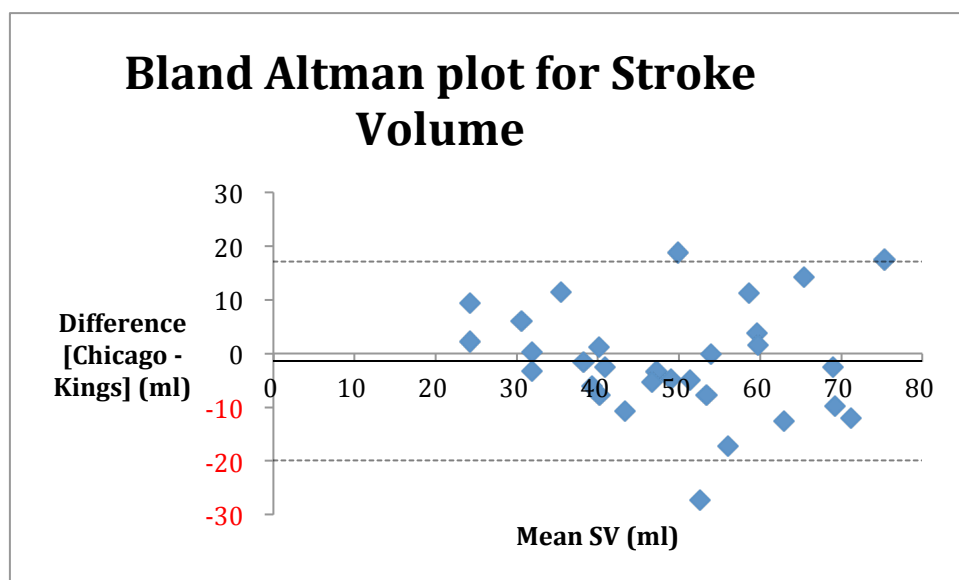


Figure 5.7 Bland Altman plot for Ejection Fraction. Solid line indicates bias and dashed lines indicate 95% confidence intervals

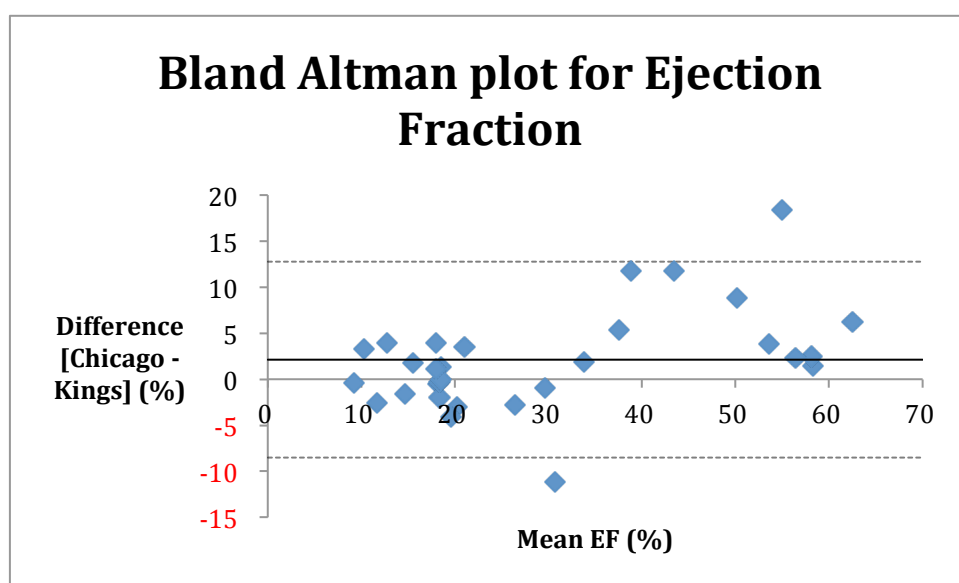


Figure 5.8 Bland Altman plot for SDI-I. Solid line indicates bias and dashed lines indicate 95% confidence intervals

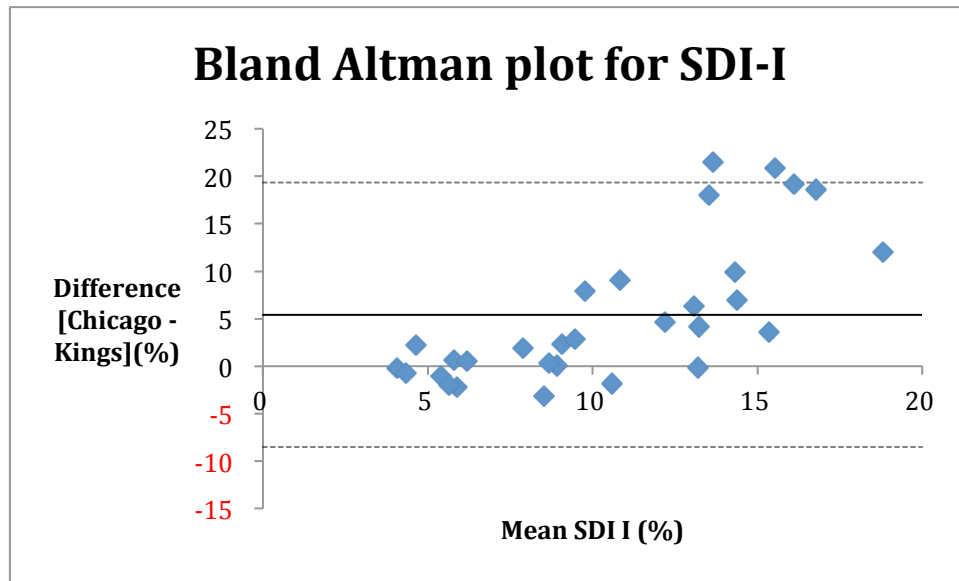
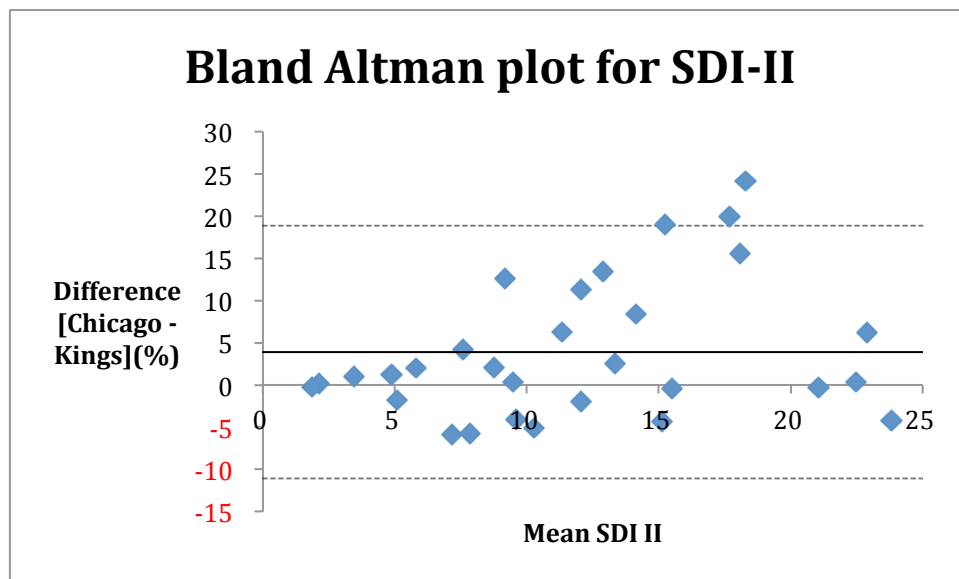


Figure 5.9 Bland Altman plot for SDI-II



We investigated the reasons behind the variability in dyssynchrony measures. Many of the datasets from the Chicago group included 2 “loops”. The terminology can be confusing as each full volume dataset is made up of 4 smaller volumes acquired over 4 consecutive heart beats, but the Philips ie33 machine has the ability to acquire for a longer period than a single cardiac cycle. The Philips system terms this the number of loops

acquired which can be single or dual for 3D acquisitions. It was realised that the TomTec software used at both sites was a different software revision, and that the Chicago group had the earlier iteration of the software which was unable to parse 2 loop acquisitions as separate loops and therefore the peaks were distributed across both loops resulting in large values for dyssynchrony. This was confirmed by a comparative analysis in a single patient of single and dual loop acquisitions by the Chicago group who demonstrated that the dyssynchrony parameters were doubled in the 2 loop acquisition, whilst the volumes remained identical. We also realised that the groups had not been analysing the same volume as each patient had multiple volumes acquired, and furthermore the initialisation frame differed between the groups, with the Chicago group setting the initial border at end-systole, whilst the author had set the initial border at end-diastole.

We therefore proceeded to repeat the analysis after standardisation of the method. The software version used was confirmed to be identical at both sites, the individual volume to be analysed for each patient was defined, and it was decided to use the end-systolic frame as the initialisation frame. The end-systolic frame was defined as the frame before opening of the mitral valve. The analysis was performed again for the group with DCM and LBBB. Individual results are collated and Bland-Altman plot displayed in Figures 5.10 to 5.17.



Figure 5.10 Bland-Altman plot for End Diastolic Volume

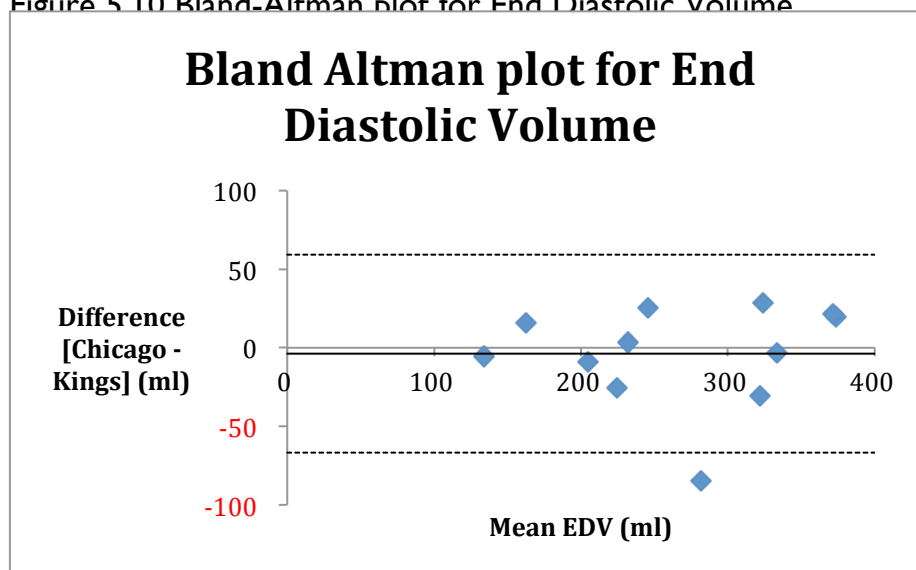


Figure 5.11 Bland-Altman plot for End Systolic Volume

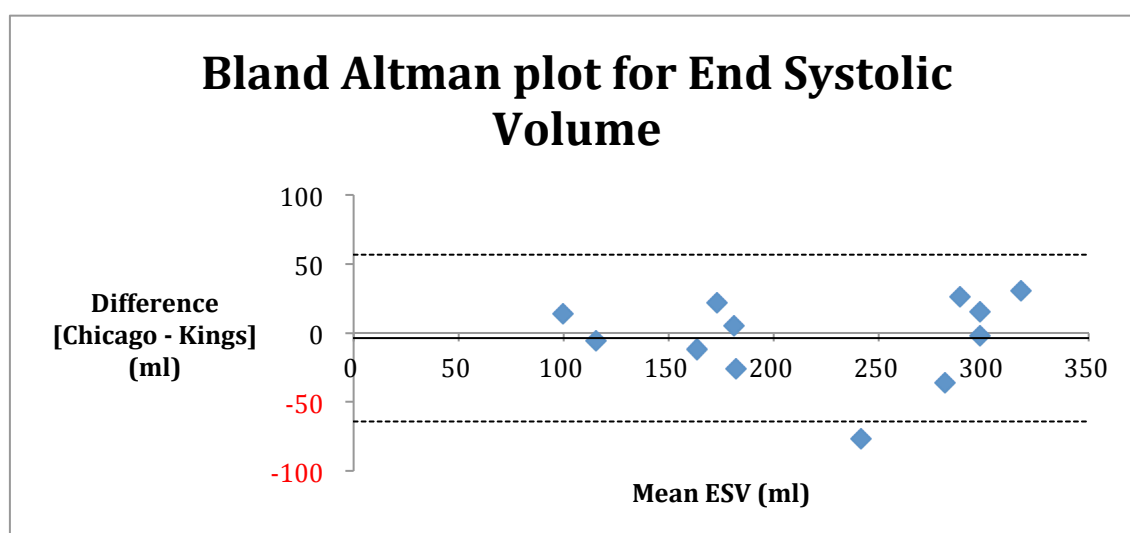


Figure 5.12 Bland-Altman plot for Stroke Volume

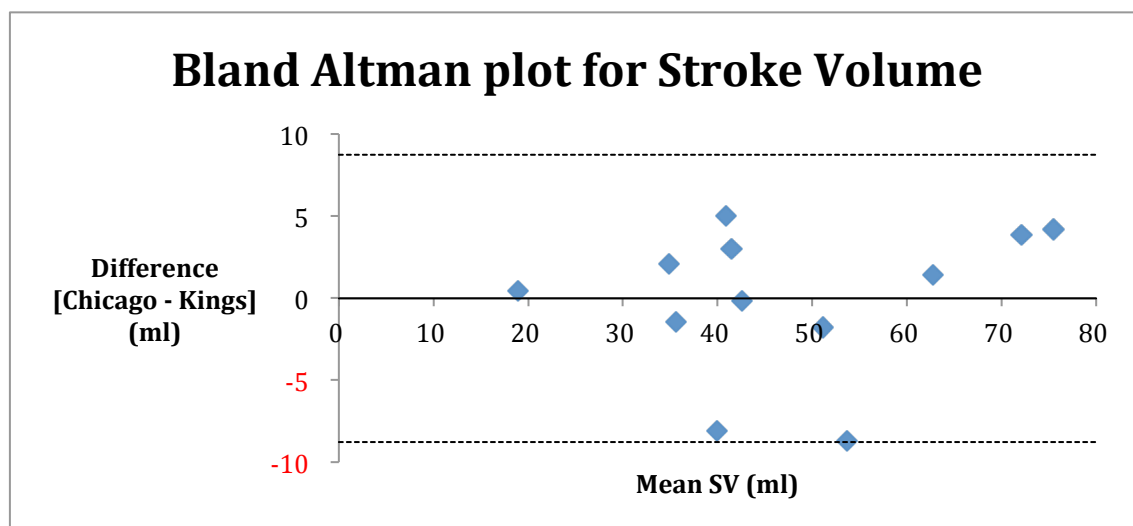


Figure 5.13 Bland-Altman plot for Ejection Fraction

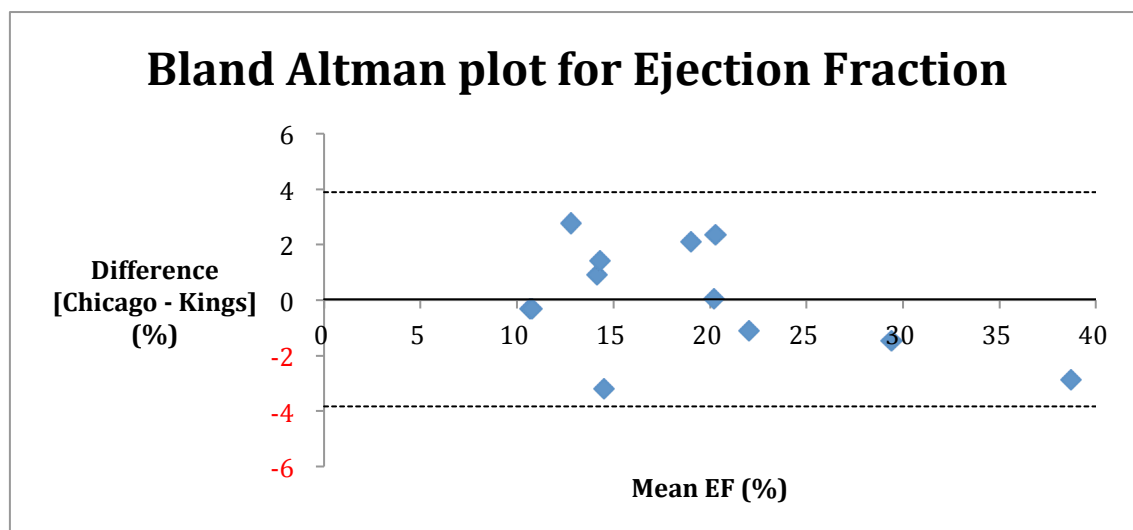


Figure 5.14 Bland-Altman plot for SDI-I

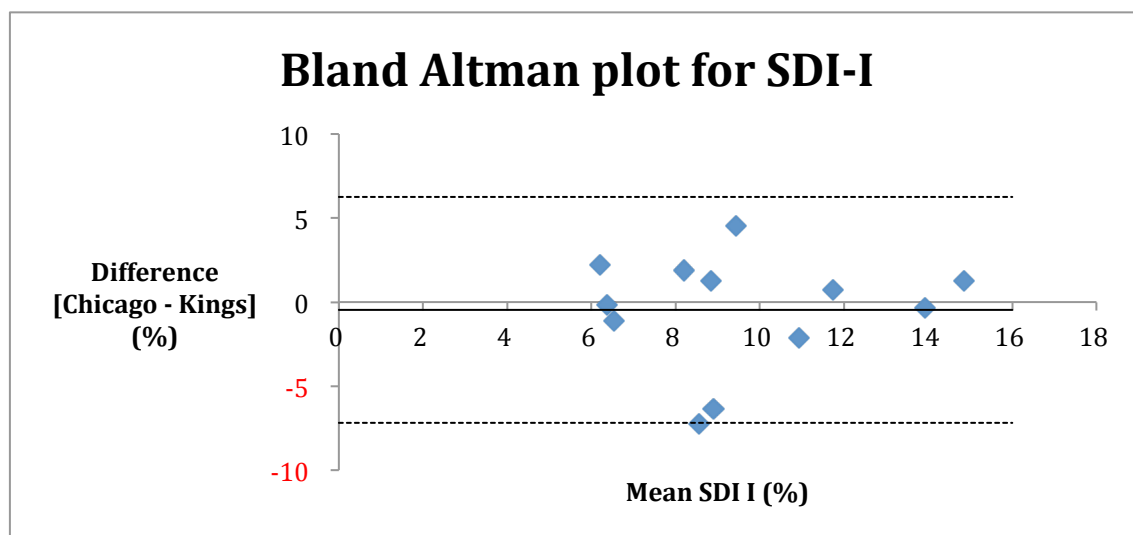


Figure 5.15 Bland-Altman plot for SDI-II

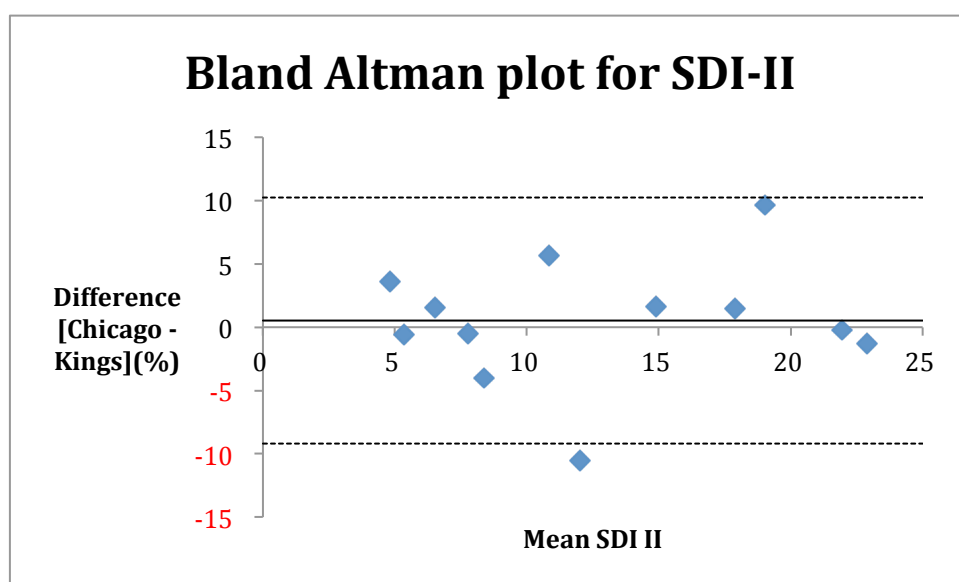


Figure 5.16 Bland-Altman plot for GLS

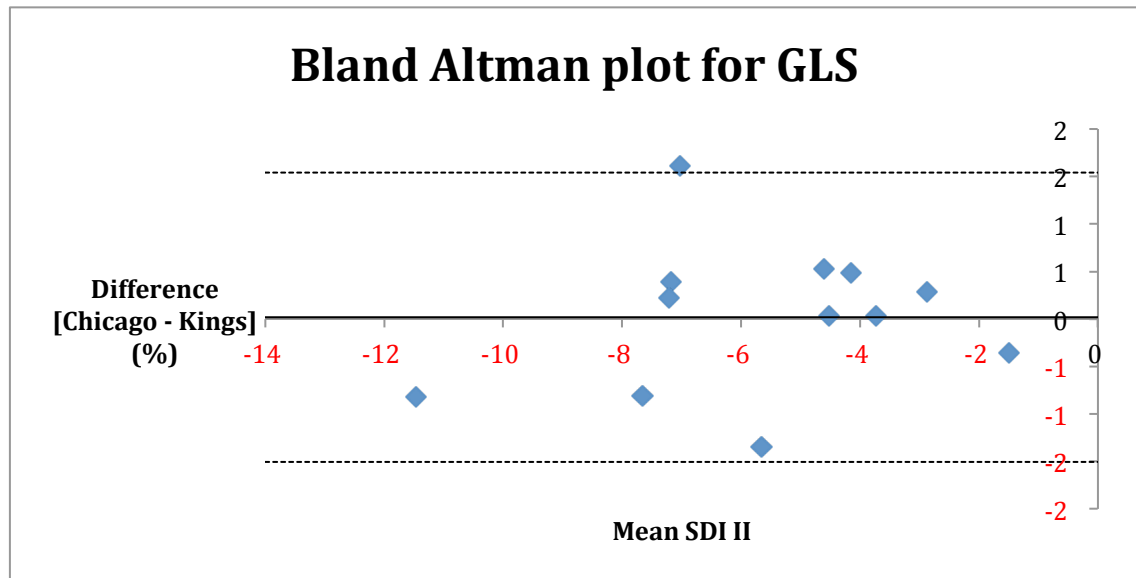
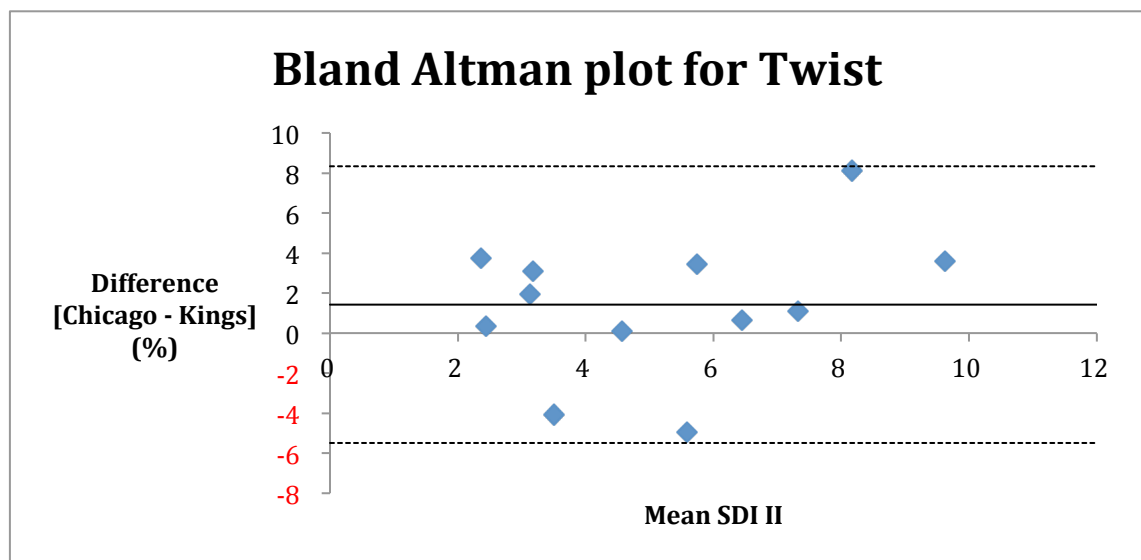


Figure 5.17 Bland-Altman plot for Twist



In the majority of patients, the volumes agreed closely between the two groups, though there were a few outliers that combined with a small sample meant that the limits of agreement were high. The mean EDV was 267.4ml, with a mean difference of 3.8ml, limits of agreement of 63ml; mean ESV 219.9ml, mean difference 3.7ml, limits of agreement 60.4ml, mean stroke volume 47.5ml, mean difference 0ml limits of agreement 8.8ml and a mean EF of 18.9%, mean difference of 0%, limits of agreement 3.9%. There were greater differences in the dyssynchrony indices, with a mean SDI-I of 9.5%,

mean difference 0.5%, limits of agreement 6.7% and SDI-II of 12.7%, mean difference 0.5%, limits of agreement 9.7%. Although the limits of agreement are likely to be an over-estimate given the sample size, nevertheless for the measures of dyssynchrony the limits of agreement approach the mean value calling into question their utility.

The outlier datasets were reviewed and it became apparent that these datasets had the worst image quality. Issues with image quality could be divided into a number of considerations, namely those with segmental dropout during at least part of the cardiac cycle or those due to poor myocardial definition such as a hazy ground glass appearance rather than a distinct specular pattern.

In order to be able to use this method in a majority of patients, it was important to develop a tool that could work with real world datasets. We therefore investigated if excluding poorly visualised segments from the analysis would improve the variability. We also decided to recruit patients with perfect datasets, to ensure that the method was robust in perfect datasets.

In the same cohort of patients with DCM and LBBB, the datasets were independently evaluated at both sites with regard to image quality and which segments should be excluded. These assessments were exchanged between sites and reviewed to generate a common list of datasets and segments to exclude, which is listed in Table 5.2. These datasets were analysed at both sites using the new speckle tracking software. As a reference comparator, further analysis of the same datasets was performed at the Kings site by myself and Dr Stamatis Kapetanakis using the previous non-speckle tracking software (i.e. the contour detection method as employed by the software package TomTec LV analysis 3.0). As the focus was on dyssynchrony indices, only these data were received from the Chicago group. These results are tabulated with Bland-Altman plots,

correlation coefficients as well as intraclass correlation coefficients in Figures 5.18 to 5.20. Using the new software, the mean difference  $\pm$  limits of agreement were 0.18%  $\pm$  3.68%, 1.38%  $\pm$  10.44%, -0.42%  $\pm$  13.00% for SDI-I, SDI-II and SDI of time to 3D minimum strain respectively. Similarly, Intraclass correlation coefficients were 0.91, 0.75 and 0.49 respectively.

Using the contour detection method, the mean difference  $\pm$  limits of agreement were -2.36ml  $\pm$  29.6ml for EDV, -0.91%  $\pm$  6.5% for Ejection Fraction, and -0.52%  $\pm$  3.6% for SDI-16, with intraclass correlation coefficients of 0.98, 0.96 and 0.90 respectively.

**Table 5.2**

Patient Number	Identifier	Datset volume to be analysed	Excluded Basal Segments	Excluded Mid Segments	Excluded Apical segments
1	OS	88	-	7,8	13,15
2	PBH	2	3	9	13,14,16
4	RH	69	2	8	13
5	EH	48	2	8	13,14,16
6	JD	65	-	-	13,14,15,16
7	EE	94	-	9	-
8	MR	51	-	8	13,15
9	EV	2	-	7,9	13,14,15
10	AC	68	-	-	15
12	YC	78	-	8	13

## Key to segments

- 1 Basal anteroseptal
- 2 Basal anterior
- 3 Basal antero-lateral
- 4 Basal infero-lateral
- 5 Basal inferior
- 6 Basal infero-septal
- 7 Mid antero-septal
- 8 Mid anterior
- 9 Mid antero-lateral
- 10 Mid infero-lateral
- 11 Mid inferior
- 12 Mid infero-septal
- 13 Apical anterior
- 14 Apical lateral
- 15 Apical inferior
- 16 Apical septal

reference <sup>176</sup>

Figure 5.18 Bland-Altman plot for SDI-I

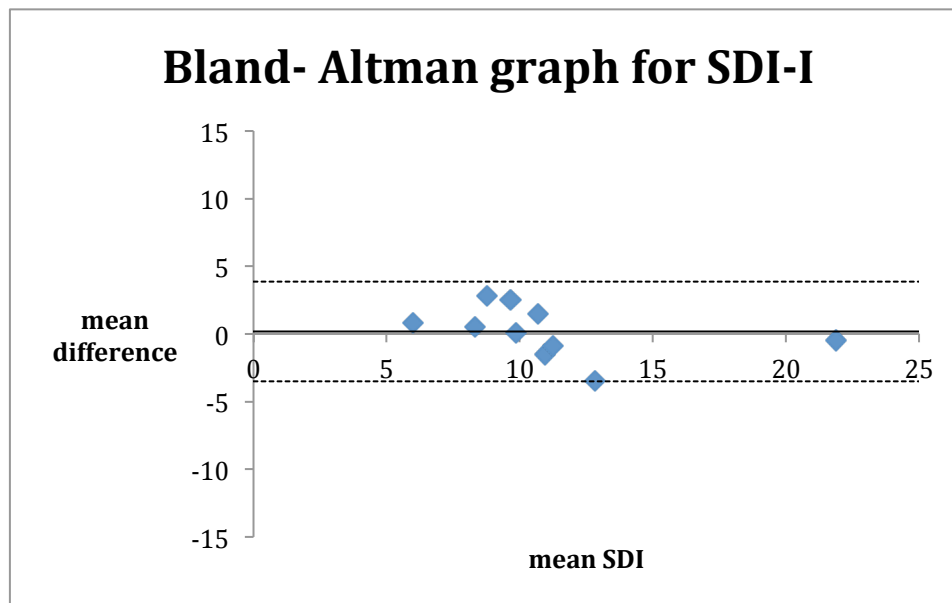


Figure 5.19 Bland-Altman plot for SDI-II

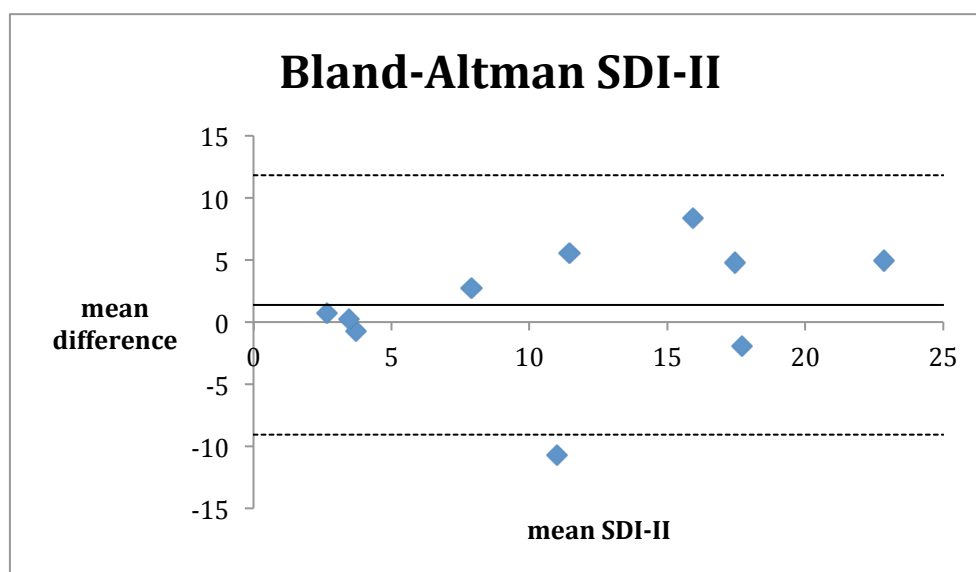
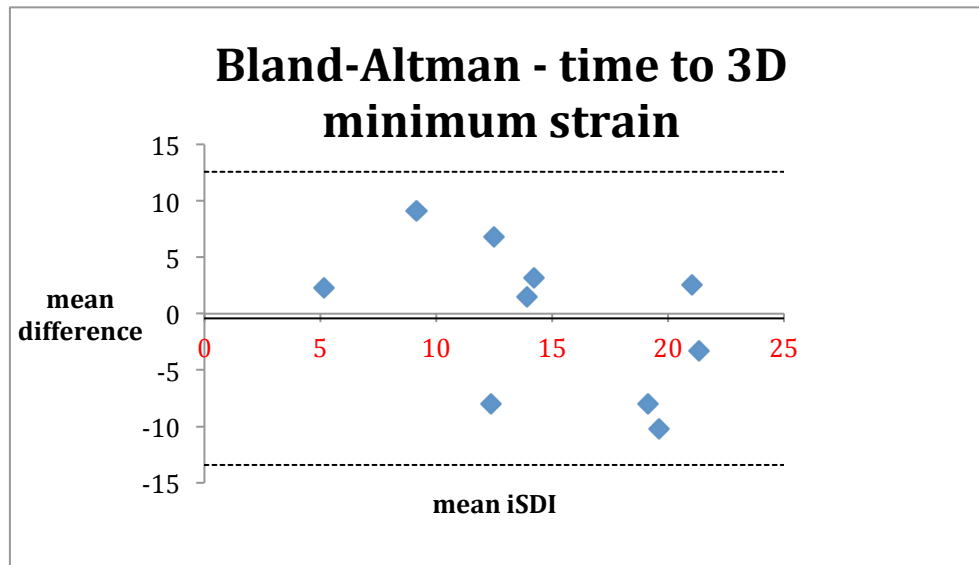




Figure 5.20 Bland-Altman plot for SDI time to 3D minimum strain



## 5.5 Conclusions

Speckle tracking is an attractive method to use in the analysis of left ventricular function in 3 dimensions. It has a number of potentially useful characteristics over existing validated methods in that it is likely to track correctly in the area of papillary muscle insertion, as well as giving direct information about myocardial mechanics. However, the development of software requires that the reproducibility of the technique is sufficiently good enough to produce reliable data. The work delineated above describes the importance in standardising methods of analysis so that the reproducibility of the software analysis with clinical data can be explored. This work used 2 major versions of the software. The first was an early software build with a different workflow to the second. As the workflow was significantly simpler in the second major version, all datasets were reanalysed with this version. We also found that using different software revisions of the same later version gave differing results, so the final comparison between centres ensured the software versions were the same. This is an important point for future studies highlighting that even minor revision builds in some circumstances give differing results.

Initially, reproducibility between centres was poor when using different datasets of the same patient and different initialisation frames. Once this had been standardised, it was discovered that reproducibility was poor when segments that were poorly visualised throughout the cardiac cycle or were noisy were included.

When poor datasets and poorly visualised datasets were excluded from the analysis, reproducibility of the standard 3 dimensional dyssynchrony index was good (SDI-I, the standard deviation of the time to minimum volume of the included segments). Reproducibility of strain based dyssynchrony indices (i.e. SDI-II and SDI of time to 3D minimum strain) was fair to poor.

The Bland-Altman plot gives an easily comprehensible method for calculating any systematic bias between groups and the limits of agreement between groups but the limits of agreement will be wide in a small cohort. This work has therefore been continued by my colleagues to analyse the rest of the cohort of normal, DCM and normal with left bundle branch block patients, as well as to recruit more perfect datasets across these groups so that we can determine the reproducibility of the technique across a range of cardiac diseases in optimal circumstances.

Further work to define the reproducibility of measurements within patients is also necessary before work on the clinical utility of these techniques is performed.

## Chapter 6 Conclusions

### 6.1 Aims of this thesis

Three-dimensional echocardiography has emerged as a promising technique to investigate mechanical dyssynchrony and quantify left ventricular function. The aim of this thesis was to utilise this technique to examine the effect of cardiac pacing on left ventricular function and in particular the optimisation of cardiac pacing with respect to site and timing. This thesis also investigated the reproducibility of three-dimensional echocardiographic speckle tracking across a range of patients.

Four discrete projects were undertaken. The first investigated three-dimensional echocardiographic measurements with invasive measurements of left ventricular function including intra-cavitary left ventricular pressure measurements as well as impedance measurement between right and left ventricular pacing leads, performed during cardiac pacing. The second project examined the effect of pacing the right ventricle as compared to intrinsic rhythm in patients paced from the mid-inter-ventricular septum or the right ventricular apex. The third project examined the effect of biventricular pacing on left ventricular function serially in patients with an aim to investigate the utility of measurements to predict echocardiographic and clinical outcomes. The final project examined the determinants of reproducibility of left ventricular function assessment using novel three-dimensional echocardiographic speckle tracking.

### 6.2 Summary of main findings

The comparisons of three-dimensional echocardiographic assessments of left ventricular function with invasive measurements of  $dp/dt$  and

impedance have not previously been performed. This study demonstrated that the agreement between these methods in the selection of optimal atrioventricular delays was poor. There may be a number of reasons underlying this - intrinsic variability, alterations in loading situations, intrinsic variability on different days, or indeed limitations in the techniques investigated. This may well explain why randomised controlled trials of echo methods to optimise atrioventricular delays have demonstrated little clinical benefit over default atrioventricular delay programming. Randomised controlled trials looking a clinical benefit for invasive measurements have not been performed, but the lack of agreement brings the question as to the reference standard for optimisation. Given the lack of a reference method, the gold standard should remain long-term clinical outcome measures though that brings its own issues of measurement and unrelated health issues.

The second study demonstrated that pacing results in impairment of left ventricular function when compared to intrinsic rhythm. These data suggest that whilst pacing from the mid RV septum is equivalent to apical pacing in normal hearts; in patients with impaired LV function, mid-septal pacing results in a smaller fall in left ventricular ejection fraction compared to apical pacing. This is the first study of the effects of mid-inter-ventricular pacing as an alternative site for right ventricular pacing using three dimensional echocardiography. In the wider context, there is good data to indicate that conventional right ventricular apical pacing causes impairment in left ventricular function. Since this study has been performed, biventricular pacing has been demonstrated to be better than right ventricular apical pacing in patients with impaired LV function<sup>167</sup>. Furthermore the results of PROTECT-PACE trial have been published<sup>177</sup>, which demonstrated that in patients with normal left ventricular function and requiring a high percentage of ventricular pacing, right ventricular apical pacing was equivalent to right ventricular outflow tract pacing. In

both groups there was a decrease in left ventricular ejection fraction of 2%. Smaller trials have demonstrated that mid-ventricular pacing is comparable to apical pacing in patients with preserved left ventricular function using nuclear medicine techniques<sup>178</sup>. Haemodynamic data suggest that the basal-mid septum is the most favourable site for RV pacing<sup>179</sup>.

Our data suggests that mid inter-ventricular septal pacing is superior to apical pacing in impaired LV function, but the question remains as to whether mid-septal pacing, or indeed right ventricular outflow tract pacing is equivalent to biventricular pacing in impaired LV function. A single recent study has attempted to answer this by measuring the ejection fraction in 22 patients scheduled for CRT. They underwent temporary dual chamber pacing prior to CRT. They found that both right ventricular outflow tract and mid-septal pacing were superior to apical pacing, but that biventricular pacing was better still<sup>180</sup>.

The third study investigated the utility of the change in dyssynchrony in predicting response to CRT and to CRT optimisation. We found that the change in dyssynchrony was a better predictor of response to CRT than baseline dyssynchrony, or other conventional selection criteria. We found that patients who were not dyssynchronous after CRT had little benefit from CRT optimisation. We confirmed the importance of LBBB, female sex, sinus rhythm, non-ischaemic aetiology in predicting a better outcome from CRT. This investigation confirms the importance of dyssynchrony as an important determinant in the response to CRT. We have confirmed prior work on the utility of baseline dyssynchrony measures in predicting outcome, but have also demonstrated that improvement in dyssynchrony after CRT is a better predictor of echocardiographic response than baseline measurements. We have also used three-dimensional echocardiography as an independent method of assessing the immediate response to Doppler echo-guided CRT optimisation. We confirm that optimisation makes a clinically significant difference to left ventricular function in a few patients,

but that the majority of patients see little acute benefit. The presence of dyssynchrony after CRT implantation may be a useful marker to select patients with a higher probability of responding to CRT optimisation.

Finally a series of investigations were performed using speckle tracking software. Although this has excellent reproducibility for volumes, dyssynchrony assessment was less reliable. We demonstrated that the removal of imperfectly visualised segments and standardisation of technique led to greater reproducibility. The applicability of this technique as investigated in this study is unlikely to be broad given the issues with image quality, however, it does demonstrate that the technique could be improved by the ability to identify and exclude poorly visualised segments. Further software development may improve the tracking ability as well as automatic identification of poorly visualised segments. This work highlights the necessity of training programs to ensure reliability in measurements and this work has been extended by colleagues<sup>181</sup>.

## 6.3 Conclusion

Real time 3 dimensional echocardiography has proven to be a valuable technique for the accurate measurement of ejection fraction and in the assessment of left ventricular dyssynchrony. Current guidelines do not recommend echocardiographic indices of dyssynchrony be used for patient selection for CRT. These data show that this technique may give valuable information that helps guide treatment for patients. Novel 3 dimensional speckle tracking software requires refinement to improve its reproducibility and reliability for dyssynchrony assessments, though it is promising for the measurement of left ventricular volumes.

## 7 References

1. McWilliam JA. Electrical stimulation of the heart in man. *British Medical Journal* 1889;1:348–50.
2. Mond HG, SLOMAN JG, EDWARDS RH. The First Pacemaker. *Pacing Clin Electrophysiol* 1982;5(2):278–82.
3. W G Bigelow JCCJAH. General Hypothermia for Experimental Intracardiac Surgery: The Use of Electrophrenic Respirations, an Artificial Pacemaker for Cardiac Standstill, and Radio-Frequency Rewarming in General Hypothermia. *Annals of Surgery* 1950;132(3):531.
4. Zoll PM. Resuscitation of the heart in ventricular standstill by external electric stimulation. *N Engl J Med* 1952;247(20):768–71.
5. Elmqvist R. Review of early pacemaker development. *Pacing Clin Electrophysiol* 1978;1(4):535–6.
6. Mohin A. Arne H. W. Larsson, 86; Had First Internal Pacemaker - *New York Times*. The New York Times. 2002;
7. FURMAN S, SCHWEDEL JB. An intracardiac pacemaker for Stokes-Adams seizures. *N Engl J Med* 1959;261:943–8.
8. Goldman BS, Black LL, Lipton IH. Implantable transvenous cardiac pacemakers: indications, complications and management. *Can Med Assoc J* 1970;103(11):1163–7.
9. Travill CM, Sutton R. Pacemaker syndrome: an iatrogenic condition. *Br Heart J* 1992;68(2):163–6.
10. Connolly SJ, Kerr C, Gent M, Yusuf S. Dual-chamber versus ventricular pacing. Critical appraisal of current data. *Circulation* 1996;94(3):578–83.
11. Lamas GA, Pashos CL, Normand SL, McNeil B. Permanent pacemaker selection and subsequent survival in elderly Medicare pacemaker recipients. *Circulation* 1995;91(4):1063–9.
12. Recommendations for pacemaker prescription for symptomatic bradycardia. Report of a working party of the British Pacing and Electrophysiology Group. *Br Heart J*. 1991;66(2):185–91.

13. Dreifus LS, Fisch C, Griffin JC, Gillette PC, Mason JW, Parsonnet V. Guidelines for implantation of cardiac pacemakers and antiarrhythmia devices. A report of the American College of Cardiology/American Heart Association Task Force on Assessment of Diagnostic and Therapeutic Cardiovascular Procedures (Committee on Pacemaker Implantation). *Journal of the American College of Cardiology* 1991;18(1):1–13.
14. Andersen HR, Thuesen L, Bagger JP, Vesterlund T, Thomsen PE. Prospective randomised trial of atrial versus ventricular pacing in sick-sinus syndrome. *Lancet* 1994;344(8936):1523–8.
15. Andersen HR, Nielsen JC, Thomsen PEB, et al. Long-term follow-up of patients from a randomised trial of atrial versus ventricular pacing for sick-sinus syndrome. *The Lancet* 1997;350(9086):1210–6.
16. Lamas GA, Orav EJ, Stamler BS, et al. Quality of life and clinical outcomes in elderly patients treated with ventricular pacing as compared with dual-chamber pacing. Pacemaker Selection in the Elderly Investigators. *N Engl J Med* 1998;338(16):1097–104.
17. Connolly SJ, Kerr CR, Gent M, et al. Effects of physiologic pacing versus ventricular pacing on the risk of stroke and death due to cardiovascular causes. Canadian Trial of Physiologic Pacing Investigators. *N Engl J Med* 2000;342(19):1385–91.
18. Kerr CR. Canadian Trial of Physiological Pacing: Effects of Physiological Pacing During Long-Term Follow-Up. *Circulation* 2004;109(3):357–62.
19. Lamas GA, Lee KL, Sweeney MO, et al. Ventricular Pacing or Dual-Chamber Pacing for Sinus-Node Dysfunction. *N Engl J Med* 2002;346(24):1854–62.
20. Toff WD, Camm AJ, Skehan JD, United Kingdom Pacing and Cardiovascular Events Trial Investigators. Single-chamber versus dual-chamber pacing for high-grade atrioventricular block. *N Engl J Med* 2005;353(2):145–55.
21. Hochleitner M, Hörtnagl H, Ng CK, Hörtnagl H, Gschnitzer F, Zechmann W. Usefulness of physiologic dual-chamber pacing in drug-resistant idiopathic dilated cardiomyopathy. *Am J Cardiol* 1990;66(2):198–202.
22. Brecker SJD, Xiao HB, Sparrow J, Gibson DG. Effects of dual-



chamber pacing with short atrioventricular delay in dilated cardiomyopathy. *The Lancet* 1992;340(8831):1308–12.

23. Hochleitner M, Hortnagl H, Hortnagl H, Fridrich L, Gschnitzer F. Long-Term Efficacy of Physiologic Dual-Chamber Pacing in the Treatment of End-Stage Idiopathic

Dilated Cardiomyopathy. *Am J Cardiol* 1992;70:1320–5.

24. Saxon LA, Stevenson WG, Middlekauff HR, Stevenson LW. Increased risk of progressive hemodynamic deterioration in advanced heart failure patients requiring permanent pacemakers. *Am Heart J* 1993;125(5 Pt 1):1306–10.
25. Wilkoff BL, Cook JR, Epstein AE, et al. Dual-chamber pacing or ventricular backup pacing in patients with an implantable defibrillator: the Dual Chamber and VVI Implantable Defibrillator (DAVID) Trial. *JAMA* 2002;288(24):3115–23.
26. Sweeney MO, Hellkamp AS, Ellenbogen KA, et al. Adverse effect of ventricular pacing on heart failure and atrial fibrillation among patients with normal baseline QRS duration in a clinical trial of pacemaker therapy for sinus node dysfunction. *Circulation* 2003;107(23):2932–7.
27. Sweeney MO, Bank AJ, Nsah E, et al. Minimizing ventricular pacing to reduce atrial fibrillation in sinus-node disease. *N Engl J Med* 2007;357(10):1000–8.
28. Cazeau S, Ritter P, Bakdach S, et al. Four chamber pacing in dilated cardiomyopathy. *Pacing Clin Electrophysiol* 1994;17(11 Pt 2):1974–9.
29. Cazeau S, Leclercq C, Lavergne T, et al. Effects of multisite biventricular pacing in patients with heart failure and intraventricular conduction delay. *N Engl J Med* 2001;344(12):873–80.
30. Linde C, Leclercq C, Rex S, et al. Long-term benefits of biventricular pacing in congestive heart failure: results from the MULTISite STimulation in cardiomyopathy (MUSTIC) study. *Journal of the American College of Cardiology* 2002;40(1):111–8.
31. Abraham WT, Fisher WG, Smith AL, et al. Cardiac resynchronization in chronic heart failure. *N Engl J Med* 2002;346(24):1845–53.

32. Auricchio A, Stellbrink C, Sack S, et al. Long-term clinical effect of hemodynamically optimized cardiac resynchronization therapy in patients with heart failure and ventricular conduction delay. *Journal of the American College of Cardiology* 2002;39(12):2026–33.
33. Bristow MR, Saxon LA, Boehmer J, et al. Cardiac-resynchronization therapy with or without an implantable defibrillator in advanced chronic heart failure. *N Engl J Med* 2004;350(21):2140–50.
34. Cleland J, Daubert J-C, Erdmann E, et al. The effect of cardiac resynchronization on morbidity and mortality in heart failure. *N Engl J Med* 2005;352(15):1539–49.
35. Moss AJ, Hall W, Cannom D, et al. Cardiac-Resynchronization Therapy for the Prevention of Heart-Failure Events. *N Engl J Med* 2009;
36. European Society of Cardiology, Heart Failure Association of the ESC HFA, European Society of Intensive Care Medicine ESICM, et al. ESC guidelines for the diagnosis and treatment of acute and chronic heart failure 2008: the Task Force for the diagnosis and treatment of acute and chronic heart failure 2008 of the European Society of Cardiology. Developed in collaboration with the Heart Failure Association of the ESC (HFA) and endorsed by the European Society of Intensive Care Medicine (ESICM). *Eur J Heart Fail* 2008;10(10):933–89.
37. Cazeau S, Bordachar P, Jauvert G, et al. Echocardiographic modeling of cardiac dyssynchrony before and during multisite stimulation: a prospective study. *Pacing Clin Electrophysiol* 2003;26(1 Pt 2):137–43.
38. JOHNSON RL, AVERILL KH, LAMB LE. Electrocardiographic findings in 67,375 asymptomatic subjects. VI. Right bundle branch block. *Am J Cardiol* 1960;6:143–52.
39. LAMB LE, KABLE KD, AVERILL KH. Electrocardiographic findings in 67,375 asymptomatic subjects. V. Left bundle branch block. *Am J Cardiol* 1960;6:130–42.
40. McCullough PA, Hassan SA, Pallekonda V, et al. Bundle branch block patterns, age, renal dysfunction, and heart failure mortality. *Int J Cardiol* 2005;102(2):303–8.
41. Barold SS, Ilercil A, Leonelli F, Herweg B. First-degree

- atrioventricular block. *J Interv Card Electrophysiol* 2007;17(2):139–52.
42. CHEN J, GARCIA E, FOLKS R, et al. Onset of left ventricular mechanical contraction as determined by phase analysis of ECG-gated myocardial perfusion SPECT imaging: Development of a diagnostic tool for assessment of cardiac mechanical dyssynchrony. *Journal of Nuclear Cardiology* 2005;12(6):687–95.
  43. Chen J, Bax JJ, Henneman MM, Boogers MJ, Garcia EV. Is nuclear imaging a viable alternative technique to assess dyssynchrony? *Europace* 2008;10 Suppl 3:iii101–5.
  44. Nakamura K, Takami M, Shimabukuro M, et al. Effective prediction of response to cardiac resynchronization therapy using a novel program of gated myocardial perfusion single photon emission computed tomography. *Europace* 2011;
  45. Pennell DJ. Cardiovascular Magnetic Resonance. *Circulation* 2010;121(5):692–705.
  46. Truong QA, Singh JP, Cannon CP, et al. Quantitative Analysis of Intraventricular Dyssynchrony Using Wall Thickness by Multidetector Computed Tomography. *JACC Cardiovasc Imaging* 2008;1(6):772.
  47. Schmidt M, Rittger H, Marschang H, et al. Left ventricular dyssynchrony from right ventricular pacing depends on intraventricular conduction pattern in intrinsic rhythm. *Eur J Echocardiogr* [Internet] 2009;10(6):776–83. Available from: <http://ehjcmimaging.oxfordjournals.org/cgi/doi/10.1093/ejechocard/jep069>
  48. Miyatake K, Yamagishi M, Tanaka N, et al. New method for evaluating left ventricular wall motion by color-coded tissue Doppler imaging: in vitro and in vivo studies. *Journal of the American College of Cardiology* 1995;25(3):717–24.
  49. Tei C, Ling LH, Hodge DO, et al. New index of combined systolic and diastolic myocardial performance: a simple and reproducible measure of cardiac function--a study in normals and dilated cardiomyopathy. *J Cardiol* 1995;26(6):357–66.
  50. Chow C-M. Tei Index [Internet]. csecho.ca. [cited 2016 Jul 28]; Available from: <http://www.csecho.ca/wp-content/themes/twentyeleven->

51. Yu C-M, Chau E, Sanderson JE, et al. Tissue Doppler echocardiographic evidence of reverse remodeling and improved synchronicity by simultaneously delaying regional contraction after biventricular pacing therapy in heart failure. *Circulation* 2002;105(4):438–45.
52. Langeland S, D'hooge J, Wouters PF, et al. Experimental Validation of a New Ultrasound Method for the Simultaneous Assessment of Radial and Longitudinal Myocardial Deformation Independent of Insonation Angle. *Circulation* 2005;112(14):2157–62.
53. Chung ES, Leon AR, Tavazzi L, et al. Results of the Predictors of Response to CRT (PROSPECT) trial. *Circulation* 2008;117(20):2608–16.
54. Kapetanakis S, Kearney MT, Siva A, Gall N, Cooklin M, Monaghan MJ. Real-time three-dimensional echocardiography: a novel technique to quantify global left ventricular mechanical dyssynchrony. *Circulation* 2005;112(7):992–1000.
55. Soliman OII, van Dalen BM, Nemes A, et al. Quantification of left ventricular systolic dyssynchrony by real-time three-dimensional echocardiography. *J Am Soc Echocardiogr* 2009;22(3):232–9.
56. Conca C, Faletra FF, Miyazaki C, et al. Echocardiographic parameters of mechanical synchrony in healthy individuals. *Am J Cardiol* 2009;103(1):136–42.
57. Bland JM, Altman DG. Statistical methods for assessing agreement between two methods of clinical measurement. *Lancet* 1986;1(8476):307–10.
58. Gwet KL. Intrarater Reliability. In: *Wiley Encyclopedia of Clinical Trials*. Wiley; 2008. p. 1–14.
59. Bland JM, Altman DG. A note on the use of the intraclass correlation coefficient in the evaluation of agreement between two methods of measurement. *Comput Biol Med* 1990;20(5):337–40.
60. HISS RG, LAMB LE, ALLEN MF. Electrocardiographic findings in 67,375 asymptomatic subjects. X. Normal values. *Am J Cardiol* 1960;6:200–31.

61. Baker GH, Hlavacek AM, Chessa KS, Fleming DM, Shirali GS. Left ventricular dysfunction is associated with intraventricular dyssynchrony by 3-dimensional echocardiography in children. *J Am Soc Echocardiogr* 2008;21(3):230–3.
62. Gimenes VML, Vieira MLC, Andrade MM, Pinheiro J, Hotta VT, Mathias W. Standard values for real-time transthoracic three-dimensional echocardiographic dyssynchrony indexes in a normal population. *J Am Soc Echocardiogr* 2008;21(11):1229–35.
63. de Castro S, Faletra F, Di Angelantonio E, et al. Tomographic Left Ventricular Volumetric Emptying Analysis by Real-Time 3-Dimensional Echocardiography: Influence of Left Ventricular Dysfunction With and Without Electrical Dyssynchrony. *Circulation: Cardiovascular Imaging* 2008;1(1):41.
64. Samet P, Bernstein WH, Nathan DA, Lopez A. Atrial Contribution to Cardiac Output in Complete Heart Block. *Am J Cardiol* 1965;16:1–10.
65. Samet P, Castillo C, Bernstein WH. Hemodynamic sequelae of atrial, ventricular, and sequential atrioventricular pacing in cardiac patients. *Am Heart J* 1966;72(6):725–9.
66. Haas JM, Strait GB. Pacemaker-induced cardiovascular failure. Hemodynamic and angiographic observations. *Am J Cardiol* 1974;33(2):295–9.
67. Barold SS, Linhart JW, Hildner FJ, Samet P. Hemodynamic comparison of endocardial pacing of outflow and inflow tracts of the right ventricle. *Am J Cardiol* 1969;23(5):697–701.
68. Abbasi AS, Eber LM, MacAlpin RN, Kattus AA. Paradoxical motion of interventricular septum in left bundle branch block. *Circulation* 1974;49(3):423–7.
69. Gomes JA, Damato AN, Akhtar M, et al. Ventricular septal motion and left ventricular dimensions during abnormal ventricular activation. *Am J Cardiol* 1977;39(5):641–50.
70. Xiao HB, Brecker SJ, Gibson DG. Differing effects of right ventricular pacing and left bundle branch block on left ventricular function. *Br Heart J* 1993;69(2):166–73.
71. Leclercq C, Gras D, Le Helloco A, Nicol L, Mabo P, Daubert C. Hemodynamic importance of preserving the normal sequence of ventricular activation in permanent cardiac pacing. *Am Heart J*

1995;129(6):1133–41.

72. Schwaab B, Fröhlig G, Alexander C, et al. Influence of right ventricular stimulation site on left ventricular function in atrial synchronous ventricular pacing. *Journal of the American College of Cardiology* 1999;33(2):317–23.
73. Victor F, Leclercq C, Mabo P, et al. Optimal right ventricular pacing site in chronically implanted patients: a prospective randomized crossover comparison of apical and outflow tract pacing. *Journal of the American College of Cardiology* 1999;33(2):311–6.
74. Mera F, DeLurgio DB, Patterson RE, Merlino JD, Wade ME, León AR. A comparison of ventricular function during high right ventricular septal and apical pacing after his-bundle ablation for refractory atrial fibrillation. *Pacing Clin Electrophysiol* 1999;22(8):1234–9.
75. Kolettis TM, Kyriakides ZS, Tsiapras D, Popov T, Paraskevaides IA, Kremastinos DT. Improved left ventricular relaxation during short-term right ventricular outflow tract compared to apical pacing. *Chest* 2000;117(1):60–4.
76. Deshmukh P, Casavant DA, Romanyshyn M, Anderson K. Permanent, direct His-bundle pacing: a novel approach to cardiac pacing in patients with normal His-Purkinje activation. *Circulation* 2000;101(8):869–77.
77. Szili-Torok T, Kimman GP, Theuns D, Poldermans D, Roelandt JRTC, Jordaens LJ. Deterioration of left ventricular function following atrio-ventricular node ablation and right ventricular apical pacing in patients with permanent atrial fibrillation. *Europace* 2002;4(1):61–5.
78. Tantengco MVT, Thomas RL, Karpawich PP. Left ventricular dysfunction after long-term right ventricular apical pacing in the young. *Journal of the American College of Cardiology* 2001;37(8):2093–100.
79. Nielsen JC, Kristensen L, Andersen HR, Mortensen PT, Pedersen OL, Pedersen AK. A randomized comparison of atrial and dual-chamber pacing in 177 consecutive patients with sick sinus syndrome. *Journal of the American College of Cardiology* 2003;42(4):614–23.
80. Stambler BS, Ellenbogen K, Zhang X, et al. Right ventricular

outflow versus apical pacing in pacemaker patients with congestive heart failure and atrial fibrillation. *J Cardiovasc Electrophysiol* 2003;14(11):1180–6.

81. Nahlawi M, Waligora M, Spies SM, Bonow RO, Kadish AH, Goldberger JJ. Left ventricular function during and after right ventricular pacing. *journal of the American College of Cardiology* 2004;44(9):1883–8.
82. Thambo J-B, Bordachar P, Garrigue S, et al. Detrimental ventricular remodeling in patients with congenital complete heart block and chronic right ventricular apical pacing. *Circulation* 2004;110(25):3766–72.
83. Liu W-H, Chen M-C, Chen Y-L, et al. Right ventricular apical pacing acutely impairs left ventricular function and induces mechanical dyssynchrony in patients with sick sinus syndrome: a real-time three-dimensional echocardiographic study. *J Am Soc Echocardiogr* 2008;21(3):224–9.
84. Vassallo JA, Cassidy DM, Marchlinski FE, et al. Endocardial activation of left bundle branch block. *Circulation* 1984;69(5):914–23.
85. Rodriguez L-M, Timmermans C, Nabar A, Beatty G, Wellens HJJ. Variable patterns of septal activation in patients with left bundle branch block and heart failure. *J Cardiovasc Electrophysiol* 2003;14(2):135–41.
86. Vassallo JA, Cassidy DM, Miller JM, Buxton AE, Marchlinski FE, Josephson ME. Left ventricular endocardial activation during right ventricular pacing: effect of underlying heart disease. *journal of the American College of Cardiology* 1986;7(6):1228–33.
87. Kvitting J-PE, Wigström L, Strotmann JM, Sutherland GR. How Accurate Is Visual Assessment of Synchronicity in Myocardial Motion? An In Vitro Study with Computer-Simulated Regional Delay in Myocardial Motion: Clinical Implications for Rest and Stress Echocardiography Studies. *Journal of the American Society of Echocardiography* 1999;12(9):698–705.
88. JANSEN A, VANDANTZIG J, BRACKE F, et al. Qualitative Observation of Left Ventricular Multiphasic Septal Motion and Septal-to-Lateral Apical Shuffle Predicts Left Ventricular Reverse Remodeling After Cardiac Resynchronization Therapy. *Am J Cardiol* 2007;99(7):966–9.

89. Yu C-M, Zhang Q, Chan Y-S, et al. Tissue Doppler velocity is superior to displacement and strain mapping in predicting left ventricular reverse remodelling response after cardiac resynchronisation therapy. *Heart* 2006;92(10):1452–6.
90. Bleeker GB, Schalij MJ, Molhoek SG, et al. Relationship Between QRS Duration and Left Ventricular Dyssynchrony in Patients with End-Stage Heart Failure. *J Cardiovasc Electrophysiol* 2004;15(5):544–9.
91. BLEEKER G, SCHALIJ M, MOLHOEK S, et al. Frequency of left ventricular dyssynchrony in patients with heart failure and a narrow QRS complex. *Am J Cardiol* 2005;95(1):140–2.
92. Cho G-Y, Song J-K, Park W-J, et al. Mechanical Dyssynchrony Assessed by Tissue Doppler Imaging Is a Powerful Predictor of Mortality in Congestive Heart Failure With Normal QRS Duration. *journal of the American College of Cardiology* 2005;46(12):2237–43.
93. Cazeau S, Daubert J-C, Tavazzi L, Frohlig G, Paul V. Responders to cardiac resynchronization therapy with narrow or intermediate QRS complexes identified by simple echocardiographic indices of dyssynchrony: The DESIRE study. *European Journal of Heart Failure* 2008;10(3):273–80.
94. van Bommel RJ, Tanaka H, Delgado V, et al. Association of intraventricular mechanical dyssynchrony with response to cardiac resynchronization therapy in heart failure patients with a narrow QRS complex. *Eur Heart J* 2010;31(24):3054–62.
95. Beshai JF, Grimm RA, Nagueh SF, et al. Cardiac-resynchronization therapy in heart failure with narrow QRS complexes. *N Engl J Med* 2007;357(24):2461–71.
96. Williams L, Ellery S, Patel K, et al. Short-Term Hemodynamic Effects of Cardiac Resynchronization Therapy in Patients With Heart Failure, a Narrow QRS Duration, and No Dyssynchrony. *Circulation* 2009;120(17):1687–94.
97. Suffoletto MS, Dohi K, Cannesson M, Saba S, Gorcsan J. Novel speckle-tracking radial strain from routine black-and-white echocardiographic images to quantify dyssynchrony and predict response to cardiac resynchronization therapy. *Circulation* 2006;113(7):960–8.
98. Gorcsan J, Oyenuga O, Habib PJ, et al. Relationship of



- echocardiographic dyssynchrony to long-term survival after cardiac resynchronization therapy. *Circulation* 2010;122(19):1910–8.
99. Delgado V, Ypenburg C, van Bommel RJ, et al. Assessment of left ventricular dyssynchrony by speckle tracking strain imaging comparison between longitudinal, circumferential, and radial strain in cardiac resynchronization therapy. *Journal of the American College of Cardiology* 2008;51(20):1944–52.
  100. Lim P, Buakhamsri A, Popović ZB, et al. Longitudinal strain delay index by speckle tracking imaging: a new marker of response to cardiac resynchronization therapy. *Circulation* 2008;118(11):1130–7.
  101. Becker M, Kramann R, Franke A, et al. Impact of left ventricular lead position in cardiac resynchronization therapy on left ventricular remodelling. A circumferential strain analysis based on 2D echocardiography. *Eur Heart J* 2007;28(10):1211–20.
  102. Zeng X, Shu X-H, Pan C-Z, et al. Assessment of left ventricular systolic synchronicity by real-time three-dimensional echocardiography in patients with dilated cardiomyopathy. *Chin Med J* 2006;119(11):919–24.
  103. Burgess MI, Jenkins C, Chan J, Marwick TH. Measurement of left ventricular dyssynchrony in patients with ischaemic cardiomyopathy: a comparison of real-time three-dimensional and tissue Doppler echocardiography. *Heart* 2007;93(10):1191–6.
  104. Takeuchi M, Jacobs A, Sugeng L, et al. Assessment of left ventricular dyssynchrony with real-time 3-dimensional echocardiography: comparison with Doppler tissue imaging. *J Am Soc Echocardiogr* 2007;20(12):1321–9.
  105. Pérez de Isla L, Balcones DV, Fernández-Golfín C, et al. Three-dimensional-wall motion tracking: a new and faster tool for myocardial strain assessment: comparison with two-dimensional-wall motion tracking. *J Am Soc Echocardiogr* 2009;22(4):325–30.
  106. van Dijk J, Dijkmans PA, Götte MJW, Spreeuwenberg MD, Visser CA, Kamp O. Evaluation of global left ventricular function and mechanical dyssynchrony in patients with an asymptomatic left bundle branch block: a real-time 3D echocardiography study. *Eur J Echocardiogr* 2008;9(1):40–6.

107. Bax JJ, Abraham T, Barold SS, et al. Cardiac resynchronization therapy: Part 1--issues before device implantation. *Journal of the American College of Cardiology* 2005;46(12):2153–67.
108. Delgado V, Sitges M, Vidal B, et al. Assessment of Left Ventricular Dyssynchrony by Real-Time Three-Dimensional Echocardiography. *Revista Española de Cardiología (Internet)* 2008;61(8):825–34.
109. Marsan NA, Bleeker GB, Ypenburg C, et al. Real-time three-dimensional echocardiography permits quantification of left ventricular mechanical dyssynchrony and predicts acute response to cardiac resynchronization therapy. *J Cardiovasc Electrophysiol* 2008;19(4):392–9.
110. van Dijk J, Knaapen P, Russel IK, et al. Mechanical dyssynchrony by 3D echo correlates with acute haemodynamic response to biventricular pacing in heart failure patients. *Europace* 2008;10(1):63–8.
111. Soliman Oll, Geleijnse ML, Theuns DAMJ, et al. Usefulness of left ventricular systolic dyssynchrony by real-time three-dimensional echocardiography to predict long-term response to cardiac resynchronization therapy. *Am J Cardiol* 2009;103(11):1586–91.
112. Kapetanakis S, Bhan A, Murgatroyd FD, et al. Real-time 3D echo in patient selection for cardiac resynchronization therapy. *JACC Cardiovasc Imaging* 2011;4(1):16–26.
113. Porciani MC, Rao CM, Mochi M, et al. A real-time three-dimensional echocardiographic validation of an intracardiac electrogram-based method for optimizing cardiac resynchronization therapy. *Pacing Clin Electrophysiol* 2008;31(1):56–63.
114. Forfang K, Otterstad JE, Ihlen H. Optimal atrioventricular delay in physiological pacing determined by Doppler echocardiography. *Pacing Clin Electrophysiol* 1986;9(1 Pt 1):17–20.
115. Ritter P, Dib J, Lelievre T. Quick determination of the optimal AV delay at rest in patients paced in DDD mode for complete AV block. *European Journal of Cardiac Pacing and Electrophysiology* 1994;4:A163.
116. Heldman D, Mulvihill D, Nguyen H, et al. True incidence of

- pacemaker syndrome. *Pacing Clin Electrophysiol* 1990;13(12 Pt 2):1742–50.
117. Bertini M, Delgado V, Bax JJ, Van de Veire NRL. Why, how and when do we need to optimize the setting of cardiac resynchronization therapy? *Europace* 2009;11(Supplement 5):v46–v57.
118. Nishimura RA, Hayes DL, Holmes DR, Tajik AJ. Mechanism of hemodynamic improvement by dual-chamber pacing for severe left ventricular dysfunction: an acute Doppler and catheterization hemodynamic study. *Journal of the American College of Cardiology* 1995;25(2):281–8.
119. Kindermann M, Fröhlig G, Doerr T, Schieffer H. Optimizing the AV delay in DDD pacemaker patients with high degree AV block: mitral valve Doppler versus impedance cardiography. *Pacing Clin Electrophysiol* 1997;20(10 Pt 1):2453–62.
120. Kerlan JE, Sawhney NS, Waggoner AD, et al. Prospective comparison of echocardiographic atrioventricular delay optimization methods for cardiac resynchronization therapy. *Heart Rhythm* 2006;3(2):148–54.
121. Kass DA, Chen CH, Curry C, et al. Improved left ventricular mechanics from acute VDD pacing in patients with dilated cardiomyopathy and ventricular conduction delay. *Circulation* 1999;99(12):1567–73.
122. Auricchio A, Stellbrink C, Block M, et al. Effect of pacing chamber and atrioventricular delay on acute systolic function of paced patients with congestive heart failure. The Pacing Therapies for Congestive Heart Failure Study Group. The Guidant Congestive Heart Failure Research Group. *Circulation* 1999;99(23):2993–3001.
123. Gold MR, Niazi I, Giudici M, et al. A prospective comparison of AV delay programming methods for hemodynamic optimization during cardiac resynchronization therapy. *J Cardiovasc Electrophysiol* 2007;18(5):490–6.
124. Jansen AHM, Bracke FA, van Dantzig JM, et al. Correlation of echo-Doppler optimization of atrioventricular delay in cardiac resynchronization therapy with invasive hemodynamics in patients with heart failure secondary to ischemic or idiopathic dilated cardiomyopathy. *Am J Cardiol* 2006;97(4):552–7.

125. Stockburger M, Fateh-Moghadam S, Nitardy A, Langreck H, Haverkamp W, Dietz R. Optimization of cardiac resynchronization guided by Doppler echocardiography: haemodynamic improvement and intraindividual variability with different pacing configurations and atrioventricular delays. *Europace* 2006;8(10):881–6.
126. Sawhney NS, Waggoner AD, Garhwal S, Chawla MK, Osborn J, Faddis MN. Randomized prospective trial of atrioventricular delay programming for cardiac resynchronization therapy. *Heart Rhythm* 2004;1(5):562–7.
127. KEDIA N, NG K, APPERSONHANSEN C, et al. Usefulness of Atrioventricular Delay Optimization Using Doppler Assessment of Mitral Inflow in Patients Undergoing Cardiac Resynchronization Therapy. *Am J Cardiol* 2006;98(6):780–5.
128. Hardt SE, Yazdi SHF, Bauer A, et al. Immediate and chronic effects of AV-delay optimization in patients with cardiac resynchronization therapy ☆. *Int J Cardiol* 2007;115(3):318–25.
129. Zhang Q, Wing-Hong Fung J, Chan Y-S, et al. The role of repeating optimization of atrioventricular interval during interim and long-term follow-up after cardiac resynchronization therapy. *Int J Cardiol* 2008;124(2):211–7.
130. Melzer C, Knebel F, Ismer B, et al. Influence of the atrio-ventricular delay optimization on the intra left ventricular delay in Cardiac Resynchronization Therapy. *Cardiovasc Ultrasound* 2006;4:5.
131. Whinnett ZI, Briscoe C, Davies JER, et al. The atrioventricular delay of cardiac resynchronization can be optimized hemodynamically during exercise and predicted from resting measurements. *Heart Rhythm* 2008;5(3):378–86.
132. Waggoner AD, Las Fuentes de L, Faddis MN, Gleva MJ, Spence KE, Davila-Roman VG. Left ventricular diastolic filling prior to cardiac resynchronization therapy: implications for atrioventricular delay programming. *Pacing Clin Electrophysiol* 2008;31(7):838–44.
133. JONES RC, SVINARICH T, RUBIN A, et al. Optimal Atrioventricular Delay in CRT Patients Can Be Approximated Using Surface Electrocardiography and Device Electrograms. *J Cardiovasc Electrophysiol* 2010;21(11):1226–32.

134. Whinnett ZI, Nott G, Davies JER, et al. Maximizing Efficiency of Alternation Algorithms for Hemodynamic Optimization of the AV Delay of Cardiac Resynchronization Therapy. *Pacing and Clinical Electrophysiology* 2010;34(2):217–25.
135. Ellenbogen KA, Gold MR, Meyer TE, et al. Primary Results From the SmartDelay Determined AV Optimization: A Comparison to Other AV Delay Methods Used in Cardiac Resynchronization Therapy (SMART-AV) Trial: A Randomized Trial Comparing Empirical, Echocardiography-Guided, and Algorithmic Atrioventricular Delay Programming in Cardiac Resynchronization Therapy. *Circulation* 2010;122(25):2660–8.
136. Abraham WT, Gras D, Yu C-M, Guzzo L, Gupta MS, Committee OBOTFS. Rationale and design of a randomized clinical trial to assess the safety and efficacy of frequent optimization of cardiac resynchronization therapy: The Frequent Optimization Study Using the QuickOpt Method (FREEDOM) trial. *Am Heart J* 2010;159(6):944–948.e1.
137. Søgaard P, Egeblad H, Pedersen AK, et al. Sequential versus simultaneous biventricular resynchronization for severe heart failure: evaluation by tissue Doppler imaging. *Circulation* 2002;106(16):2078–84.
138. Perego G. Simultaneous vs. sequential biventricular pacing in dilated cardiomyopathy: an acute hemodynamic study. *European Journal of Heart Failure* 2003;5(3):305–13.
139. van Gelder BM, Bracke FA, Meijer A, Lakerveld LJM, Pijls NHJ. Effect of optimizing the VV interval on left ventricular contractility in cardiac resynchronization therapy. *Am J Cardiol* 2004;93(12):1500–3.
140. Burri H, Sunthorn H, Somsen A, et al. Optimizing sequential biventricular pacing using radionuclide ventriculography. *Heart Rhythm* 2005;2(9):960–5.
141. Vanderheyden M, Debacker T, Riveroayerza M, et al. Tailored echocardiographic interventricular delay programming further optimizes left ventricular performance after cardiac resynchronization therapy. *Heart Rhythm* 2005;2(10):1066–72.
142. Leon AR, Abraham WT, Brozena S, et al. Cardiac Resynchronization With Sequential Biventricular Pacing for the Treatment of Moderate-to-Severe Heart Failure. *Journal of the American College of Cardiology* 2005;46(12):2298–304.

143. Boriani G, MULLER C, SEIDL K, et al. Randomized comparison of simultaneous biventricular stimulation versus optimized interventricular delay in cardiac resynchronization therapyThe Resynchronization for the HemodyNamic Treatment for Heart Failure Management II implantable cardioverter defibrillator (RHYTHM II ICD) study. *Am Heart J* 2006;151(5):1050–8.
144. Boriani G, Biffi M, Müller CP, et al. A prospective randomized evaluation of VV delay optimization in CRT-D recipients: echocardiographic observations from the RHYTHM II ICD study. *Pacing Clin Electrophysiol* 2009;32 Suppl 1:S120–5.
145. DOLTRA A, Vidal B, SILVA E, et al. Comparison of Hemodynamic versus Dyssynchrony Assessment for Interventricular Delay Optimization with Echocardiography in Cardiac Resynchronization Therapy. *Pacing and Clinical Electrophysiology* 2011;;no–no.
146. Bertini M, Matteo Ziacchi, Biffi M, et al. Interventricular delay interval optimization in cardiac resynchronization therapy guided by echocardiography versus guided by electrocardiographic QRS interval width. *Am J Cardiol* 2008;102(10):1373–7.
147. Fischer A, Hansalia R, Buckley S, et al. Lack of clinical predictors of optimal V-V delay in patients with cardiac resynchronization devices. *J Interv Card Electrophysiol* 2009;25(2):153–8.
148. Sciaraffia E, Malmborg H, Lönnerholm S, Blomström P, Blomström Lundqvist C. The use of impedance cardiography for optimizing the interventricular stimulation interval in cardiac resynchronization therapy-a comparison with left ventricular contractility. *J Interv Card Electrophysiol* 2009;25(3):223–8.
149. Marsan NA, Bleeker GB, van Bommel RJ, et al. Cardiac resynchronization therapy in patients with ischemic versus non-ischemic heart failure: Differential effect of optimizing interventricular pacing interval. *Am Heart J* 2009;158(5):769–76.
150. Duvall WL, Hansalia R, Wijetunga MN, Buckley S, Fischer A. Advantage of Optimizing V-V Timing in Cardiac Resynchronization Therapy Devices. *Pacing Clin Electrophysiol* 2010;
151. Herweg B, ALI R, Ilercil A, et al. Site-Specific Differences in Latency Intervals during Biventricular Pacing: Impact on Paced QRS Morphology and Echo-Optimized V-V Interval. *Pacing and*

Clinical Electrophysiology 2010;33(11):1382–91.

152. Khan FZ, Virdee MS, Read PA, et al. Impact of VV optimization in relation to left ventricular lead position: an acute haemodynamic study. *Europace* 2011;13(6):845–52.
153. Tamborero D, Vidal B, Tolosana JM, et al. Electrocardiographic versus Echocardiographic Optimization of the Interventricular Pacing Delay in Patients Undergoing Cardiac Resynchronization Therapy. *J Cardiovasc Electrophysiol* 2011;;no–no.
154. Valzania C, Biffi M, Cristian Martignani, et al. Cardiac Resynchronization Therapy: Variations in Echo-Guided Optimized Atrioventricular and Interventricular Delays During Follow-Up. *Echocardiography* 2007;24(9):933–9.
155. Valzania C, Eriksson MJ, Boriani G, Gadler F. Cardiac resynchronization therapy during rest and exercise: comparison of two optimization methods. *Europace* 2008;10(10):1161–9.
156. van Gelder BM, Meijer A, Bracke FA. The optimized V-V interval determined by interventricular conduction times versus invasive measurement by LVdP/dtMAX. *J Cardiovasc Electrophysiol* 2008;19(9):939–44.
157. Zuber M, Toggweiler S, Quinn-Tate L, Brown L, Amkieh A, Erne P. A comparison of acoustic cardiography and echocardiography for optimizing pacemaker settings in cardiac resynchronization therapy. *Pacing Clin Electrophysiol* 2008;31(7):802–11.
158. Khan FZ, Virdee MS, Pugh PJ, Read PA, Fynn SP, Dutka DP. Non-invasive cardiac output measurements based on bioreactance for optimization of atrio- and interventricular delays. *Europace* 2009;11(12):1666–74.
159. Taha N, Zhang J, Ranjan R, et al. Biventricular Pacemaker Optimization Guided by Comprehensive Echocardiography- Preliminary Observations Regarding the Effects on Systolic and Diastolic Ventricular Function and Third Heart Sound. *J Am Soc Echocardiogr* 2010;
160. REINSCH N, KONORZA T, WOYDOWSKI D, et al. Iterative Cardiac Output Measurement for Optimizing Cardiac Resynchronization Therapy: A Randomized, Blinded, Crossover Study. *Pacing and Clinical Electrophysiology* 2010;33(10):1188–94.
161. Bogaard MD, Doevendans PA, Leenders GE, et al. Can

- optimization of pacing settings compensate for a non-optimal left ventricular pacing site? *Europace* 2010;12(9):1262–9.
162. Ginks MR, Sciaraffia E, Karlsson A, et al. Relationship between intracardiac impedance and left ventricular contractility in patients undergoing cardiac resynchronization therapy. *Europace* 2011;
  163. Tang WHW, Tong W. Measuring impedance in congestive heart failure: current options and clinical applications. *Am Heart J* 2009;157(3):402–11.
  164. Stahl C, Walker T, Straub A, et al. Assessing acute ventricular volume changes by intracardiac impedance in a chronic heart failure animal model. *Pacing Clin Electrophysiol* 2009;32(11):1395–401.
  165. Whinnett ZI, Davies JER, Willson K, et al. Haemodynamic effects of changes in atrioventricular and interventricular delay in cardiac resynchronisation therapy show a consistent pattern: analysis of shape, magnitude and relative importance of atrioventricular and interventricular delay. *Heart* 2006;92(11):1628–34.
  166. Karpawich PP, Rabah R, Haas JE. Altered cardiac histology following apical right ventricular pacing in patients with congenital atrioventricular block. *Pacing Clin Electrophysiol* 1999;22(9):1372–7.
  167. Curtis AB, Worley SJ, Adamson PB, et al. Biventricular Pacing for Atrioventricular Block and Systolic Dysfunction. *N Engl J Med* 2013;368(17):1585–93.
  168. Kypta A, Steinwender C, Kammler J, Leisch F, Hofmann R. Long-term outcomes in patients with atrioventricular block undergoing septal ventricular lead implantation compared with standard apical pacing. *Europace* 2008;10(5):574–9.
  169. Shimony A, Eisenberg MJ, Filion KB, Amit G. Beneficial effects of right ventricular non-apical vs. apical pacing: a systematic review and meta-analysis of randomized-controlled trials. *Europace* 2011;
  170. Liu W-H, Guo B-F, Chen Y-L, et al. Right Ventricular Outflow Tract Pacing Causes Intraventricular Dyssynchrony in Patients With Sick Sinus Syndrome: A Real-Time Three-Dimensional Echocardiographic Study. *J Am Soc Echocardiogr*



2010;23(6):599–607.

171. Cano O, Osca J, Sancho-Tello M-J, et al. Comparison of Effectiveness of Right Ventricular Septal Pacing Versus Right Ventricular Apical Pacing. *Am J Cardiol* 2010;105(10):1426–32.
172. Ng ACT, Allman C, Vidaic J, Tie H, Hopkins AP, Leung DY. Long-Term Impact of Right Ventricular Septal Versus Apical Pacing on Left Ventricular Synchrony and Function in Patients With Second- or Third-Degree Heart Block. *Am J Cardiol* 2009;:1–6.
173. Mond HG, FELDMAN A, KUMAR S, Rosso R, HUNG TT, PANG B. Alternate Site Right Ventricular Pacing: Defining Template Scoring. *Pacing and Clinical Electrophysiology* 2011;:no–no.
174. Porciani MC, Dondina C, Macioce R, et al. Echocardiographic Examination of Atrioventricular and Interventricular Delay Optimization in Cardiac Resynchronization Therapy. *Am J Cardiol* 2005;95(9):1108–10.
175. Porciani MC, Dondina C, Macioce R, et al. Temporal Variation in Optimal Atrioventricular and Interventricular Delay During Cardiac Resynchronization Therapy. *J Card Fail* 2006;12(9):715–9.
176. Lang RM, Bierig M, Devereux RB, et al. Recommendations for Chamber Quantification: A Report from the American Society of Echocardiography’s Guidelines and Standards Committee and the Chamber Quantification Writing Group, Developed in Conjunction with the European Association of Echocardiography, a Branch of the European Society of Cardiology. *Journal of the American Society of Echocardiography* 2005;18(12):1440–63.
177. Kaye GC, Linker NJ, Marwick TH, et al. Effect of right ventricular pacing lead site on left ventricular function in patients with high-grade atrioventricular block: results of the Protect-Pace study. *Eur Heart J* 2014;
178. Domenichini G, Sunthorn H, Fleury E, Foulkes H, Stettler C, Burri H. Pacing of the interventricular septum versus the right ventricular apex: a prospective, randomized study. *Eur J Intern Med* 2012;23(7):621–7.
179. Vancura V, Wichterle D, Melenovský V, Kautzner J. Assessment of optimal right ventricular pacing site using invasive

measurement of left ventricular systolic and diastolic function. *Europace* 2013;15(10):1482–90.

180. Alhous MHA, Small GR, Hannah A, Hillis GS, Frenneaux M, Broadhurst PA. Right ventricular septal pacing as alternative for failed left ventricular lead implantation in cardiac resynchronization therapy candidates. *Europace* 2014;;euu259.
181. Tsang W, Kenny C, Adhya S, et al. Interinstitutional measurements of left ventricular volumes, speckle-tracking strain, and dyssynchrony using three-dimensional echocardiography. *J Am Soc Echocardiogr* 2013;26(11):1253–7.